HOST AND VIRAL FACTORS INVOLVED IN REGULATION OF NUCLEAR EGRESS OF HERPES SIMPLEX VIRUS

A Dissertation

Presented to the Faculty of the Graduate School

of Cornell University

in Partial Fulfillment of the Requirements for the Degree of

Doctor of Philosophy

by

Fan Mou

January 2009

HOST AND VIRAL FACTORS INVOLVED IN REGULATION OF NUCLEAR EGRESS OF HERPES SIMPLEX VIRUS

Fan Mou, Ph. D.

Cornell University 2009

The nascent nucleocapsids of Herpes Simplex Virus (HSV) egress from the infected cell nuclei by budding at the inner nuclear membrane (INM), and become enveloped primary virions in the perinuclear space. The envelope then fuses with the outer nuclear membrane (ONM) and the capsids are released into the cytosol, where they acquire tegument proteins and the final envelope at the trans-Golgi network and are delivered to the extracelluar space via secretory vesicles. This complicated process involves interactions between both viral and host factors.

The products of viral U_L31 and U_L34 genes form a complex on the INM that is essential to initiate the primary envelopment reaction. The proper positioning of this complex requires a kinase encoded by the viral U_S3 gene. In the absence of pU_S3 kinase activity, pU_L31/pU_L34 complexes aggregate on the nuclear rim and perinuclear virions accumulate within invaginations of the INM. I discovered that the nuclear lamina was dramatically perforated near those pU_L31/pU_L34 aggregations, and identified lamin A/C as a putative substrate of U_S3 kinase *in vitro*. The kinase activity was found to be sufficient to induce partial dissolution of lamin A/C from permeabilized cell nuclei. Two-dimensional electrophoretic analyses confirmed that lamin A/C was phosphorylated in HSV-infected cells, and the optimal phosphorylation required U_S3 kinase activity. These data suggest that U_S3 kinase activity regulates HSV-1 capsid nuclear egress at least in part by phosphorylation of lamin A/C.

Lamins A/C and B1 were shown to interact with pU_L34. To determine the roles of these interactions on viral infectivity and pU_L34 targeting, the localization of pU_L34 was examined in lamin knockout mouse embryonic fibroblasts (MEFs) in the presence or absence of pU_S3 kinase activity. It was determined that both lamin proteins directly or indirectly modified pU_L34 distribution but neither was required for its INM targeting during viral infection. The elimination of lamin B1 made cells less permissive for viral replication, whereas lamin A/C was dispensable for viral infection. Furthermore, in cells infected by the U_S3 defective virus, the lack of lamin A/C precluded accumulation of perinuclear virions and partially restored replication of this virus. These observations reveal different roles of specific lamins in HSV infection, suggesting that lamin A/C normally impedes viral nuclear egress and that U_S3 kinase helps alleviate this impediment, whereas lamin B1 is necessary for efficient viral replication, probably through its effects on many cellular signaling pathways.

pU_L31, the binding partner of pU_L34, is also a substrate of pU_S3. The N-terminus of pU_L31 was found to be critical for the protein's normal function and contains multiple phosphorylation sites for U_S3 kinase. The phosphorylation was not essential for productive infection, but was necessary for optimal viral growth kinetics. Phosphorylation-deficient pU_L31 caused pU_L31/pU_L34 complex aggregation as well as perinuclear virion accumulation, similar to the phenotype caused by abolishing U_S3 kinase activity. Mimicking phosphorylation of pU_L31 by replacement of phosphorylated residues with glutamic acid largely restored the smooth distribution of pU_L34/pU_L31, and precluded the perinuclear virion herniations, regardless of U_S3 kinase activity. However, the pseudo-phosphorylated protein hindered the primary envelopment of capsids. These results indicate that pU_L31 phosphorylation is a dynamic event, which mediates pU_S3 regulatory functions in both primary envelopment of nucleocapsids and subsequent de-envelopment of perinuclear virions.

BIOGRAPHICAL SKETCH

Fan Mou was born and raised in Enshi, a beautiful town surrounded by mountains in central China. At age of 16, she left home and went to Wuhan, where she spent four years of undergraduate life at Huazhong Agricultural University. In May 2003, she graduated with a Bachelor of Science degree in Animal Science. Later this year, she was awarded a fellowship to attend Cornell University to pursue a doctorate degree in the field of Comparative Biomedical Sciences. After one year rotation, she joined the lab of Dr. Joel Baines in 2004 and began the thesis research on Herpes Simplex Virus. The degree work was completed by January of 2009.

This work is dedicated to my dear mom and dad

ACKNOWLEDGEMENTS

First and foremost I would like to thank my mentor, Dr. Joel Baines for his guidance and patience throughout my Ph. D. study. I would also like to thank the people who have assisted in this research in so many different ways: my committee advisors Dr. Volker Vogt, Dr. Mark Roberson and Dr. Eric Denkers for their expert advice and opinions; all the people in the Baines' lab Elizabeth Wills, Jarek Okulicz-Kozaryn, Carol Duffy, Li Liang, Tom Forest, Kui Yang, Richard Park, Luella Scholtes and Kari Roberts for their inspiring discussions when I was stuck; all the faculty and staff in the Department of Microbiology and Immunology for their generous sharing of equipments and reagents. Finally I would like to thank my parents for their support and nurturing. I would not be here without any one of these people.

The research was supported by grants (R01 AI52341 and S10 RR020981) awarded to Dr. Joel Baines from the National Institutes of Health.

TABLE OF CONTENTS

LIST OF FIGURES

LIST OF TABLES

CHAPTER I

INTRODUCTION

Herpes simplex viruses are members of the Herpesviridae family. Members of this family are enveloped DNA viruses that produce life-long infections (168). Based upon details of tissue tropism, pathogenicity, and behavior under conditions of culture in the laboratory, the herpesviruses have been classified into three groups (171, 172): the alpha-herpesviruses which are neurotropic, have a rapid replication cycle and usually a broad host and cell range, and the beta- and gamma-herpesviruses which differ in genome size and structure. Both beta- and gamma-herpesviruses replicate more slowly and in a much more restricted range of cells of glandular and/or lymphatic origin. The human herpesviruses include herpes simplex virus type 1 and type 2 (HSV-1 and HSV-2, respectively), varicella-zoster virus (VZV), human cytomegalovirus (HCMV) and Epstein-Barr virus (EBV) (168).

Herpes simplex viruses belong to alpha-herpesviruses (168). The infection by HSV-1 and -2 initiates at oral and genital mucosa respectively (226, 227). Viruses enter sensory nerve termini and travel through neuronal axons in a retrograde manner to the dorsal root and trigeminal ganglia, where latent infection is established (8, 9, 42, 65). During latency, viruses maintain their quiescent genomes in the neuronal nucleus (41, 122, 167). However, lytic infection can be reactivated by a variety of stimuli including mental stress, menstruation, UV light etc (170, 227). Once activated, viruses resume replication and can disseminate progeny into nearby cells, peripheral nerve endings in skin, and/or the central nervous system (65, 212, 226). The release of viruses from the nerve terminals permits reinfection of the original epithelial tissues (e.g., creation of “cold sore” for HSV-1 or “genital herpes” for HSV-2). These lesions can be painful and recur for the host’s entire life. If the infection spreads into the cen-

tral nervous system, it may result in life threatening, or fatal viral encephalitis. There is no cure for herpes infection currently, as neither vaccines nor antiviral drugs can affect the latent virus.

HSV-1 virion structure

The herpesvirus virion is composed of four elements (Fig. 1.1A): a core containing a linear double-stranded DNA genome, an icosahedral capsid protecting genetic material, a tegument protein matrix surrounding the capsid, and an outer lipid bilayer envelope. The HSV-1 particle is approximately 186nm in diameter (73, 169). Twelve different viral glycoproteins and at least 2 nonglycosylated proteins are embedded in the envelope (170). The tegument contains around 20 different proteins and is largely unstructured. Abundance of individual components varies from 100 to 2000 copies per virion (74, 112). The 125nm diameter capsid is not centrally positioned (73). It is composed of 150 hexons and 12 penton capsomeres, which are composed of four proteins. VP5, the major capsid protein, is present in five copies in each penton and six copies in hexon (179). Six copies of VP26 form a ring on the top of VP5 in each hexon (240). The adjacent capsomers are linked together by triplexes formed by one copy of VP19C and two copies of VP23 (239). There are also a number of minor capsid-associated proteins such as U_L6 protein and VP24; they are not capsid building blocks, but are involved in DNA encapsidation (209, 222).

Genome organization

The 152 Kbp genome of HSV is packed in a liquid crystalline array in the capsid (16). As represented in Fig 1.1B, it contains two covalently linked segments of nonrepeated DNA designated unique long (U_L) (128 Kbp) and unique short (U_S) (25 Kbp) (169). These unique components are flanked by inverted repeats of DNA designated R_L and R_S respectively. A common nomenclature for HSV genes refers to their

A

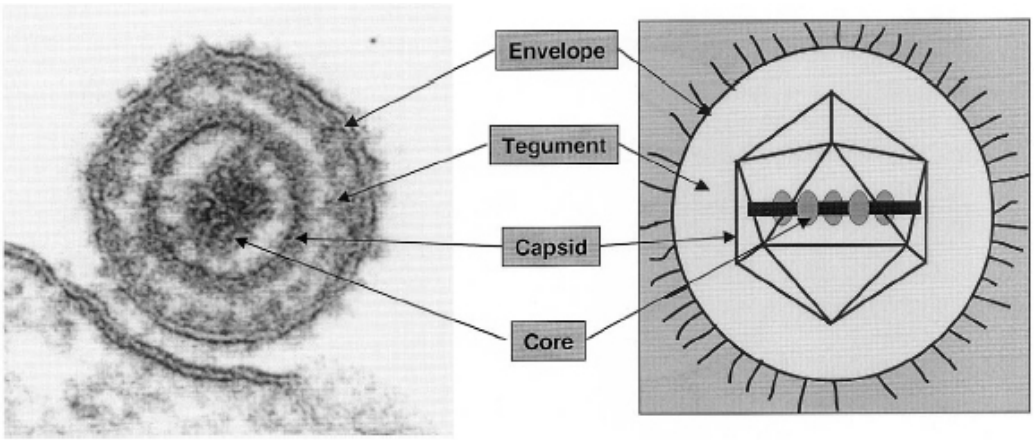

B

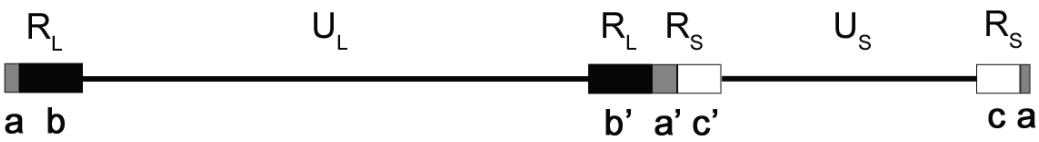

Figure 1.1 Structure of herpes virion and viral genome. (A) Electron micrograph (left) of a herpesvirus particle and schematic representation (right) of virion structural components [reprinted from reference (124)]. **(B)** Schematic illustration of HSV genome. The genome is divided into a U_L and U_S region. The unique sequences are separated by inverted repeats (shown as boxes and designated as R_L and R_S).

location in the genome, e.g. U_L1-56, U_S1-11. Genes mapped within the inverted repeats are present in two copies e.g. ICP4 (R_S1).

The R_L sequences can be more specifically indicated as ab at the genome terminus and b'a' in the opposite orientation at the L/S junction, whereas R_S is represented as a'c' and ca. More than one "a" sequence can be present in the terminal R_L, while the terminal R_S invariably contains a single "a" sequence (220). The "a" sequence structure is highly conserved but its sequence composition and size vary from strain to strain. The "c" sequences harbor two copies of a viral DNA replication origin (oriS). A third origin, oriL, was identified in the middle of the U_L component. The three origins function redundantly such that deletion of oriL or both oriS have only slight impacts on viral replication (5, 169).

Until now, more than 90 unique transcriptional units have been identified on both strands of the genome; 84 of them encode proteins (170). Of the proteins potentially encoded, it is estimated that more than 40 accompany the viral particle itself, while the remainder are thought to modulate infectivity. With few exceptions, most viral genes do not contain introns and each produces a single protein (169). So far, more than two gene clusters have been noted. For example, a set of beta genes involved in viral DNA synthesis is located near the oriL, and a set of gamma genes encoding glycoproteins is positioned within the U_S component (170).

HSV-1 replication

HSV infection begins when virus penetrates into a host cell by fusion of its envelope with the cell membrane. The de-enveloped particle is then transported to the nuclear pore, through which genomic DNA is released into the nucleus for transcription and genome replication. Assembly of new capsids and genome packaging take place in the nucleus. Following that, nucleocapsids bud across the nuclear membrane into

the cytoplasm, where they acquire tegument and viral envelopes at the Golgi network to become a mature virion. Afterwards, the progeny virus can be released into the extracellular space by exocytic vesicle transport, or can spread to neighboring cells through virus-induced cell fusion or direct cell-cell spread.

Viral entry

Two pathways coexist for HSV to enter cells, but which serves as a primary route is cell-type dependent (65). In cells like Hep2 cells, Vero cells and neurons, viral entry is mainly mediated by direct fusion at the plasma membrane and subsequent release of the capsid into cytosol. For keratinocytes and HeLa cells, the virus is first endocytosed and later fuses with the membrane of endosomal vesicles (141). Whatever pathway is used, recognition of and binding to target cells and subsequent fusion are key events, which depend upon interactions between cell surface receptors and viral glycoproteins on the viral envelope. By current count, there are at least 12 glycoproteins on the viral envelope, and four of these glycoproteins: gB (U_L27), gD (U_S6), and the complex of gH (U_L22) and gL (U_L1) are known to be essential for entry in both pathways (161).

Attachment to the cell surface involves at least three glycoproteins—gB, gC (U_L44), and gD. gC and gB mediate the initial interaction with cells, recognizing heparan sulfate proteoglycans (HSPGs) on the cell surface; gC is not essential for entry inasmuch as gB can substitute for gC (75). Simultaneous mutations of the HSPG-binding sites of gC and gB abolish high-affinity interaction with HSPGs and decrease the efficiency of entry (54, 115). This initial heparin-sensitive attachment to cells is relatively weak, and is followed by more stable association to enable entry; the latter step apparently requires gD. Three cellular receptors can bind gD and mediate HSV entry independently: herpesvirus entry mediator (HVEM), nectins, or 3-O-sulfotransferase-modified heparan sulfate (3-O-HS). These molecules do not act as co-

receptors for entry, and the existence of a co-receptor was not known until a recent discovery that association of immunoglobulin-like type 2 receptor (PILRα) with gB was required for entry even in the presence of HVEM (178).

The subsequent fusion of the viral envelope with the cell plasma membrane takes place at physiological pH and temperature in most cells (229), and requires the concerted action of three additional viral glycoproteins: gB, gH, and gL. Although the precise fusion mechanism is still elusive, the current model is that a homotrimer of gB and heterodimer of gH/gL comprise the core fusion machinery. The conformational switch in gD upon receptor binding brings gB and gH/gL together, and activates their fusion activities. Both gB and gH are fusogenic; they can act sequentially or they can form a complex (3, 200).

As for the endocytic entry of HSV, the same glycoproteins (gB, gD, gH/gL) are required (142). A gD receptor is absolutely needed, but it is unclear whether it requires the same receptors as those involved in the direct fusion pathway. The mode of endocytic uptake is cell-type specific and is not always clathrin-dependent. Actin rearrangement and RhoA GTPases are likely to be involved (26). In some cells, low pH is another critical trigger of fusion machinery in addition to receptor mediated activation (141).

Translocation of the capsid to the nucleus

After viral fusion, the tegument is the first to be exposed to the intracellular environment. Most of the outer tegument proteins have been shown to dissociate from the capsid upon viral entry. This dissociation is likely induced by phosphorylation through virion associated and/or cellular kinases (127). Some of the released proteins provide important functions both early and late in infection. For example, the virion host shut-off (VHS, U_L41) protein remains in the cytoplasm to selectively degrade mRNA early

in infection (52), whereas protein VP16 (U_L48) is transported into the nucleus independently of the capsid to act as immediate-early gene trans-inducing factor (αTIF), and later interacts with and blocks the pU_L41 RNase activity (11, 190).

As the majority of the tegument disassembles, the capsid then needs to be transported to the nucleus for genome replication and transcription. Diffusion alone may eventually allow delivery of the capsid to its destination. But the slow rate is clearly not compatible with the need for the capsid to travel long distances in human neurons. In this case, translocation becomes an active transport event. Studies have shown that dynein, a microtubule (MT)-based motor, is bound to capsids after entry, and these results prompted the theory that the incoming capsid is transported along the cellular microtubule network in a retrograde direction towards the nucleus (192). Other supporting evidence includes the observation that movement of incoming viral particles was blocked by microtubule depolymerizing drugs (97, 206), or by over-expression of dynamitin, a protein disrupting the dynein complex (46). However, the HSV receptors for MT motors are not yet known. A series of non-essential tegument proteins and a potential dynein binding capsid protein, VP26 (U_L35) (47), were tested for roles in incoming viral retrograde transport, but did not seem to actively participate. The tegument proteins pU_L36 and pU_L37 now emerge as candidates based on the fact that both proteins are associated with capsids as they traverse the cytosol to the nucleus (71, 111). Moreover pU_L36, but not pU_L37, is required for the anterograde transport of capsids along microtubules during the egress phase of infection (112).

When the capisd arrives in the nucleus, it docks at the nuclear pore complex (NPC). The attachment is importin-β dependent (144). Electron microscopy (EM) analyses support a mechanism in which the HSV-1 genome is rapidly and efficiently ejected from capsids bound to the nuclear pore complex, and empty capsids dissociate from the NPC after release of the genome (10, 113, 192). Experiments have also

shown that the tegument protein VP1/2 (U_L36) is critical in liberating the HSV-1 genome from the nucleocapsid. A temperature-sensitive mutation in the U_L36 gene caused capsids to accumulate at nuclear pores, but they did not release their DNA at the non-permissive temperature. After a shift to the permissive temperature, the DNA was released successfully into the nucleus (10). Recently, the VP1/2 protein was shown to be proteolytically cleaved only after capsid binding to the NPC, and inhibition of this cleavage by protease inhibitors prevented the release of viral DNA (88). It is therefore proposed that the proteolytic cleavage of VP1/2 induced by binding to the NPC translates into structural changes in the capsid pentons on a particular vertex, which might be identical to the portal of DNA entry during capsid maturation and genome packaging (138).

The transfer of the viral genome through the NPC channel also requires metabolic energy (144). A study using atomic force microscopy (AFM) analyzed interactions between HSV-1 capsid and the NPC; it revealed that the HSV-1 genome was delivered to the nucleus through the NPC central channel as a highly condensed, rod-like structure, and that translocation of the viral genome is associated with a remarkable widening of the NPC central channel (181).

Viral gene expression

Once viral DNA enters the host nucleus, it circularizes quickly without viral protein synthesis and prior to DNA replication (64, 81, 149). The DNA is circularized through joining of the genomic termini (199) by cellular DNA ligase IV and its cofactor XRCC4. This conclusion came from the observations that RNAi-mediated depletion of either protein largely inhibited the formation of circular genomes and caused significant reduction of viral DNA synthesis (131).

The viral genome is faced with an important "decision": whether to proceed to productive infection or to establish a latent infection (21). In the latent state, the viral genome is retained quiescently in the circular form as an episome associated with host nucleosomes; gene expression is repressed except for some non-encoding transcripts. In contrast, the lytic cycle is characterized by a progressive cascade of gene expression and DNA replication. In this case, the circular genome serves as a template for initial "θ" type replication followed by rolling circle replication (104).

Viral gene expression during the productive infection is highly coordinated. In general, each viral gene has its own promoter and transcription is catalyzed by RNA polymerase II (pol II) of the infected host cell (30). All genes have been classified into three categories according to their transcriptional kinetics: α (immediate early, IE), β (early, E), and γ (late, L) genes.

α genes are the first to be expressed, and are expressed optimally at approximately 2 to 4 hours post infection. Their promoters harbor multiple binding sites for cellular transcriptional factors, such as a TATA element, CAAT elements, and SP1 binding sites (223). Their transcription does not require other *de novo* synthesized viral proteins, but are distinctively regulated by the tegument protein VP16 (U_L48), which is translocated into the nucleus upon release of the tegument after viral entry. In the nucleus, VP16 forms a complex with host transcription factors Oct-1 and HCF (Host Cell Factor). Oct-1 specifically binds to the characteristic element TAATGArAT in the upstream region of all α gene promoters, and enables VP16 to exert its transcriptional activation functions through promoting the formation of pol II preinitiation complexes on the promoters (114).

α gene products include ICP0 (R_L2), ICP4 (R_S1), ICP22 (U_S1), ICP27 (U_L54), ICP47 (U_S12) and $U_S1.5$. Excluding ICP47, the other five α proteins have been implicated in stimulating β and γ gene expression. In particular, ICP4 is required for all

post-α gene expression (27, 45), and its effect is exerted at the transcriptional level (68). ICP4 is also responsible for down regulation of α products including itself and ICP0. In this case, specific consensus binding sites appear to be responsible for ICP4 mediated repression (66, 98). ICP0 is a nonspecific transactivator of α, β, and γ genes (170). It promotes viral infection and gene expression, especially at a low multiplicity of infection (MOI) where its absence leads to a 100 fold decrease in virus yield (187, 198). The shut-off of α genes involves auto down regulation (e.g ICP4), and also re-pression mediated by β and γ products (169).

β genes produce proteins involved in viral DNA replication (219), such as a sin-gle stranded DNA binding protein ICP8 (U_L29) and viral DNA polymerse pU_L30. The transcription of β genes starts at 3 hours post infection and reaches peak rates between 4 to 8 hours post infection (169). Its activation requires at least the presence of func-tional ICP4 but not viral DNA synthesis (223). Soon after the production of β proteins, viral DNA replication ensues.

Efficient levels of γ gene transcription require α and β products including ICP4, ICP22, ICP27, and ICP8, and also the synthesis of viral DNA. γ genes predominantly encode proteins comprising the virion particle, and have been subdivided into two groups based on timing of expression and their dependence on viral DNA replication: The expression of γ1 (leaky-late) genes does not require accumulation of viral DNA synthesis whereas the expression of γ2 (true late) genes is entirely dependent on DNA replication (219). Typical γ1 products include the major capsid protein VP5, gB, and gD; and typical γ2 proteins include gC, pU_L41 (VHS), and pU_L36.

DNA replication

Once β proteins are expressed, several proteins localize to the nucleus where they assemble on the parental viral genome to promote DNA replication. The initial round

of replication starts on the circular viral DNA molecule, creating a "θ" structure. At some point, the replication pattern switches to a rolling circle mechanism and produces head-to-tail concatemers of progeny DNA (82). Seven viral proteins are necessary for viral DNA replication. These are the viral DNA polymerase (pU_L30) (154) and its processivity factor (pU_L42) (29), an origin binding protein (pU_L9), the single stranded DNA binding protein (ICP8), and the helicase-primase complex of three proteins, pU_L5, pU_L8, and pU_L52 (22, 231). Host factors also participate in the replication event. For example, the host DNA polymerase α-primase, DNA ligase, and topoisomerase II are certainly required.

There are three replication origins in the viral genome: *oriS*, a 45 bp palindromic sequence located in "c" sequences of the genome and present in two copies; and *oriL*, also a palindromic sequence of 144 bp mapped between the U_L29 and U_L30 genes (34, 108, 224). However, only one origin is required for replication to occur (79, 151). The reason for the presence of three redundant replication origins is unclear. It may reflect the evolutionary history of the virus (169), and the *oriL* may be important for replication and reactivation from latency in certain types of tissue (7).

The basic model for HSV genome replication proceeds as follows. First, U_L9 protein binds to the origin sequences and unwinds the viral DNA by its helicase activity. ICP8 is then recruited by pU_L9 and binds to the single stranded DNA of the unwound portion. Next, the remaining five proteins (pU_L5, pU_L8, pU_L52, pU_L30, and pU_L42) are targeted to the origin by pU_L9 and ICP8. They assemble into a helicase–primase complex and viral DNA polymerase complex to initiate "θ" form replication. The reaction takes place at one or more origins and proceeds bidirectionally. Through an unknown mechanism, replication switches from the "θ" form to a rolling circle form, and U_L9 protein is no longer required for rolling circle replication; such replication is not origin dependent. The rolling circle replication generates long head-to-tail con-

catameric DNA complexes, which become cleaved into individual units during packaging of viral DNA into progeny capsids (170).

It is well known that the parental HSV genome and associated replication proteins initially localize to sites adjacent to intranuclear structures containing components of nuclear domain 10 (ND-10) (110, 213). It has been reported that the viral DNA replication origins promoted the localization of viral genome to the ND-10 domains (193), suggesting viral DNA replication proteins may play a role in targeting viral DNA to the ND-10 structures. Alternatively, it has been shown by a more recent study that ND-10 proteins localized to viral genomes, rather than *vice versa* (53). Thus, viral DNA and replication proteins initially localize to other intranuclear sites and induce redistribution of pre-existing ND-10 proteins leading to formation of novel ND-10 bodies located at sites containing viral genomes.

HSV genome replication initiates at punctate ICP8 foci near the ND-10-like structures (116), and these foci are named "pre-replicative sites". As DNA replication progresses, the pre-replicative sites expand and coalesce to form replication compartments (33, 193, 203) that eventually fill the nucleus. At this point, replication takes place in "replication compartments" that consist of accumulating DNA molecules and replication complexes (158). It has been reported that this compartmentalization of viral proteins is necessary for efficient viral DNA replication as well as late gene transcription (121).

Capsid assembly

After the onset of viral DNA replication, the γ genes are transcribed, including those that encode viral capsid proteins. In the nucleus, these proteins assemble into closed shells with an internal scaffold; viral DNA is then inserted into the capsids and the internal scaffold is expelled giving rise to a mature nucleocapsid. In the infected

nucleus, there are four types of capsids with morphological differences that can be distinguished by electron microscopy (EM): procapsids and type A-, B-, and C-capsids (134). Although the procapsid contains an internal scaffold, it is morphologically distinct from all other capsids because of its porous and roughly spherical appearance (134, 208). A-, B- and C-capsids share a common angularized icosahedral structure of approximately 120 nm in diameter. A-capsids contain only an icosaheral shell without the scaffold. B-capsids contain a spherical internal scaffold but no DNA. The C-capsid is the mature nucleocapsid; it contains DNA and lacks the scaffold (16, 179, 241).

The procapsid has been widely accepted as the precursor of all capsid types; its formation requires interactions of the major capsid protein VP5 (U_L19), triplex proteins VP19C (U_L38) and VP23 (U_L18), and a scaffold protein VP22a ($U_L26.5$) (39, 135, 136). Although the final assembly occurs in the nucleus, some initial interactions take place in the cytoplasm (140, 165). VP5, VP23, and the hexon outer tip protein VP26 are not capable of nuclear localization on their own. However, VP5 can be transported into the nucleus by the triplex protein VP19C and/or by the uncleaved precursor form of scaffold protein VP22a, pre-VP22a. VP23 nuclear localization is VP19C dependent, while VP26 nuclear import requires the presence of both VP5 and VP19C or pre-VP22a (140, 165). Once in the nucleus, VP5/pre-VP22a complexes come together as a result of self assembly of pre-VP22a. The triplex proteins VP19C and VP23 are then added to form a partial capsid. As hexons and pentons are added, the structure assembles into a round procapsid (134). In the procapsid, the internal scaffold is composed of many copies of the pre-VP22a protein encoded by $U_L26.5$ gene, and another unprocessed protein encoded by U_L26. The $U_L26.5$ transcript initiates within the U_L26 gene and is in the same coding frame. As a result, the U_L26 protein shares its C-terminal sequence with $pU_L26.5$ (i.e. pre-VP22a). It is this C-terminal domain that mediates the interactions with VP5 and leads to incorporation of the scaf-

fold proteins into the capsid structure during assembly (37, 78, 221). Uniquely, the pU_L26 possesses an N-terminus with intrinsic protease activity. Upon activation, it cleaves itself at two sites and produces two functional units, a serine protease VP24 and a scaffold protein VP21; it also cleaves pre-VP22a into VP22a (148, 222). The procapsid undergoes a structural transformation and becomes polyhedral around the time that the internal scaffold proteins are cleaved (25, 183). The protease activity is required for capsid assembly (63), and its role is presumably to release the capsid shell from constraints that preclude maturation into more angualrized capsid forms. A do-decamer of U_L6 proteins is also assembled onto the procapsid through interactions with $pU_L26.5$ to form a portal structure that is required for DNA packaging (133, 139, 147).

In the current view, A-, B- and C-capsids are considered to be three different outcomes of the procapsid maturation pathway. A-capsids arise when DNA is not inserted or not retained but the internal scaffold is lost or degraded. B-capsids arise as DNA is not inserted and the internal scaffold is trapped within the capsid. C-capsids are the only capsids to contain properly packaged with DNA; their internal scaffold is released and the DNA is sealed inside by the conformational changes in the capsid shell.

DNA packaging

Encapsidation of HSV DNA is a process in which cleavage of unit length viral genomes from concatamers is tightly coupled to their packaging into preformed capsids. It has been observed that viral DNA cleavage does not occur in cells infected with viruses that fail to produce capsids, suggesting that capsids contain essential parts of the cleavage/packaging machinery (36).

The cleavage and packaging machinery is complex and requires seven viral proteins pU_L6, pU_L15, pU_L17, pU_L25, pU_L28, pU_L32, and pU_L33 (5, 170). They interact

with the capsid either during capsid assembly or in the course of DNA packaging (5). As described above, viral DNA is believed to enter the capsid through a ring-shaped portal formed by 12 copies of U_L6 protein located at one vertex of the capsid (137).

By analogy with bacteriophage DNA packaging systems, the terminase complex comprising pU_L15, pU_L28 and pU_L33 drives the HSV genome into the capsid with energy provided by ATPase activity. The terminase also functions to cleave the concatemeric DNA to yield a monomeric genome. Supporting evidence for this proposition includes sequence similarity between pU_L15 and the large subunit of bacteriophage T4 terminase, the ability of pU_L28 to bind to the viral DNA packaging signals, and the interaction of pU_L15 and pU_L28 with the portal protein pU_L6 (2, 32, 225, 237). Within the complex, direct interactions have been characterized between pU_L15 and pU_L28, and also between pU_L28 and pU_L33, but not between pU_L15 and pU_L33 (1, 12, 83, 95, 96, 233). A recent study suggested that the three proteins assemble in the cytoplasm and are transported into the nucleus by the nuclear localization signal (NLS) of pU_L15 (234).

The final step of DNA packaging is “capsid completion”. This term refers to the formation of a stable DNA-containing capsid. Earlier studies have indicated that the U_L25 protein of HSV-1 is not required for cleavage of newly replicated viral DNA but is necessary for stable encapsidation. It was suggested that pU_L25 may function as a head completion protein or plug which seals the portal channel after DNA packaging (120). pU_L25 has also been reported to interact with the capsid shell and viral DNA, further suggesting a role in anchoring of the genome to the capsid (143). The addition of pU_L25 to the capsid is proposed to occur in response to the release of the internal capsid proteins (182).

The functions of pU_L17 and pU_L32 are less well defined. The infection of U_L17 or U_L33 null HSV-1 mutant shows a common phenotype: newly replicated concate-

meric DNA is not cleaved into unit-length genomes, and, accordingly, in infected cell nuclei no C capsids are detectable while scaffold-containing B capsids accumulate and mislocalize (101, 176, 202). These observations have suggested pU_L17 and pU_L32 are involved in properly targeting capsids to viral DNA replication compartments for encapsidation. More light has been cast recently on pU_L17 with the finding that pU_L17 appears to bind to pU_L25 on C-capsids, thus implying a role in stabilizing the capsid-DNA structure (204, 210).

The cleavage of viral DNA also needs cis-acting elements in the viral genome. Two signal segments designated *pac1* and *pac2* in the "a" sequence define the cleavage sites (35, 191, 216). It is proposed that the packaging complex binds to the DNA concatemer and scans for the first pac2 site in proper orientation. Cleavage occurs at a fixed distance from pac2, generating the L end of one genome that is inserted into the capsid. As the DNA engagement continues, the complex keeps scanning the following DNA until a directly repeated junction is encountered. Then a second cleavage is executed to produces a monomeric genome.

Viral egress

After the viral genome is packaged, nucleocapsids exit the nucleus, become enveloped virions in cytoplasm, and eventually gain access to the extracellular space. Enveloped capsids have been observed in the perinuclear space between the inner and outer nuclear membrane (INM and ONM, respectively), and this led to two proposed models of viral egress. The first model (Fig 1.2), also called the "double envelopment" pathway, proposed that nucleocapsids are enveloped at the INM, become de-enveloped by fusion of the virion envelope with the ONM, and then undergo secondary envelopment at cytoplasmic membranes. These virions are transported in vesicles to the plasma membrane and are released into the extracellular space through fusion

between the vesicle membrane and plasma membrane (51, 123). In the second model, known as the "single nuclear envelopment" pathway, the capsids acquire the initial envelope at the INM, enter into a vesicle at the ONM, and retain their primary and final envelope as they leave the cell through the secretory pathway (19, 86). In this model, virion glycoproteins are modified in transit to the plasma membrane and perinuclear virions should contain the entire complement of tegument and envelope proteins present on mature extra-cellular virions. However, this model is inconsistent with multiple lines of evidence. First, according to electron microscopic examinations, the primary envelope and primary tegument in perinuclear virions clearly differ in ultrastructure from the final envelope and tegument in cytoplasmic and extracellular virions (67, 70). Second, biochemical studies revealed compositional differences between perinuclear virions and extracellular virions. In an HSV-1 mutant, when gD was retained in the endoplasmic reticulum (ER), gD was detected on the perinuclear virions but was absent from extracellular virions (188). Moreover, pU_L34 and pU_L31 are components of perinuclear virions, but are missing in extracellular ones (163), whereas the major tegument protein pU_L49 is associated with cytoplasmic and extracellular virions but not with perinuclear particles (94). Moreover, the phospholipid composition differs between the envelope of extracellular HSV-1 virions and the host cell nuclear membrane (214). All of these differences can only be explained by the two-step envelopment model.

Alternatively, a third model was suggested by a recent report. Wild et al. observed that, in bovine herpesvirus-1 infected cells, nuclear pores were dilated to a size readily allowing capsids to pass through (228); and so they proposed that virus exits the cell via a "dual pathway single envelopment" model (105). In this model, a minor

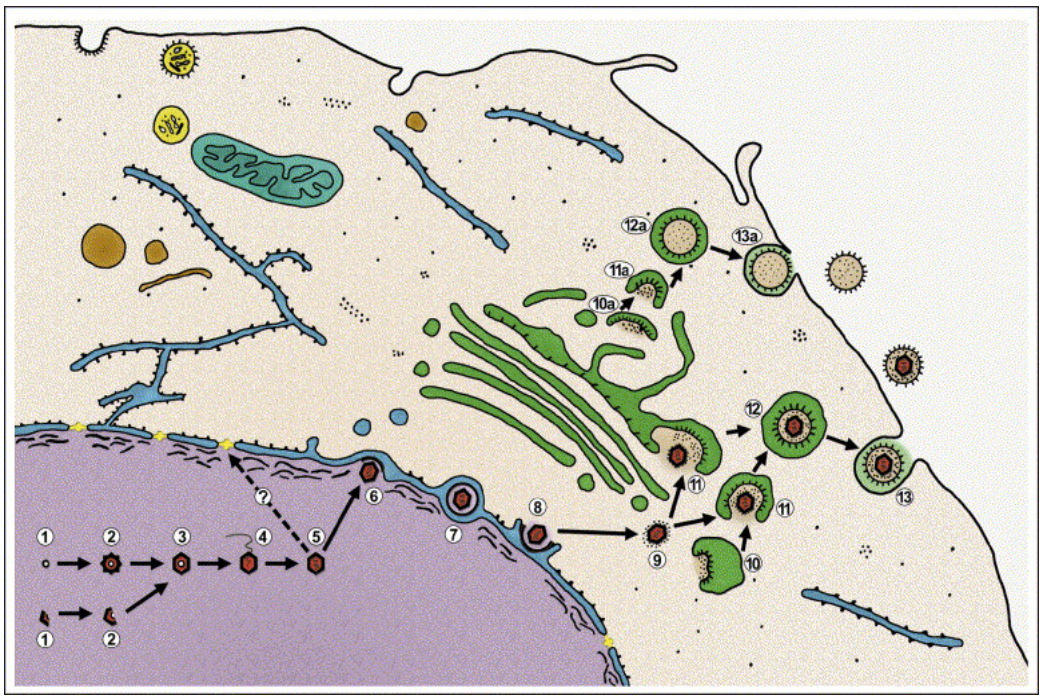

Figure 1.2 Diagram of herpesvirus egress pathway [reprinted from reference (125)]. In the nucleus capsids assemble around a scaffold (1 – 3), then DNA is packaged (4) into preformed capsids. DNA-filled capsids (5) contact the inner nuclear membrane at the sites where the nuclear lamina has been locally dismantled (6), bud into perinuclear space resulting in enveloped primary virions (7). The primary envelope fuses with the outer nuclear membrane (8), releasing the nucleocapsid into the cytosol where capsid-proximal tegument proteins assemble onto the capsid (9). Concurrently at the trans-Golgi apparatus, glycoproteins and outer tegument proteins assemble together (10). Two subassemblies join to complete the final envelopment (11) and the mature virion is then transported in a vesicle (12) to the plasma membrane for release (13). (10a – 13a) Formation and release of capsid-free particles.

population of capsids egress via a "single nuclear envelopment" pathway early in infection, whereas the majority exit the nucleus through enlarged nuclear pores, become enveloped in the cytoplasm and are released by secretory vesicles. At face value, this model could also be compatible with the above results supporting the "double envelopment" model. Nevertheless, it faces challenges that have not been resolved at this time. For instance, an HSV-1 defective in U_S3 kinase induced accumulation of enveloped virions in the perinuclear space and slowed viral production, indicating at least capsid budding into the perinuclear space is not a minor egress pathway (174).

Nuclear egress

HSV nuclear egress is a complex process, involving interactions of viral proteins and cellular components. Nucleocapsids initiate the event by budding at the inner nuclear membrane (INM), acquire INM-derived envelope (specified as the primary envelope), and translocate into the perinuclear space. De-envelopment occurs when the primary envelope fuses with the outer nuclear membrane (ONM); capsids are then released into cytoplasm.

Primary envelopment at the INM

It is believed that DNA packaging is a prerequisite for nuclear egress of capsids. In wild type virus infections, a preference has been noted for primary envelopment of C-capsids over other non-DNA-containing capsid forms. The mechanism underlying this preferential envelopment of C capsids is unclear. In an early study, the conserved capsid-associated protein pU_L25 was suggested to play a role in this process (197); more recently, the pU_L25 homolog in pseudorabies virus was found to be necessary for the nuclear egress of capsids (92). However, no capsid nor capsid-associated protein has been identified so far that physically interacts with the egress complex (pU_L31/pU_L34) to drive primary envelopment. DNA-filled capsids move from in-

tranuclear assembly sites to contact the inner nuclear membrane prior to primary envelopment. This intranuclear transport of HSV-1 capsids appears to be actin dependent, inasmuch as it could be inhibited by latrunculin B (60). This is additionally supported by the finding of actin filaments in the host cell nucleus induced by HSV-1 infection (58).

Two HSV-1 proteins, pU_L31 and pU_L34 are required to initiate the primary envelopment at the INM (163). Analysis of U_L31 and U_L34 deletion mutants has indicated that the absence of either protein results in a drastic impairment in primary envelopment with capsids trapped within the nucleus (24, 62, 94, 163, 173). The U_L34 or U_L31 null viruses failed to replicate on most non-complementing cell lines. An exception is that rabbit skin cells were permissive to U_L31 null virus to a limited extent (107).

pU_L31 and pU_L34 are highly conserved in the herpesviridae family. pU_L34 is predicted to be a type II integral membrane protein with a 22 amino acid transmembrane domain at the C-terminus (157, 173, 184), while pU_L31 is a nuclear phosphoprotein (23). In wild type virus infected cells, pU_L31 and pU_L34 co-localize on the nuclear rim. In the absence of pU_L34, pU_L31 is exclusively intranuclear, whereas without pU_L31, pU_L34 redistributes to the ER, although the protein appears to possess an intrinsic nuclear targeting signal (94, 163). Physical interaction between the two proteins has been demonstrated; and a 50 amino acid region of pU_L34 is known as an essential domain interacting with pU_L31 (106). It is very clear that the complex formation of two proteins is important for proper positioning of both partners at the inner nuclear membrane, which is a prerequisite for primary envelopment (163). Both proteins are incorporated into the perinuclear virions, but are likely lost at the ONM through de-envelopment (164).

The pU_L31/pU_L34 complex is considered to act as a membrane receptor for capsids to recognize, bind, and then bud into the perinuclear space. However, it is unclear whether additional viral or cellular proteins are required in this process. In an *in vitro* system, reconstruction of nuclear egress required cytosol, whereas infected cytosol was not necessary (160). This data strongly implied involvement of host factors. In another study, co-expression of pU_L31 and pU_L34 induced vesicles to form from the INM in the absence of viral infection; those vesicles resembled primary envelopes without a nucleocapsid (91). This also argues for the contribution of cellular factors in the budding reaction. Such factors might be recruited from their natural cytoplasmic location, or were previously unrecognized in the nucleus.

Alteration of the nuclear lamina has been observed after HSV infection and may be required so that the inner nuclear membrane is accessible to capsids (103, 162, 180). Multiple lines of evidence indicate that pU_L31 and pU_L34 play a role in lamina modification. Over expression of pU_L31 alone was sufficient to relocalize lamin A/C from the nuclear rim into nucleoplasmic aggregates, whereas over-expression of pU_L34 causes some lamin A/C redistribution into the cytoplasm (162). More importantly, both pU_L31 and pU_L34 are able to directly bind lamins A/C and/or B, suggesting that pU_L31 and pU_L34 modify the conformation of the nuclear lamina in infected cells, possibly by direct interaction with lamin proteins (69, 162). Given that the nuclear lamina potentially excludes nucleocapsids from envelopment sites at the inner nuclear membrane, the lamina alteration may reflect a role of the pU_L31/pU_L34 protein complex in perturbing the lamina to promote nucleocapsid egress from the nucleus. Lamins A/C and B appear to participate in viral infection in different ways; their respective roles are covered in more detail in Chapter III,

In addition, the complex can also recruit protein kinases to modify the lamina. Cellular protein kinase C (PKC) is enriched on the nuclear rim in a pU_L31/pU_L34-

dependent manner, which in turn phosphorylates lamins A/C and/or B (130, 146). This could result in local dismantling of the lamina network and the underlying chromatin layer (185), enabling the capsids to access the inner nuclear membrane. Viral encoded kinases are also involved in this process. The U_L13 kinase of human cytomegalovirus (HCMV) is targeted to the lamin B receptor via interaction with cellular protein p32, causing redistribution of lamins A/C and B (115). In a pU_L34-dependent manner, HSV-1 U_S3 kinase hyperphosphorylates emerin, a lamin-interacting nuclear membrane protein, and induces localizational changes of this protein (103). This kinase has also been found to phosphorylate lamin A/C during infection, as reported in Chapter II. Transient expression of pU_S3 alone is sufficient to disrupt the nuclear lamina (15).

The U_S3 kinase also assists pU_L31/pU_L34 in proper positioning, and is needed for efficient nuclear egress. Deletion or deactivation of the kinase induces aggregation of pU_L31/pU_L34 on the nuclear rim in infected cells, and results in a delay in viral production, but has little effect on the final peak yield of infectious virus (164, 174). Electron microscopic examinations of cells infected by a U_S3-defective HSV mutant have revealed perinuclear virions that accumulate in invaginations of the inner nuclear membrane (164, 174). These structures are assumed to form as a result of delayed perinuclear virion de-envelopment, and they appear to cause restriction of nucleocapsid envelopment to certain sites within the inner nuclear membrane. Therefore, U_S3 kinase activity modulates pU_L31/pU_L34 distribution in the nuclear membrane as well as the fusion of the primary envelope with the outer nuclear membrane.

pU_S3 is a PKA-like serine/threonine kinase (14, 155). Interestingly, both pU_L31 and pU_L34 are phosphorylated by pU_S3 *in vivo* (89, 156). Although the catalytic relationship between pU_S3 and pU_L34 has been examined in details, the phosphorylation of pU_L34 is not demonstrably important to nuclear egress (174). Instead, I show in

Chapter IV that pU_L31 is a functionally important downstream effecter of the U_S3 kinase.

De-envelopment at the ONM

Several glycoproteins have been identified as components of the perinuclear virion, including gD, gB and gM (6, 188, 195, 207). It is reasonable to assume that the fusion of the primary envelope with the ONM is conducted by the same set of glycoproteins involved in entry and other fusion events. In earlier studies, however, deletion of these major glycoproteins required in other membrane fusion did not affect the de-envelopment process (18, 70, 84). The core fusion machinery of the perinuclear virion has been elusive. Recently, an HSV-1 mutant lacking both gB and gH produced a large number of perinuclear virions, indicating a failure of de-envelopment, whereas a single deletion of either gene had no detectable effect on the de-envelopment process (56). This observation indicates that fusion relevant to nuclear egress requires both gB and gH, and these proteins function in a redundant manner. It also suggests that fusion during nuclear egress is mechanistically different from that of viral entry, because in the latter, both gB and gH are required and are not functionally redundant.

Tegumentation in the cytoplasm

After translocation into the cytoplasm, capsids undergo tegumentation and secondary envelopment through a highly ordered network of protein-protein interactions. The tegument proteins interact with the capsid on one side and with the viral envelope proteins on the other in order to link the structural components to the final envelope of the HSV-1 virion and to secure the integrity of the virus particle (123). It has become clear that final tegumentation can initiate at two different sites, the capsid and the future envelope, resulting in two "subassemblies" that combine to produce a mature virion (125).

The first layer of tegument around the capsid is composed of pU_L36 and pU_L37. pU_L36 has been shown to interact with the major capsid protein VP5 (139, 238), whereas pU_L37 is likely incorporated via interaction with pU_L36 (90). pU_L36 and pU_L37 are the only tegument components conserved in the Herpesviridae family. The absence of pU_L36 and pU_L37 abolishes virus maturation (38, 40). The level of these proteins in the virion is strictly controlled, whereas stoichiometry of outer tegument proteins can vary extensively (126). As mentioned in a previous section, pU_L36 and pU_L37 remain associated with incoming capsids while outer tegument proteins disperse after viral entry (71, 111), and are involved in intracytoplasmic transport of capsids during entry and exit (112, 230). Besides these conserved components, other non-conserved proteins might also be components of the inner tegument. For instance, pU_S3 is also encompassed in the capsid-proximal tegument.

Concurrently, at the final envelopment site in the trans-Golgi network, another subset of tegument proteins including pU_L46, pU_L47 and pU_L49, are assembled together with viral glycoproteins (211). Viral glycoproteins are recruited to cytoplasmic envelopment sites by an envelope protein gM, which is also thought to retain other glycoproteins at the envelopment site, or to retrieve them from the cell surface (31). Tegument proteins may also be recruited by a small myristoylated protein pU_L11, which has intrinsic targeting properties to the Golgi apparatus (17, 109).

The capsids coated with pU_L36 and pU_L37 are then transported to the cytoplasmic envelopment site where the remaining tegument and envelope glycoproteins await them. Although it is not yet clear which proteins form the bridge between the two subassemblies, some experiments indicate that pU_L48 (VP16) may play a role in this process (62, 218). pU_L48 has been shown to interact with tegument proteins pU_L49 and pU_L41 (VHS) (189). Mutant forms of pU_L41 that do not bind pU_L48 fail to be-

come incorporated into the virion (159). Cross-linking studies have indicated interactions between pU_L48 and gB, gD, and gH (242).

Secondary Envelopment and release

Following tegumentation, HSV-1 capsids bud into cytoplasmic vesicles derived from the trans-Golgi Network (TGN) or endosomes by wrapping the membranous cisterna around the capsid to form a mature herpesvirus particle within a cellular vesicle. This vesicle is then transported to the plasma membrane. After fusion of the vesicle and plasma membrane, the nascent virion is released into the extracellular space.

Studies of viral mutants have shed light on the roles of certain viral envelope proteins in this event. As revealed by EM, HSV-1 mutants lacking either U_L20 or gK produced dramatic accumulations of un-enveloped and aberrantly enveloped capsids in the cytoplasm with a marked absence of extra-cellular virion (61, 84). A triple mutant lacking gD, gE, and gI had a severe defect in the final envelopment step. It is proposed that gD and the gE/gI heterodimeric complex act in a redundant fashion to anchor the virion envelope onto tegumented capsids (54). In contrast, it is also possible that deletion of multiple glycoproteins indirectly disrupts the integrity of many different protein protein interactions required for the final envelopment step and that the resulting phenotype results from the compound effects of an abnormal glycoprotein profile.

Secondary envelopment does not require the presence of capsids. Capsid-free particles can be formed by enclosing tegument proteins in an envelope in a process mimicking normal capsid envelopment (119, 166). These structures are called light (L) particles. These particles form in abundance in cells infected with particular mutant viruses, in which normal capsid assembly and tegument formation is inhibited (119, 166). This demonstrates that capsids are not required to trigger secondary envelopment. It has been proposed that normal tegumentation requires pU_L36 and pU_L37 in-

teractions with the capsid and that pU_L49 may be required for proper interactions with viral glycoproteins in the final envelopment step (123). In the absence of capsids, tegument assembly could be mediated through U_L49 anchoring, resulting in the formation of L particles.

The release of nascent virions following final envelopment mimics the cellular secretory pathway. Viral proteins are apparently involved, although their functions in this particular step remain elusive. It is also known that the late stages in viral egress may differ depending on the cell type (85, 125). For example, in polarized epithelial cells, wild type virions are sorted predominantly to cell junctions, whereas gE/gI null virions are released nonspecifically into the extracellular space (44).

Cell-cell spread

Dissemination of HSV occurs via both the release of progeny viruses into the extracellular environment and direct cell-to-cell spread. In the process of cell-cell spread, nascent virions are targeted to cell junctions that contact neighboring cells. These virions are then released and bound immediately by the adjacent cell for internalization (85). In the host, HSV disseminate mostly by spreading from cell to cell. This strategy is expected to enhance viral spread and enable viruses to avoid host immune defenses.

The glycoproteins that are required for HSV cell-cell spread are gB, gD, gH/gL and gE/gI (85). The requirements for gD and its receptor as well as gB and gH/gL parallel those involved in entry of cell free virions. gE and gI, although not required for entry of cell free virions, are important in promoting HSV cell-cell spread (150, 175). Viruses lacking gE or gI cause no disease in rodents and produce smaller plaques in culture compared to wild type virus (43). Subsequent studies showed that gE/gI is involved in routing virions to the basolateral surfaces of polarized cells (55, 87). It is proposed that gE/gI is concentrated at cell junctions through interaction with

an as-yet-unidentified extracelluar ligand, and so diverts viral trafficking from apical to basolateral membranes (150). Moreover, the enrichment of nectins at junctions of neurons and epithelial cells, coupled with the ability of gD to bind them, suggests an alternative mechanism by which virions are directed towards the neuronal terminal (85).

In addition, cells infected by HSV-1 or PRV can form extended protrusions to contact neighboring cells and deliver virions to the contacted cell (57, 100, 215). These F actin-associated structures can be induced by U_S3 kinase in PRV and can be reproduced by inhibition of the Rho-associated kinase (ROCK) when pU_S3 is absent (57).

Brief outline of dissertation research

The goal of the work herein was to shed some light on the machinery of HSV nuclear egress. With the proposal that viral U_S3 kinase phosphotylates viral and/or cellular fators to regulate the capsid primary envelopment at the INM and subsequent de-envelopment at the ONM, several putative substrates of pU_S3 were identified and the functional relevance of their catalytic relationships was evaluated. In Chapter II, the distribution of lamin A/C was observed to be modified by pU_S3 kinase activity, and lamin A/C was identified as a substrate of the kinase. Therefore I hypothesized that lamin A/C might be the factor required for pU_S3 functions. However, this hypotheis was not favored by the data shown in Chapter III, where I examined the respective roles of lamin A/C and lamin B1 during viral infection. Finally, in Chapter IV, I determined that pU_L31 is a major substrate mediating pU_S3 regulatory effects, and found the phosphorylation of pU_L31 to be a dynamic event during nuclear egress.

CHAPTER II

U_S3 OF HERPES SIMPLEX VIRUS TYPE I ENCODES A PROMISCUOUS PROTEIN KINASE THAT PHOSPHORYLATES AND ALTERS LOCALIZATION OF LAMIN A/C IN INFECTED CELLS*

Fan Mou, Tom Forest, and Joel D. Baines

Department of Microbiology and Immunology, College of Veterinary Medicine

Cornell University, Ithaca, NY 14853

* Reprinted from **Mou, F., T. Forest, and J. D. Baines.** (2007). U_S3 of herpes simplex virus type 1 encodes a promiscuous protein kinase that phosphorylates and alters localization of lamin A/C in infected cells. J Virol 81:6459-70.

Abstract

The herpes simplex virus type 1 (HSV-1) U_S3 gene encodes a serine/threonine kinase that, when inactivated, causes capsids to aggregate aberrantly between the inner and outer nuclear membranes (INM and ONM, respectively) within evaginations/extensions of the perinuclear space. In both Hep2 cells and an engineered cell line derived from Hep2 cells expressing lamin A/C fused to enhanced green fluorescent protein (eGFP-lamin A/C), lamin A/C localized mostly in a reticular pattern with small regions of the INM devoid of eGFP-lamin A/C when they were either mock infected or infected with wild-type HSV-1(F). Cells infected with HSV-1(F) also contained some larger diffuse regions lacking lamin A/C. Proteins U_L31 and U_L34, markers of potential envelopment sites at the INM and perinuclear virions, localized within the regions devoid of lamin A/C and also in regions containing lamin A/C. Similar to previous observations with Vero cells (S. L. Bjerke and R. J. Roller, Virology 347:261-276, 2006), the proteins U_L34 and U_L31 localized exclusively in very discrete regions of the nuclear lamina lacking lamin A/C in the absence of U_S3 kinase activity. To determine how U_S3 alters lamin A/C distribution, U_S3 was purified and shown to phosphorylate lamin A/C at multiple sites in vitro, despite the presence of only one putative U_S3 kinase consensus site in the lamin A/C sequence. U_S3 kinase activity was also sufficient to invoke partial solubilization of lamin A/C from permeabilized Hep2 cell nuclei in an ATP-dependent manner. Two-dimensional electrophoretic analyses of lamin A/C revealed that lamin A/C is phosphorylated in HSV-infected cells, and the full spectrum of phosphorylation requires U_S3 kinase activity. These data suggest that U_S3 kinase activity regulates HSV-1 capsid nuclear egress at least in part by phosphorylation of lamin A/C.

Introduction

Like orthologues in other members of the subfamily Alphaherpesvirinae, the U_S3 gene of herpes simplex virus type 1 (HSV-1) encodes a serine/threonine kinase (60, 160). These proteins have been implicated in nuclear egress, prevention of apoptosis, and modulation of the actin cytoskeleton to promote the cell-to-cell spread of virions (55, 63, 85, 94, 107, 170, 176, 183, 220). The current study focuses on the role of the U_S3 gene-encoded kinase activity in nuclear egress of nucleocapsids and virions.

Although models of HSV virion egress differ as to the extent of its contribution, all models propose that at some point during the course of infection with wild-type herpesviruses, nucleocapsids assemble in the nucleoplasm and bud through the inner nuclear membrane (INM) and into the perinuclear space (87, 199, 226). This compartment is delimited by the INM and outer nuclear membrane (ONM) and is continuous with the lumen of the endoplasmic reticulum. To become enveloped, capsids must bypass the nuclear lamina, a fibrous meshwork lining the nucleoplasmic face of the INM. The nuclear lamina provides structural rigidity to the nucleus and is essential for transcription and DNA replication (73, 189). The lamina contains a series of type 5 intermediate filaments composed of lamin types A, B1, B2, and C; types A and C are products of RNA splice variants from the *Lmna* transcript, whereas types B1 and B2 are derived from other genes (57, 76, 77). Like all intermediate filaments, lamins comprise globular head and tail domains that flank a rod domain (59). The rod domains of two lamins intertwine to form protomers, whereas regions bordering the rod/head and rod/tail domains likely interact with other lamin protomers to form longer filaments (162). The globular domains interact with a variety of proteins in the lamina and INM.

One remarkable feature of the lamina is its dynamic nature. The lamina expands by the addition of protomers during interphase, is completely disassembled prior to

mitosis, and is partially disrupted during apoptosis. Phosphorylation likely plays a role in lamin dynamics in all phases of the cell cycle. The disassembly of the lamina during mitosis is associated with phosphorylation of lamin A/C by cdc2 kinase at Ser390 and Ser392 and during apoptosis by protein kinase C (PKC) delta (26, 30, 46, 150, 151). Protein kinase C can phosphorylate lamin A/C at Ser572 *in vitro* (48).

The architecture of the nuclear lamina is altered from its normal state during HSV-1 infection (13, 147, 168, 184, 190). Depending on the cell line and time after infection, these changes include (i) limited displacement and conformational changes of lamin A/C (13, 168, 190), (ii) redistribution of lamin B to a perinuclear region (147, 184), and (iii) increased mobility and mislocalization of lamin B receptor, one of several integral membrane proteins that anchor the nuclear lamina to the INM (184, 189). In attempts to understand the mechanism(s) by which the lamina becomes displaced, it was found that PKC of the alpha and delta subfamilies are recruited to the nuclear rim of HSV-1-infected cells and that lamin B becomes hyperphosphorylated during HSV infection, in part due to phosphorylation by PKC (146). Given these observations, it was postulated that HSV coopts cellular mechanisms to disrupt the nuclear lamina and thereby promotes egress of nucleocapsids (146). The state of phosphorylation of lamin A/C in HSV-infected cells is unknown, in contrast to that of lamin B. Previous analyses using one-dimensional gel electrophoresis indicated that HSV infection did not drastically alter the electrophoretic mobility of lamin A/C from human foreskin fibroblasts or from Hep2 cells, suggesting that phosphorylation is not extensive(164, 168).

As detected by immunoelectron microscopy, nascent virions located in the perinuclear space contain the U_S3 kinase and at least two of its substrates, the proteins encoded by the U_L31 and U_L34 genes (as products pU_L31 and pU_L34, respectively) (90, 156, 161, 170). The proteins pU_L31 and pU_L34 are required for efficient envelopment of nucleocapsids at the INM (22, 110, 169, 175). The observations that proteins pU_S3,

pU_L31, and pU_L34 are located within perinuclear virions and at the INM suggest that these proteins are incorporated into the virion during budding at the INM (164). Interestingly, all of the HSV-1-induced alterations in lamin A and B distribution/conformation require expression of pU_L31 and pU_L34 (13, 147, 168, 191). How pU_L31 and pU_L34 alter the structure of the nuclear lamina is not known, but the alteration likely involves multiple mechanisms. For example, both pU_L31 and pU_L34 are required for the recruitment of protein kinase C alpha and delta to the nuclear rim, and both can interact with lamin A/C in vitro (147, 168). Thus, U_L31/U_L34 might interrupt the nuclear lamina by mechanical interference with lamin-lamin interactions, by a disruption of lamin folding, by recruitment of lamina-disrupting kinases, or by all three mechanisms.

Deletion of U_S3 delays the onset of production of infectious virus and reduces peak infectious titers by approximately 10- to 30-fold with Hep2 cells (170, 176). The absence of U_S3 or its kinase activity does not preclude budding at the INM, nor incorporation of the pU_L31/pU_L34 into perinuclear virions, but causes these virions to aggregate aberrantly within the perinuclear space (94, 170, 176, 183, 220). These observations with both the HSV and the pseudorabies herpesvirus (PRV) systems have led to the conclusion that U_S3 is involved in the exit of virions from the perinuclear space into the cytoplasm (94, 170). On the other hand, if the exit from the perinuclear space was the sole contribution of U_S3 to nuclear egress, one might expect that $pU_S3(–)$ perinuclear virions would distribute evenly throughout the perinuclear space, but this is not the case. Rather, virions are tightly packed together within discrete invaginations/extensions of the nuclear membrane (NM). How U_S3 kinase activity precludes this aberrant aggregation of perinuclear virions is unknown.

In vitro biochemical studies characterized a U_S3 kinase minimal consensus sequence as (R)n-X-(S/T)-Y-Y, where n is >2, S/T is the target site where either serine

or threonine is phosphorylated, X can be absent or any amino acid but preferably Arg, Ala, Val, Pro, or Ser, and Y is similar to X except that it cannot be an absent amino acid, proline, or an acidic residue (105, 158, 159). The optimal consensus sequence is similar except that X is not absent and n is 3. Both pU_L34 and pU_L31 have one or more sequences matching this consensus motif (117). Of the known U_S3 kinase substrates localizing at the NM, the lack of phosphorylation of pU_L34 is not likely responsible for the aberrant NM morphology in U_S3 mutant-infected cells (174), whereas the role of pU_L31 phosphorylation has not yet been tested. The current studies were initiated under the hypothesis that substrates in addition to pU_L31 and pU_L34 may be involved in capsid and virion egress from the NM.

Materials and methods

Cells and viruses. Wild-type HSV-1(F) virus and a U_S3 deletion mutant virus, R7041, have been described and were obtained from B. Roizman (48, 160). Virus vRR1204, containing a mutation at U_S3 codon 220 changing lysine to alanine (K220A) in an HSV-1(F) background, was a kind gift of R. J. Roller (174). The viruses were grown and titers were determined on Vero cells as described previously (132).

An enhanced green fluorescent protein (eGFP)-lamin A/C-expressing cell line was made by transfection of DNA containing a cDNA of *Lmna* fused to eGFP-C1 and encoding neomycin resistance (a kind gift from D. Gilbert, Upstate Medical Center) into human Hep2 cells (80). Individual eGFP-positive cells were sorted based on the intensity of fluorescence determined using an ExCalibur fluorescence-activated cell sorter (FACS), into individual wells of a 96-well plate. The cells were grown in growth medium (Dulbecco's minimal essential medium supplemented with 10% fetal bovine serum and antibiotics) supplemented with 250 μg/ml Geneticin (Invitrogen).

The highest-expression cells failed to expand further, whereas some intermediate expressers and all low expressers expanded into colonies (not shown). A single clone of several, containing intermediate levels of nuclear fluorescence, was further amplified in growth medium supplemented with 50 to 250 μg/ml Geneticin and was used for further studies.

Construction of recombinant baculoviruses. Full-length U_S3 and U_S3(K220A) were PCR amplified from viral DNA of HSV-1(F) or the U_S3 mutant virus vRR1204, respectively. The PCRs used primers with a BglII restriction endonuclease site incorporated into the forward primer (5'-TAA T*AG ATC T*AT GGC CTG TCG TAA GTT TTG-3') and an EcoRI site in the reverse primer (5'-ATA T*GA ATT C*TC ATT TCT GTT GAA ACA GCG-3'; restriction sites are in italics). PCR products were then cloned into the BamHI and EcoRI sites of the pGEX4T-1 vector such that they were in frame with the gene encoding glutathione-*S*-transferase (GST). DNA in the plasmid clones was sequenced, and those clones with the proper GST-U_S3 fusions were used as templates for a second PCR to amplify GST-U_S3 and GST-U_S3(K220A). This second PCR used primer 5'-AGG C*AG ATC T*AT TCA TGT CCC CTA TAC TAG-3' containing another BglII site (italicized) and the U_S3 reverse primer. Amplicons were then subcloned into the BglII/EcoRI sites of the pBacPAK8 vector (Clontech). This construct was then transfected into insect Sf9 cells along with BacPAK6 baculoviral DNA (Clontech) according to the instructions of the BacPAK baculovirus expression system, and recombinant baculoviruses expressing the target proteins were plaque purified and amplified to produce viral stocks.

Antibodies and immunofluorescence. Polyclonal chicken antibody against pU_L34 was a kind gift from R. J. Roller (163). Chicken anti-lamin A/C polyclonal and rabbit anti-pU_L31 antisera were prepared in our laboratory and were described previ-

ously (168, 169). Lamin B-specific goat polyclonal antibody was purchased from Santa Cruz Biotechnology (catalog number sc-6218).

To characterize the localization of pU_L31 and lamin A/C in infected cells, 200 μl of rabbit anti-pU_L31 antisera was adsorbed against an acetone powder (177) prepared from approximately 2×10^8 Hep2 cells that were infected 24 h previously with a U_L31 deletion virus (107). The powder and antisera were added to 4 ml phosphate-buffered saline (PBS) containing 1% bovine serum albumin (BSA) and were mixed overnight. After centrifugation, the supernatant was passed through a 0.2-μm-pore-sized filter.

Hep2 cells growing on glass coverslips were mock infected or infected with wild-type HSV-1(F), U_S3 null, or U_S3(K220A) HSV-1 at a multiplicity of infection (MOI) of 5.0 for 16 h. Cells were fixed with 3% paraformaldehyde for 15 min, followed by treatment for 5 min at –20°C in methanol. The cells were then permeabilized with 0.1% Triton X-100 and reacted with 10% human serum in PBS to block nonspecific immunoreactivity and were subsequently probed with the preadsorbed pU_L31 rabbit polyclonal antibody diluted 1:50 in PBS supplemented with 1% BSA. Ten percent BlockHen II (Aves Lab) was used for a second round of blocking before probing with a 1:200 dilution of chicken anti-lamin A/C polyclonal antibody. Bound primary antibodies were recognized by Texas Red-conjugated donkey anti-rabbit and fluorescein isothiocyanate (FITC)-conjugated donkey anti-chicken immunoglobulin (Jackson ImmunoResearch).

In some experiments, the cell line expressing eGFP-lamin A/C was mock infected or infected as described above, fixed in 3% paraformaldehyde, and permeabilized with 0.1% Triton X-100. Epitopes were then blocked by incubation with 10% human serum in PBS for 1 h, followed by blocking with 10% BlockHen II and reaction with pU_L34-specific antisera diluted 1:200. After extensive washing, primary antibody was recog-

nized by Texas Red-conjugated donkey anti-chicken immunoglobulin (Jackson ImmunoResearch).

Images were visualized and recorded using either an Olympus or a Zeiss laser scanning confocal microscope equipped with a 488-nm argon or 568-nm krypton laser, respectively, and associated software. Digital images were exported in a tagged image file format (TIFF) to Adobe Photoshop for processing.

Purification of wild-type and mutant HSV-1 pU$_S$3. Sf9 cells were infected with recombinant baculoviruses expressing GST-pU$_S$3 or GST-pU$_S$3(K220A) and were lysed 42 hr post infection by brief sonication in ice-cold lysis buffer (50 mM Tris [pH 7.5], 100 mM NaCl, 5 mM $MgCl_2$, 0.1% NP-40, 10% glycerol) containing 1x Complete protease inhibitor cocktail (Roche). The U$_S$3 proteins were purified from the lysates by affinity chromatography using glutathione Sepharose beads (Amersham) as previously described (89). Proteins were eluted in 100 mM reduced glutathione according to the manufacturer's protocol and dialyzed into storage buffer (20 mM Tris-HCl [pH 7.5], 25 mM KCl, 0.1 mM EDTA, 2 mM dithiothreitol [DTT], 50% glycerol). Protein concentration was determined by an RC DC protein assay kit (Bio-Rad), and aliquots were frozen at –80°C.

GST fusion proteins were partially purified from *Escherichia coli* lysates, as described previously (162), and retained on the Sepharose beads without elution for reactions. Protein concentration was estimated by elution and separation by sodium dodecyl sulfate-polyacrylamide gel electrophoresis (SDS-PAGE), followed by comparison with known amounts of BSA standards stained with Coomassie brilliant blue.

***In vitro* kinase assay.** A kinase assay was performed using purified GST-pU$_S$3 or GST-pU$_S$3(K220A) essentially as described previously, with minor modifications (21). Briefly, 0.1 μg GST-pU$_S$3 or at least an equivalent amount of GST-pU$_S$3(K220A) was

incubated separately with 1 to 3 µg of partially purified *E. coli*-expressed GST fusion proteins for 30 min at 30°C in 50 µl U_S3-specific kinase buffer (50 mM Tris [pH 9.0], 20 mM MgCl2, 0.1% NP-40, 1 mM DTT) containing 10 µM ATP, and 10 µCi [γ-^{32}P]ATP (Amersham). The Sepharose beads bearing the fusion proteins were then washed three times with TNE buffer (20 mM Tris-HCl [pH 8.0], 100 mM NaCl, 1 mM EDTA) and in some cases were resuspended in bacteriophage lambda pyrophosphatase (λ-PPase) buffer containing 200 U of enzyme (New England Biolabs) and incubated for another 30 min at 30°C. The proteins on the beads were again washed three times in TNE. All the samples were dissolved in SDS-PAGE sample buffer (10 mM Tris-HCl [pH 8.0], 10 mM ß-mercaptoethanol, 20% glycerol, 5% SDS, trace amounts of bromophenol blue) and subjected to electrophoresis in a 12% polyacrylamide gel in the presence of 0.1% SDS. Gels were then stained with Coomassie brilliant blue, dried, and autoradiographed using X-ray film (Pierce).

Lamin disassembly assay. A previously described lamin disassembly assay was modified for the current studies (28). Approximately 1 x 10^7 Hep2 cells were homogenized in 5.0 ml nuclear buffer (250 mM sucrose, 5 mM MgCl2, 25 mM KCl, 10 mM Tris [pH 7.4], 1 mM DTT, 1x Complete protease inhibitor cocktail [Roche]) by three strokes of a Dounce homogenizer. Nuclei were pelleted at 800 x *g* for 10 min in a refrigerated tabletop centrifuge (Eppendorf). The supernatant was discarded, and pelleted nuclei were resuspended in nuclear buffer and then permeabilized by the addition of 0.1% Triton X-100, followed by incubation on ice for 20 min. Nuclei were again pelleted at 800 x *g* for 10 min, and the supernatant was removed. The pelleted permeabilized nuclei were then washed twice with an excess volume of U_S3-specific kinase buffer and finally resuspended in 400 µl of this buffer.

For the in vitro disassembly assay, three 80-µl aliquots of resuspended nuclei were incubated with 1 µg GST-pU_S3 or GST-pU_S3(K220A) in 120 µl kinase buffer in the presence or absence of 1 mM ATP. After 30 min of incubation at 30°C, the reaction mixture tubes were gently vortexed, and 10 µl of the reaction mixtures (samples designated L) were set aside. All subsequent steps were performed at 0 to 4°C. After centrifugation at 2,000 x *g* for 5 min, supernatants of each sample (30 µl) were collected and were designated S1. The remaining nuclei were centrifuged again at 10,000 x *g* for 2 min, and equal volumes of the supernatants were collected and designated S2. Proteins in the L, S1, and S2, samples were denatured in SDS-PAGE sample buffer, electrophoretically separated in denaturing polyacrylamide gels, and transferred to nitrocellulose for immunoblotting with lamin-specific antibodies.

Two-dimensional gel electrophoresis. To solubilize lamins, 2 x 10^6 infected Hep2 cells were lysed directly on culture dishes into 250 µl of urea rehydration buffer {9 M urea, 4% CHAPS [3-[(3-cholamidopropyl)-dimethylammonio]-1-propanesulfonate], 50 mM DTT, 0.2% ampholytes [Bio-Rad]} containing 1x Complete protease inhibitor cocktail (Roche) and a serine/threonine phosphatase inhibitor (10 mM NaF) (99). Approximately 100 µg of protein was subjected to isoelectric focusing in a Bio-Rad Protean isoelectric focusing cell using an 11-cm-long pH 3.0 to 10.0 nonlinear or a pH 5.0 to 8.0 linear immobilized pH gradient ReadyStrip (Bio-Rad). For separation in the second dimension, the strips were loaded on precast Criterion 10% bis-Tris polyacrylamide gels (Bio-Rad), followed by electrophoresis. The separated proteins were then transferred electrically to nitrocellulose for immunoblotting.

In some experiments, cells were first permeabilized in 0.5% CHAPS on ice for 5 min in the presence of Complete protease inhibitor, clarified by centrifugation at 800 x

g for 5 min at 4°C, and incubated with 400 U of λ-PPase in a supplied buffer (New England Biolabs) at 30°C for 30 min. After this reaction, cells were repelleted and lysed in urea rehydration buffer, followed by two-dimensional electrophoresis and immunoblotting.

Immunoblotting. Nitrocellulose sheets bearing proteins of interest were blocked in 5% nonfat milk plus 0.2% Tween 20 for at least 2 h. Membranes were then probed with lamin A/C chicken polyclonal antibody and lamin B goat polyclonal antibody if needed. Primary antibodies were detected by horseradish peroxidase-conjugated rabbit anti-chicken (Jackson ImmunoResearch) and/or bovine anti-goat secondary antibodies (Santa Cruz Biotechnology). Bound immunoglobulin was visualized by enhanced chemiluminescence (Pierce) followed by exposure to X-ray film. Signal intensities were quantified and calibrated using a Syngene Chemi-Genius imaging system and associated GeneTools software as needed.

Results

U_S3 kinase activity modifies nuclear lamin A/C organization and localization of pU_L31 and pU_L34 during HSV-1 infection. Because Hep2 cells are generally resistant to HSV-induced cytoskeletal changes, one goal of these studies was to investigate whether the nuclear lamina of Hep2 cells was affected by U_S3, as was previously reported with Vero cells (15). In considering the design of such experiments, we noted in previous studies that some commercial lamin A/C antibodies are rendered less immunoreactive upon infection with HSV-1 (162). To avoid the potentially misleading effects of antibody staining, we attempted to use eGFP-lamin A/C in transient-expression assays but found that overexpression of such constructs disrupted the nuclear lamina in many cells, even in the absence of infection (not shown). To avoid

these overexpression artifacts, and under the expectation that cells experiencing associated cytotoxic effects should be outgrown by healthy cells expressing the construct, we sought to produce a cell line stably expressing eGFP-lamin A/C. Hep2 cells were therefore transfected with a plasmid conferring G418 resistance and encoding eGFP fused to lamin A/C. Individual cells expressing eGFP were cloned by FACS, followed by amplification in G418-containing medium. Cell lines expressing fluorescence in association with the nuclear rim were selected for further study.

One such cell line was either mock infected or infected with wild-type HSV-1(F) or virus vRR1204 bearing a mutation inactivating U_S3 kinase activity [designated U_S3(K220A) in Fig. 2.1] (174). At 16 h postinfection, cells were fixed, permeabilized, and reacted with chicken antibody directed against U_L34 protein. Bound chicken antibody was revealed by reaction with Texas Red-conjugated donkey anti-chicken antibody, followed by confocal microscopy.

In general, the shape of nuclei infected with HSV-1(F) was more irregular than that of uninfected cells. As revealed upon collection of confocal images at high magnification, followed by digital enlargement, eGFP-lamin A/C appeared mostly as a series of filaments and dots linking larger solid areas of fluorescence. Overall, the fluorescence appeared in a reticular pattern in the nuclear rim of both the mock-infected and the HSV-1(F)-infected cells. The reticular pattern was most readily noticeable in optical sections of the tops and bottoms of the cells in which a planar view of the nuclear lamina was most readily apparent (Fig. 2.1B). In both mock-infected and HSV-1(F)-infected cells, the reticular filaments were bordered by spaces that lacked eGFP fluorescence. Although the reticular pattern of NM fluorescence in mock-infected and HSV-1-infected cells did not differ significantly, most cells infected with HSV-1(F) contained larger regions near the bottom of the cell that were devoid of fluorescence (Fig. 2.1B, arrow). In general, the appearance of these cells is in contrast to the

Figure 2.1 Confocal analyses of a Hep2-derived cell line stably expressing eGFP-lamin A/C. Cells were either mock infected (Mock) or infected with 5.0 PFU/cell of wild-type HSV-1(F) (designated F) or mutant U_S3(K220A), lacking pU_S3 kinase activity. Cells were fixed and permeabilized at 16 h postinfection and stained with polyclonal anti-pU_L34 chicken polyclonal antibody, followed by Texas Red-conjugated secondary antibody, and examined with confocal microscopy. (A) Analysis of optical sections taken through the middle of cells. (B) Optical sections taken at the bottom of cells. Regions indicated in white rectangles in panels D, E, F, J, K, and L are digitally magnified in the panel immediately below them (panels G, H, I, L, M and N, respectively). Coincident signals in the merged images (rightmost column) are indicated by a yellow color. An arrow indicates one region of the infected cell containing less lamin A/C than surrounding areas.

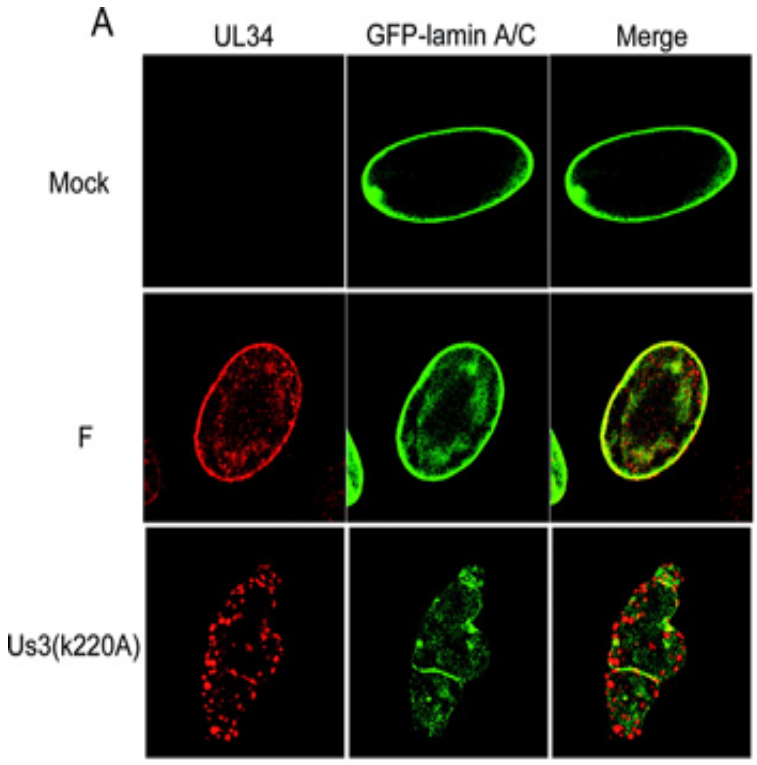
A
UL34
GFP-lamin A/C
Merge
Mock
F
Us3(k220A)

Figure 2.1 (Continued)

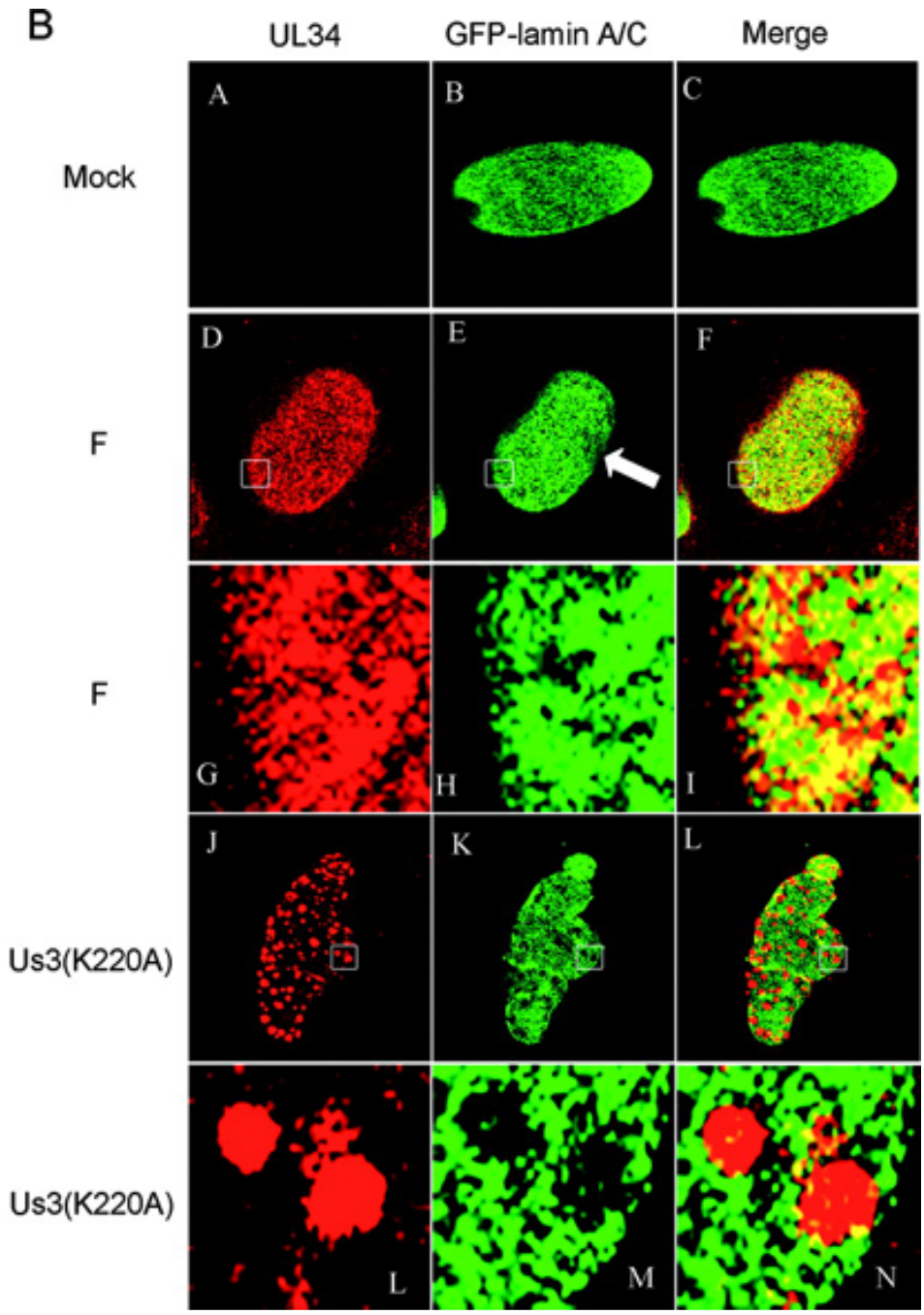

appearance reported for HSV-infected Hep2 cells expressing eGFP-lamin A/C transiently in which large discrete holes in the eGFP-specific fluorescence were seen (186). Differences in the two studies include the use of transient expression of eGFP-lamin A/C, followed by infection with 50 PFU/cell in the previous study, versus the use of a stably expressing cell line and an MOI of 5 in the current study.

In contrast to the results obtained upon infection with wild-type virus, the pattern of eGFP-lamin A/C fluorescence was markedly different after infection with the kinase-inactivated U_S3 mutant virus. Specifically, sites within the reticular pattern lacking eGFP fluorescence were substantially larger in diameter and more likely oval to round. In addition, the larger regions of HSV-1(F)-infected cells lacking the most eGFP in the nuclear rim displaying a paucity of lamin A/C were absent. These results indicated that the kinase activity of pU_S3 is necessary for the distribution of lamin A/C normally seen in cells infected with wild-type HSV.

As noted previously, pU_L34-specific immunostaining was distributed throughout the nuclear rim in Hep2 cells infected with the wild-type virus HSV-1(F) (163). This was readily apparent in optical cross-sections taken through the middle of cells (Fig. 2.1A). Superficially, eGFP-lamin A/C fluorescence and pU_L34-specific immunostaining mostly colocalized in these cross-sections. However, high magnification of planar sections near the bottom of the cells revealed regions containing only pU_L34 immunostaining or only eGFP-lamin A/C, as well as regions where eGFP-lamin A/C and pU_L34 colocalized (Fig. 2.1B). In the larger regions lacking lamin A/C, seen only in cells infected with HSV-1(F), pU_L34 immunostaining could also be detected.

In striking contrast to the localization of pU_L34 in HSV-1(F)-infected cells, cells infected with the U_S3 kinase mutant contained pU_L34 almost exclusively within punctate foci at the nuclear rim in optical cross-sections taken near the centers of cells (Fig. 2.1A) (13, 170, 176). These regions invariably corresponded to the well-defined

breaches in the reticular distribution of eGPF-lamin A/C noted above. This dramatic change in the distribution of lamin A/C became even more striking in optical sections that focused on the bottom of infected cell nuclei. In such sections (Fig. 2.1B, lower two rows), foci staining intensely with pU_L34-specific antibody coincided with regions that entirely lacked detectable eGPF-lamin A/C. We conclude that the kinase activity of pU_S3 is necessary for partial colocalization of pU_L34 and eGFP-lamin A/C at the nuclear rim and for the wide distribution of pU_L34 throughout the nuclear rim. These data are consistent with previous immunostaining studies indicating that U_S3 kinase activity is necessary for the normal distribution of pU_L34 with Vero cells (13, 170, 176).

To ensure that the above-described observations were not idiosyncratic to the eGFP-lamin A/C cell line, Hep2 cells were also mock infected or were infected with the wild-type HSV-1(F), the U_S3 kinase-dead viral mutant, or a viral mutant containing a deletion of U_S3. The cells were fixed at 16 h after infection and were immunostained with antibody against pU_L31 and a chicken polyclonal antibody directed against lamin A/C that was insensitive to HSV-induced epitope masking (162).

As shown in Fig. 2.2, lamin A/C localized in a reticular pattern in mock-infected cells that superficially resembled that of cells infected with HSV-1(F), except that some regions near the nuclear rim of infected cells did not stain with lamin A/C antibody (e.g., as shown by the arrow in Fig. 2.2D). pU_L31 immunostaining also appeared in a reticular pattern, but this pattern did not completely overlap that of lamin A/C immunostaining. Specifically, regions containing only pU_L31 immunostaining or only lamin A/C immunostaining and colocalization of these were observed. Thus, the patterns of pU_L31 immunostaining were similar to those of pU_L34, as indicated above.

More importantly for the purposes of subsequent experiments herein, planar sections of cells infected with either the U_S3 deletion virus or the kinase-dead mutant

Figure 2.2 Digital confocal images of Hep2 cells immunostained with antibodies to lamin A/C and pU_L31. Hep2 cells were mock infected (Mock) or infected with a U_S3 deletion mutant (dU_S3), a mutant lacking U_S3 kinase activity [U_S3 (K220A)], or wild-type virus HSV-1(F) (designated F). Sixteen hours after infection, the cells were fixed, permeabilized, and reacted with preadsorbed rabbit polyclonal antiserum against pU_L31 or chicken immunoglobulin Y directed against lamin A/C. Bound antibodies were revealed with Texas Red-conjugated anti-rabbit antibody or FITC-conjugated anti-chicken antibodies. Optical sections closest to the glass coverslips are shown. An arrow indicates regions of the nuclear rim that are mostly devoid of lamin A/C immunostaining. White boxes indicate areas of interest that are magnified in an inset in the same panel.

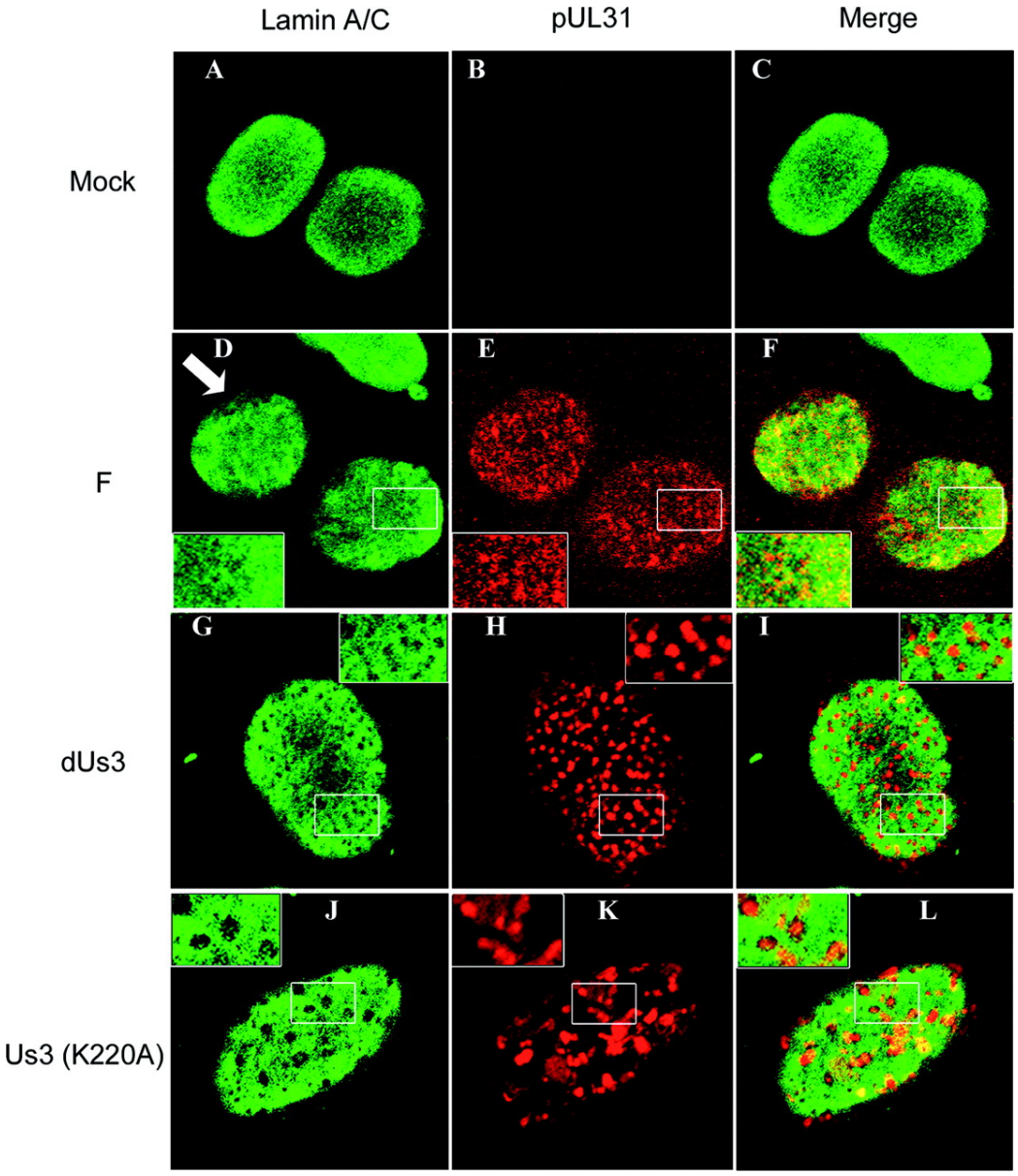
Lamin A/C
pUL31
Merge
Mock
F
dUs3
Us3 (K220A)
A
B
C
D
E
F
G
H
I
J
K
L

virus revealed well-circumscribed, roughly circular regions that completely lacked lamin A/C immunostaining. These regions invariable contained most of the pU_L31 immunostaining in the cell, i.e., there were very few regions in which pU_L31 and lamin A/C colocalized except on the edges of these "holes" in the nuclear lamina. Taken together, the results are reminiscent of the above-described study using the eGFP-lamin A/C-expressing cell line and indicate that U_S3 kinase and its activity are required for (i) partial colocalization of pU_L31/pU_L34 with lamin A/C, (ii) for the reticular distribution of lamin A/C and pU_L31/pU_L34 seen in cells infected with wild-type viruses, and (iii) for the large regions devoid of lamin A/C immunostaining as seen in cells infected with HSV-1(F).

Adaptation of a U_S3 *in vitro* kinase assay and identification of lamin A as a substrate. The above-described observations indicated that the kinase activity encoded by the U_S3 gene altered lamin A/C distribution. The simplest mechanism to explain this phenomenon would be that U_S3 phosphorylates lamin A/C directly, thereby altering lamin A/C's interaction with other proteins in the nuclear lamina. Further studies were undertaken to test this possibility.

Inasmuch as preliminary observations indicated that the Thr-10 residue of lamin A/C (within the sequence Arg_7-Arg_8-Ala_9-Thr_{10}-Arg_{11}-Ser_{12}, from GenBank accession number NP_733821) matched the optimal consensus target, experiments were designed to determine whether lamin A/C could be phosphorylated by the U_S3 kinase. Thus, U_S3 fused to GST was expressed in insect SF9 cells and was purified on glutathione beads as previously described (89). As a control, the kinase-inactivated mutant U_S3(K220A) was purified in the same manner. Coomassie blue staining of the proteins indicated at least 90% purity (Fig. 2.3A).

Figure 2.3 Analysis of *in vitro* kinase activities of purified GST-pU$_S$3 and the mutant GST-pU$_S$3(K220A). (A) Denaturing polyacrylamide gel containing purified GST-pU$_S$3 and GST-pU$_S$3(K220A) and stained with Coomassie brilliant blue. **(B)** In vitro kinase reaction. The fusion proteins indicated at the top of the left panel were mixed with 100 ng GST-pU$_S$3. After 30 min at 30°C in the presence of [γ-^{32}P]ATP, the reaction mixtures were resolved on a denaturing polyacrylamide gel and visualized by Coomassie (CBB) staining (left panel) and autoradiography (right panel). The position of the approximately 90,000 apparent Mr GST-pU$_S$3 fusion protein is shown in the right panel. GST-pU$_L$34 (amino acids 205 to 275) is a negative control inasmuch as it does not contain the phosphorylation consensus site in pU$_L$34. **(C)** *In vitro* kinase activities of GST-pU$_S$3 and GST-pU$_S$3(K220A). Purified GST-pU$_S$3 (0.1 µg) or 0.5 µg GST-pU$_S$3(K220A) was incubated with [γ-^{32}P]ATP in the presence or absence of partially purified GST-pU$_L$31 as a potential substrate, followed by subsequent incubation in the presence or absence of λ-PPase. The reaction components were denatured, electrophoretically separated, and stained with Coomassie brilliant blue (CBB, bottom panel) or dried and autoradiographed (upper panel). For comparative purposes, the molecular weight standards from the bottom panel were copied and aligned with the top panel, using Adobe Photoshop. Sizes of the standards are indicated to the left of the figure in thousands [K]).

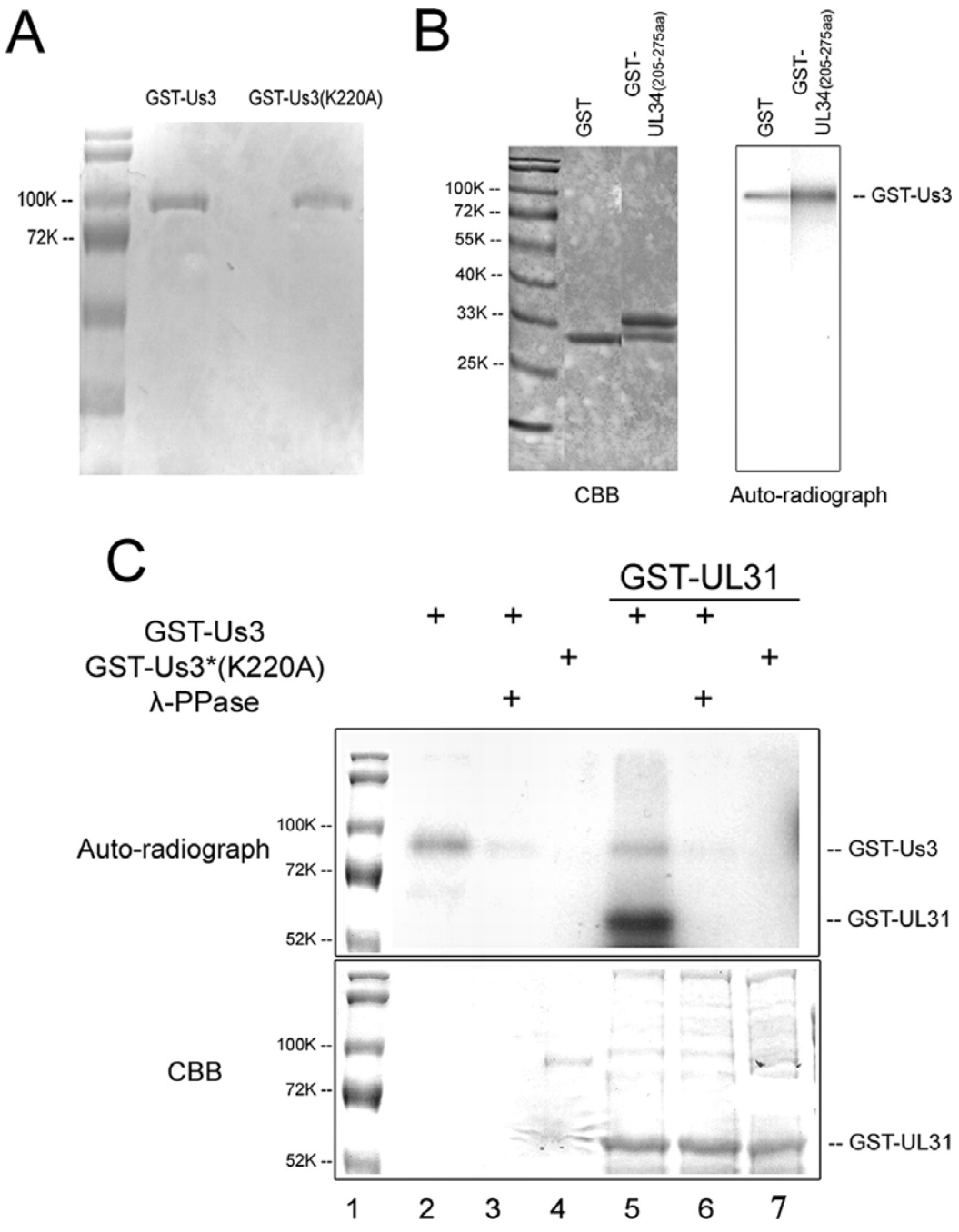
A
GST-Us3
GST-Us3(K220A)
100K --
72K --
B
GST
GST-UL34(205-275aa)
100K --
72K --
55K --
40K --
33K --
25K --
CBB
Auto-radiograph
-- GST-Us3
C
GST-UL31
GST-Us3
GST-Us3*(K220A)
λ-PPase
Auto-radiograph
100K --
72K --
52K --
-- GST-Us3
-- GST-UL31
CBB
-- GST-UL31
1 2 3 4 5 6 7

To test their enzymatic activities, 0.1 μg of the purified proteins was reacted with purified GST, or with pU_L31 fused to GST, in the presence of [γ-^{32}P]ATP. As an additional negative control, the pU_L34 amino acids 205 to 275 region, comprising a region of pU_L34 separate from that of the known U_S3 phosphorylation site, was also subjected to the kinase assay. The reaction mixtures were then electrophoretically separated on a denaturing polyacrylamide gel and subjected to autoradiography (Fig. 2.3B and C). Consistent with a previous report (89), GST-pU_S3 phosphorylated itself (Fig. 2.3B and C, lanes 2 and 5), whereas GST-pU_S3(K220A) had no such activity (Fig. 2.3C, lane 4). GST-pU_S3 also readily phosphorylated the partially purified pU_L31-GST fusion protein (Fig. 2.3C, lane 5). In contrast, GST-pU_S3 did not phosphorylate GST: GST fused to the U_L34 amino acids 205 to 275 or other *E. coli* proteins within the GST-pU_L31 preparation that were readily visible on the Coomassie blue-stained gel (Fig. 2.3B and C, lane 5). GST-pU_S3(K220A) did not phosphorylate GST-pU_L31 or other proteins in the *E. coli* lysate (Fig. 2.3C, lane 7). As expected, addition of bacteriophage λ-PPase significantly reduced the phosphorylation of GST-pU_S3 (Fig. 2.3C, lane 3) and eliminated the phosphorylation of GST-pU_L31 that was mediated by GST-pU_S3 (Fig. 2.3C, lane 6).

Collectively, these data indicate that the U_S3 gene-encoded kinase activity was functional and specific inasmuch as it induced phosphorylation of two known substrates (pU_L31 and pU_S3) but not GST or other tested proteins. In addition, the data indicate that the K220A mutation inactivated all detectable U_S3 kinase activity. Thus, an efficient and specific in vitro kinase assay system was established for testing of additional substrates.

To determine whether lamin A was a target of the U_S3 kinase, GST fused to lamin A was purified from *E. coli* and subjected to the in vitro kinase assay. The results, shown in Fig. 2.4, indicated that the lamin A-GST fusion protein was heavily

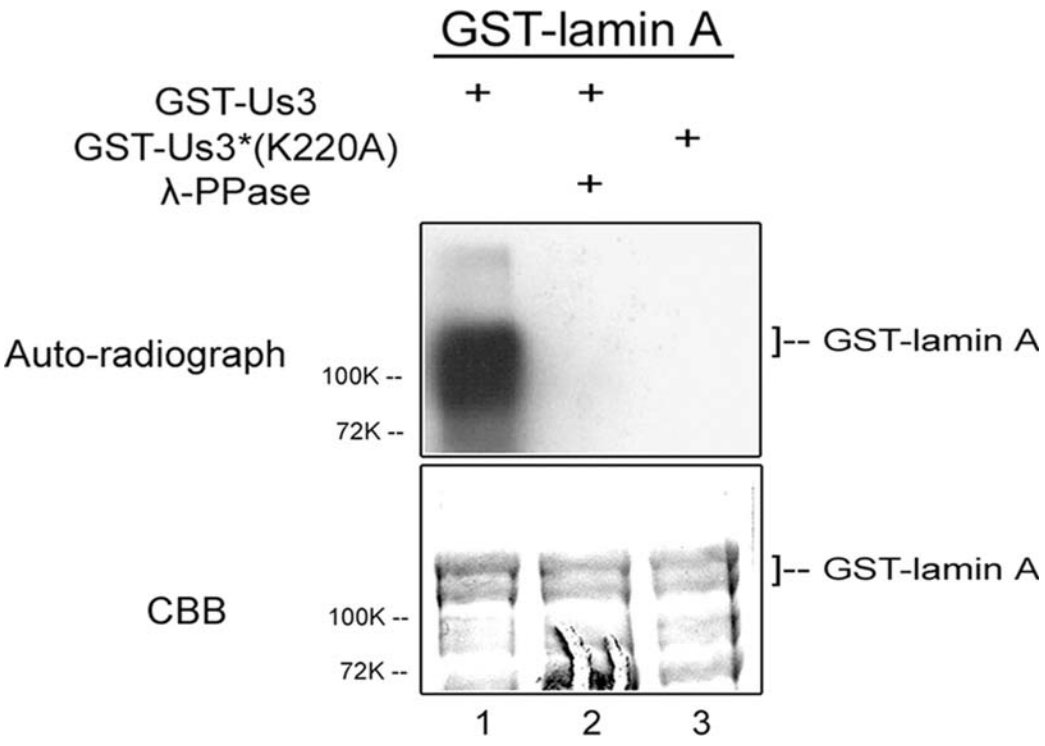

Figure 2.4 Phosphorylation of lamin A by U_S3 kinase *in vitro.* Full-length lamin A fused to GST was partially purified and reacted with either purified GST-pU_S3 or GST-pU_S3(K220A) in the presence of [γ-^{32}P]ATP, followed by incubation in the presence or absence of λ-PPase. The reaction components were separated on a polyacrylamide gel and stained with Coomassie brilliant blue (CBB, lower panel) and autoradiographed (upper panel).

phosphorylated in the presence of GST-pU$_S$3 (Fig. 2.4, lane 1) but not in the presence of GST-pU$_S$3(K220A) (Fig. 2.4, lane 3). The phosphorylation of lamin A-GST wa-seliminated upon incubation with λ-PPase (Fig. 2.4, lane 2). These data indicate that lamin A is an in vitro substrate of the U$_S$3 kinase.

U$_S$3 has broader kinase activity than predicted and phosphorylates lamin A/C at multiple sites *in vitro*. Because lamin A/C is phosphorylated at different sites depending on the physiological mechanism of lamin disassembly (see the introduction), it was of interest to identify which region of lamin A was phosphorylated by the U$_S$3 kinase. To identify the region targeted by the U$_S$3 kinase, five subfragments of lamin A fused to GST were purified from lysates of *E. coli* and incubated with GST-pU$_S$3 in the presence of [γ-^{32}P]ATP, followed by denaturing gel electrophoresis, Coomassie blue staining, and autoradiography. The amount of radioactive phosphate in a given protein band was normalized to the amount of protein present in the reaction mixtures and expressed as a percentage of the degree to which full-length lamin A was phosphorylated. The results are shown in Fig. 2.5.

Comparing the radiolabeling of full-length protein with that of truncated lamin A proteins normalized to the amount of protein in individual reaction mixtures revealed that full-length lamin A was phosphorylated to a higher degree than any single subfragment. While only Thr-10 matched the optimal U$_S$3 kinase consensus sequence, it was surprising to find that all five subfragments of lamin A were phosphorylated to various extents when reacted with purified GST-pU$_S$3. Although the head (Fig. 2.5, lane H) domain (amino acids 1 to 129) containing the U$_S$3 consensus site was phosphorylated to a level that was 14% of that of full-length lamin A/C, the tail 1 (Fig. 2.5, lane T1) domain (amino acids 369 to 519) was even more heavily phosphorylated (to 37% of that of full-length lamin A/C), despite the lack of a pU$_S$3 phosphorylation

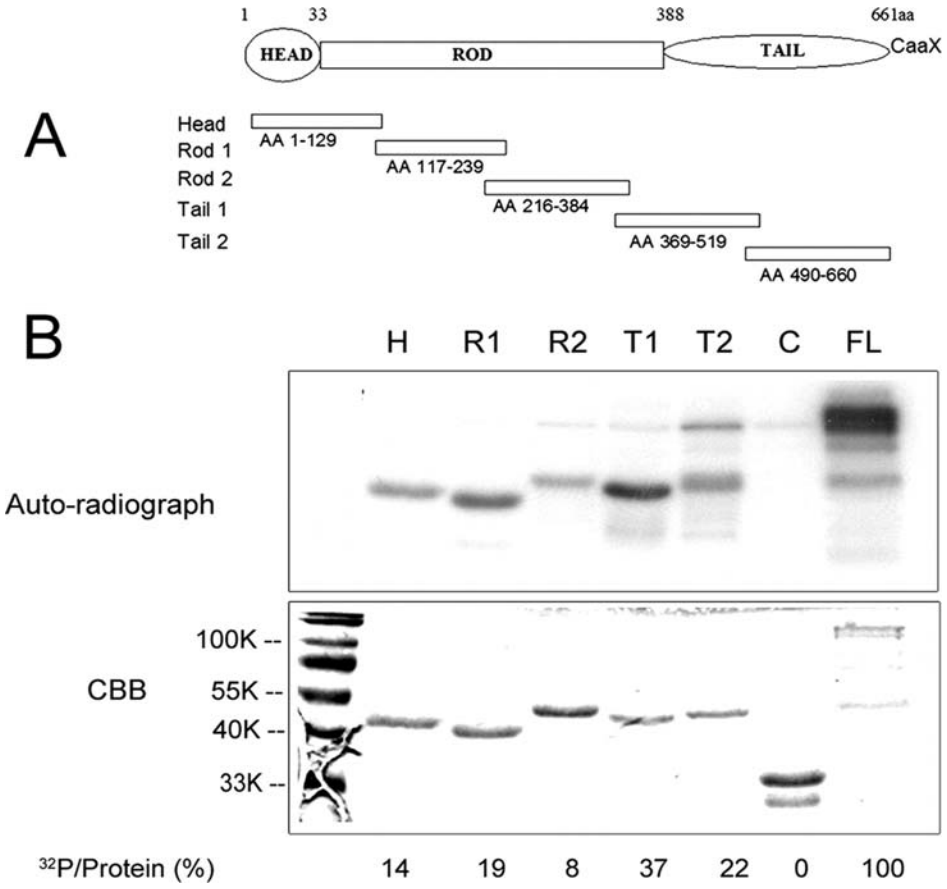

Figure 2.5 (A) Schematic diagram of lamin A primary structure and five subdomains fused to GST. The amino acids (AA) in each peptide subdomain are indicated, assuming that the start methionine codon is 1 [reprinted from reference (162)]. **(B) Full-length (FL) lamin A or lamin A fragments fused to GST and reacted with GST-pU$_S$3 kinase.** The five GST fusion proteins bearing fragments of lamin A as detailed for panel A were purified, mixed with U$_S$3-GST and [γ-^{32}P]ATP, and electrophoretically separated and stained with Coomassie brilliant blue (lower panel) and autoradiographed (upper panel). H, head; R1, rod1; R2, rod2; T1, tail 1; T2, tail2; lane C, GST-pU$_L$34 (amino acids 205 to 275).

consensus motif. As expected from previous results, GST-pU_L34 (amino acids 205 to 275) lacking the U_S3 kinase consensus motif was not phosphorylated by pU_S3 (Fig. 2.5, lane C).

Taken together, these observations indicate that the full-length lamin A-GST was phosphorylated at multiple sites within lamin A. It follows that, at least in vitro, the previously derived U_S3 kinase consensus site is overly restrictive and other sites can also be phosphorylated.

U_S3 induces partial lamin A/C solubilization in purified Hep2 cell nuclei. Because the phosphorylation of lamins is well known to regulate lamin disassembly, it was of interest to determine whether phosphorylation by U_S3 kinase could increase the solubility of lamin A/C. This was of particular interest because the complex structure of the nuclear lamina might preclude the access of pU_S3 to lamin A/C or lamin A/C phosphorylation sites. To test whether U_S3 kinase activity could modify the nuclear lamina, an in vitro lamina disassembly assay was developed.

Briefly, nuclei from Hep2 cells were isolated, permeabilized, and incubated in U_S3 kinase buffer with GST-pU_S3 or GST-pU_S3(K220A) in the presence or absence of ATP. After the reaction, nuclei were pelleted by centrifugation, and equal amounts of supernatant were collected for analysis. To ensure minimal contamination of the supernatants with insoluble material, nuclei were subjected to a second high-speed centrifugation, and a portion of the supernatants were again collected. Protein in the supernatants and pellets were denatured in SDS, electrophoretically separated, transferred to nitrocellulose, and probed with a chicken polyclonal antibody to lamin A/C.

As shown in Fig. 2.6, the presence of GST-pU_S3 and ATP increased the amount of lamin A/C solubilized into the supernatants by approximately twofold compared to that in reaction mixtures containing either GST-pU_S3(K220A) plus ATP or GST-pU_S3

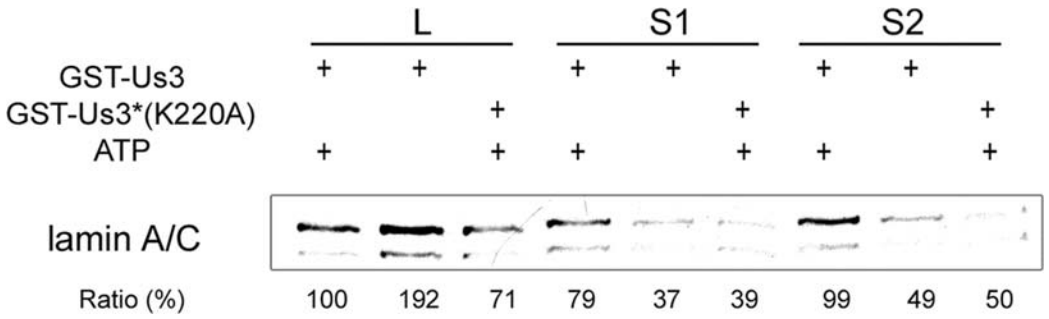

Figure 2.6 Immunoblot of total and solubilized lamin A/C from permeabilized Hep2 cell nuclei reacted with wild-type and mutant U_S3-encoded kinases. Purified and permeabilized Hep2 cell nuclei were incubated for 30 min in the presence or absence of the indicated fusion proteins and ATP. As a loading control, a sample of the total material (L) was collected immediately after the reactions. S1 was collected after centrifugation at low speed. A second supernatant fraction (S2) was collected after high-speed centrifugation. Proteins in the various fractions were denatured in SDS, electrophoretically separated, transferred to nitrocellulose, and probed with lamin A/C-specific antibody. Bound immunoglobulin was detected by a horseradish peroxidase-conjugated secondary antibody and chemiluminescence. The intensity of the chemiluminescence signals of the lamin A and C bands were quantified using a Syngene Chemi-Genius imaging system and associated GeneTools software, and the amount of chemiluminescence was pooled. The reported percentages represent the intensity of chemiluminescence in that lane relative to that detected in the first lane (sample L of GST-pU_S3 plus ATP).

without ATP. This reaction was repeated three times with similar results. We conclude that U_S3 kinase activity and ATP are sufficient to increase the solubility of lamin A/C from an endogenous preexisting nuclear lamina *in vitro*.

Lamin A/C is phosphorylated in HSV-infected cells, and the full spectrum of phosphorylation requires pU_S3 kinase activity. The studies described above were performed *in vitro*. In order to determine whether U_S3 phosphorylates lamin A/C in infected cells, two-dimensional electrophoretic analysis of lamin A/C was performed under various conditions. Specifically, Hep2 cells were mock infected or infected with 5.0 PFU/cell of wild-type HSV-1(F) or the U_S3(K220A) mutant virus and were lysed 16 h postinfection in 9 M urea to solubilize nuclear lamins (99). The proteins were separated by isoelectric focusing in the first dimension and by size in the second dimension. The electrophoretically separated proteins were transferred to nitrocellulose, and the positions of various isoforms of lamin A/C were revealed by immunoblotting with lamin A/C-specific chicken polyclonal antibody. The immunoblots were also probed with a goat antibody directed against lamin B1 and B2 with predicted isoelectric points of 5.11 and 5.29, respectively.

The results (Fig. 2.7) showed that unlike lamin A/C, neither lamin B isoform showed consistent or obvious shifts in isoelectric points under the various conditions tested. The lamin B-specific spots were therefore used as an internal control for alignment of the lamin A/C immunoblots. Upon separation in the first dimension in the pH 3.0 to 10.0 range, lamin A/C from mock-infected cells and cells infected with wild-type HSV-1(F) were broadly distributed throughout a wide pH range. Superficially, the patterns of lamin A/C-specific spots were similar in distribution, but mock-infected cells contained lamin A/C isoforms that were evenly distributed throughout the middle of the range, whereas some individual spots were more defined and easier to discern in

Figure 2.7 Two-dimensional gel electrophoresis and immunoblots of lamin A/C isoforms from mock-infected and HSV-infected cells. Hep2 cells were mock infected or infected with wild-type HSV-1(F) (panels labeled F) or mutant U_S3(K220A). Proteins were extracted in buffer containing 9 M urea to solubilize lamins and separated by isoelectric focusing in the first dimension using nonlinear pH gradients from pH 3.0 to 10.0 (A and B) or linear pH gradients 5.0 to 8.0 (C) and by size on denaturing polyacrylamide gels in the second dimension. The proteins were then transferred to nitrocellulose and probed with polyclonal chicken antibody directed against lamin A/C or a rabbit antibody against lamin B1 and lamin B2. Bound immunoglobulin was detected by appropriate horseradish peroxidase-conjugated secondary antibodies. Chemiluminescence generated by the addition of appropriate substrates was recorded on X-ray film. In some experiments (λ-PPase), proteins were reacted with λ-PPase before electrophoretic separation. For comparative purposes, the three blots in panels A and B were aligned by position of lamin B-specific spots and by distance from the cationic and anionic poles. The positions of the terminal poles on the pH strip of the four immunoblots shown in panel C are also aligned. For orientation, the positions of the lamin A-, B-, and C-specific spots are indicated to the left of the top immunoblot shown in panels A and C.

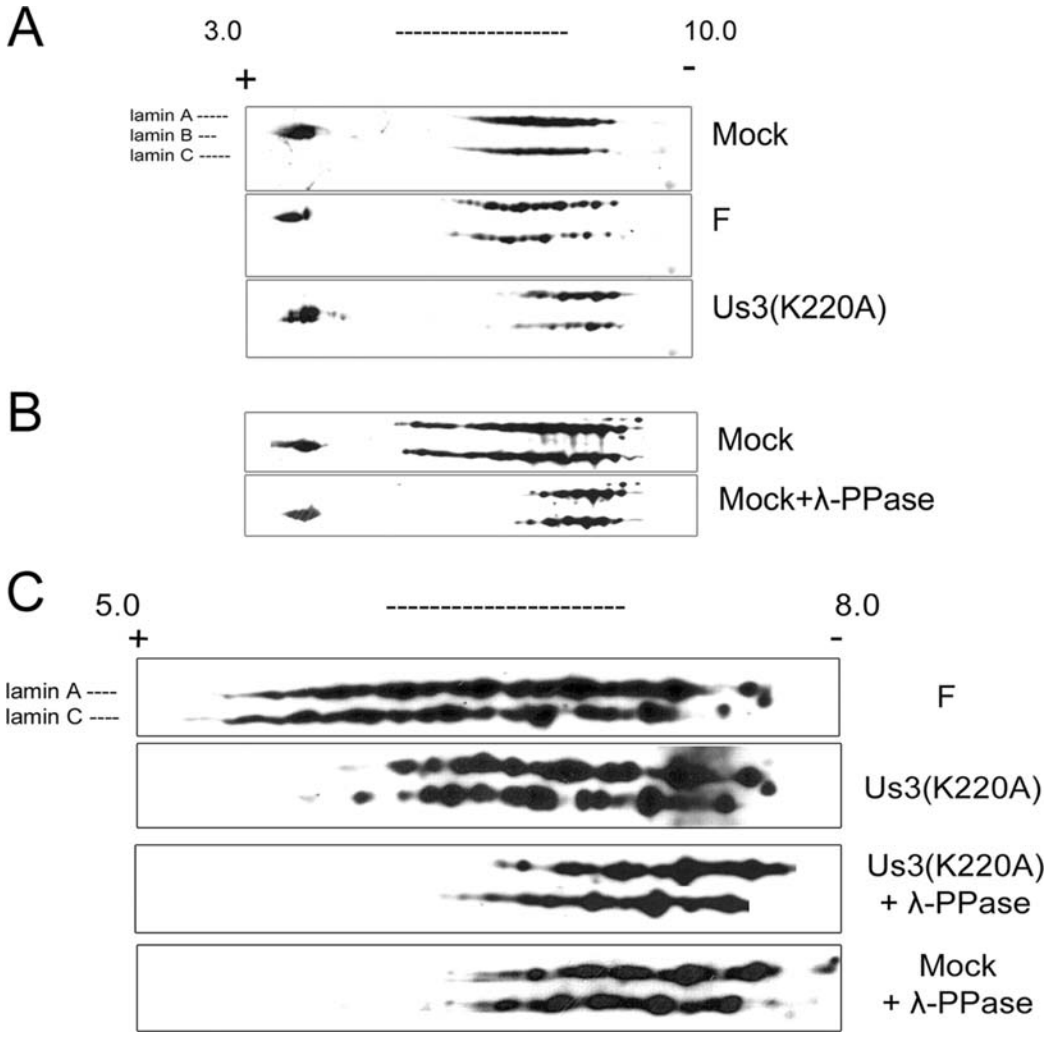
A
3.0
10.0
+
-
lamin A -----
lamin B ---
lamin C -----
Mock
F
Us3(K220A)
B
Mock
Mock+λ-PPase
C
5.0
8.0
+
-
lamin A ----
lamin C ----
F
Us3(K220A)
Us3(K220A)
+ λ-PPase
Mock
+ λ-PPase

lamin A/C taken from cells infected with HSV-1(F). This suggested that lamin A/C in HSV-1(F)-infected cells are modified differently than in mock-infected cells, but these differences are subtle, at least as viewed by two-dimensional gel electrophoresis. In contrast, however, U_S3(K220A)-infected cells lacked many of the more acidic lamin A/C species present within the populations of lamin A/C isoforms in HSV-1(F)-infected or mock-infected cells. The predicted isoelectric points of lamin A and C are 6.57 or 6.40, respectively. Separation in the first dimension using a narrower pH range, closer to the lamin A/C isoelectric point (pH 5.0 to 8.0) (Fig. 2.7C), confirmed that numerous acidic lamin A/C species detected in HSV-1(F)-infected cells were absent from cells infected with the U_S3 kinase mutant.

Because the wide range of distribution of lamin A/C on first dimension might be due to posttranslational modifications other than phosphorylation (such as polyadenylylation), samples were treated with λ-PPase, followed by two-dimensional electrophoretic separation and immunoblotting with lamin A/C antibody. As shown in Fig. 2.7B and C, phosphatase treatment of lamins from mock-infected cells resulted in a dramatic loss of the most acidic species of lamin A/C, indicating that the acidity of these species is a consequence of phosphorylation. Moreover, λ-PPase treatment of lamin A/C also eliminated some acidic species detected in cells infected with the U_S3(K220A) mutant virus. Thus, U_S3 kinase activity cannot account for all of the lamin A/C phosphorylation in HSV-infected cells.

Taken together, these data indicate that many of the acidic lamin A/C isoforms are phosphorylated species whose acidity in infected cells depends on U_S3 kinase activity. We conclude that endogenous lamin A/C is phosphorylated during HSV-1 infection and that the full spectrum of phosphorylation requires U_S3 kinase activity.

Discussion

The effect of U_S3 on the distribution of lamin A/C in HSV-1-infected cells. Using two different methods, we have shown that U_S3 kinase activity is necessary for the pattern of lamin A/C distribution in HSV-1-infected Hep2 cells. Whereas lamin A/C and pU_L31 and pU_L34 immunostaining partially colocalized in a reticular pattern in Hep2 cells infected with wild-type virus, the lack of kinase activity in infected cells caused pU_L31 and pU_L34 to localize solely within circular regions lacking lamin A/C. These regions were wider in diameter and more circumscribed than most areas of cells infected with wild-type viruses containing pU_L31/pU_L34 but lacking lamin A/C. Similar conclusions were reached in studies of Vero cells, with the exception that the disruption of the lamina induced by both wild-type and U_S3(–) viruses was considerably more dramatic than that of uninfected cells, probably as a result of using different cell lines in the two studies (146). Our results are not a consequence of epitope masking because we used an eGFP-lamin A/C-expressing cell line and a polyclonal antibody insensitive to this HSV-induced effect with similar results.

We also noted subtle differences in the distribution of lamin A/C between the lamina of uninfected and HSV-1(F)-infected Hep2 cells. In both cases, the lamina contained small regions that lacked eGFP-lamin A/C. In infected cells, many, but not all, of these contained pU_L34 and pU_L31, proteins that are incorporated into nascent virions and are required for envelopment of nucleocapsids (169, 170, 175). Unlike the regions in uninfected Hep2 cells, larger regions of the nuclear rim, as viewed in planar sections, seemed to be devoid of lamin A/C in infected cells. It is unclear if these regions also lack lamin B or correspond to regions that communicate with the HSV DNA replication compartment (185). In any event, the concentration of pU_L31 and pU_L34 in both of the larger regions lacking lamin A/C and small gaps in the reticular

pattern of lamin A/C argue that they both represent potential sites of virion egress. In contrast, the absence of U_S3 kinase or its activity restricted potential envelopment sites to fewer, very discrete, and round foci that also lacked lamin A/C.

These data suggest that during infection with wild-type virus, some potential envelopment sites (i.e., in the reticular pattern) may be very small or a consequence of localized thinning of the lamina, whereas others, while larger, remain somewhat diffuse. These observations suggest a sophisticated manipulation of the dynamics of nuclear lamins by HSV to promote virus egress while maintaining most laminar structure. This balance depends on U_S3 kinase activity, inasmuch as the absence of this activity causes very discrete breaches in the lamina as viewed by the distribution of eGFP-lamin A/C. It seems likely that capsids pass through these exaggerated breaches in the lamina and accumulate in the perinuclear space adjacent to these sites. This is supported by the observation that in the absence of U_S3, perinuclear virions accumulate in evaginations of the NM (170, 176). It would be useful to confirm this by live cell microscopy.

How does U_S3 kinase activity preclude the presence of discrete "holes" in the nuclear lamina and aggregation of virions in the perinuclear space? We speculate that there are three possibilities. The first possibility is that U_S3 kinase activity serves to increase lamin turnover and dynamics. Thus, phosphorylation by U_S3 would remove lamin A/C from some regions where U_S3 accumulates. Subsequent dephosphorylation of these lamins (not accounted for in these studies) would allow their reincorporation into gaps in the lamina, similar to mechanisms by which the lamina expands during interphase (145). The result is a more dynamic and flexible lamina to facilitate nuclear egress at multiple sites and the absence of most obvious gaps, since these are subsequently filled in. A second, related possibility is that U_S3's effects on lamin A/C distribution are unrelated to the direct phosphorylation of lamin A/C by U_S3. In this sce-

nario, U_S3 kinase would phosphorylate other proteins that would then serve to increase lamin A/C phosphorylation in infected cells, leading to fewer discrete breaches in the lamina. A third possibility is related to the effect of U_S3 kinase on the localization of pU_L31 and pU_L34. At least pU_L31 likely encodes its own depolymerizing effects on the lamina (168, 190), and its concentration in discrete areas of the nuclear rim in the absence of U_S3 kinase activity might promote highly localized lamina disruption. The converse of this hypothesis is that U_S3's kinase activity serves to redistribute the lamina depolymerizing, envelopment machinery (specifically the pU_L34/pU_L31 complex) more widely throughout the NM. Clearly, further studies are necessary to test specific aspects of these models and to determine whether U_S3's phosphorylation and displacement of lamin A/C are related to the localization of pU_L34/pU_L31.

Lamin A/C phosphorylation in infected cells. Two-dimensional gel electrophoresis was chosen to characterize lamin A/C in infected and uninfected cells because of its ability to rapidly characterize differences between soluble and insoluble isoforms of lamin A/C. While it might seem surprising that the migration of lamin A/C in uninfected and HSV-1(F)-infected cells was only subtly different, we speculate that some of the phosphorylation of lamin A/C in mock-infected cells is consequential to phosphorylation by cellular kinases like cdc2 kinase in some mitotic cells (150, 151), whereas in HSV-infected cells, lamin A/C is primarily phosphorylated by the U_S3 kinase (Fig. 2.7). Thus, while collectively the electrophoretic profiles under the two conditions are similar, the mechanisms responsible for lamin A/C phosphorylation in the two circumstances are very different. These interpretations are supported by the observations that (i) HSV-infected cells do not undergo mitosis late in infection (47), (ii) U_S3 can directly phosphorylate lamin A/C at multiple sites in vitro (Fig. 2.5), and (iii) most highly phosphorylated lamin A/C species in HSV-1(F)-infected cells are not

detected upon infection with the U_S3 kinase mutant (Fig. 2.7). On the other hand, some phosphorylated species of lamin A/C were detected even in the absence of U_S3 kinase activity, suggesting that other kinases also phosphorylate lamin A/C in HSV-1(F)-infected cells.

Substrates of the U_S3 kinase. It was surprising that multiple regions of lamin A could be phosphorylated by purified GST-pU_S3, despite the fact that only codon 10 matched the consensus sequence derived from previous analyses of peptide substrates (105, 158, 159). Indeed, some lamin A peptides lacking a bona fide pU_S3 phosphorylation consensus sequence (e.g., amino acids 369 to 519 in the tail domain) were phosphorylated more heavily than the lamin A head domain bearing this motif (Fig. 2.5). In the same reactions, the U_S3 kinase did not phosphorylate a variety of *E. coli* proteins, nor GST, suggesting kinase specificity for lamin A/C. Parenthetically, the consensus phosphorylation site of cyclic AMP-dependent PKA phosphorylation is R-*X*-S/T or R-R/K-*X*-S/T, i.e., very similar to and partially overlapping that of pU_S3, although the K_m values of the respective enzymes differ (155). Although it has been speculated that pU_S3 kinase activity functionally overlaps that of PKA in HSV-infected cells (12), the spectrum of U_S3 kinase substrates is likely broader inasmuch as protein kinase A phosphorylates lamin A/C only at N-terminal amino acids 1 to 32 *in vitro* (48).

These data indicate that the U_S3 kinase is more promiscuous than previously thought and suggest the existence of more substrates than previously predicted. Like other promiscuous kinases, it seems likely that the most important factor limiting phosphorylation by pU_S3 would be access to the substrate in the living cell or virion, rather than the presence or absence of the previously reported phosphorylation motif. Given this consideration, it is reasonable to postulate that U_S3 kinase substrates other than lamin A/C could also contribute to alterations in the nuclear lamina of HSV-

infected cells. Candidates include lamin B, various lamin receptors, and the HSV-1 U_L31 protein.

Acknowledgements

We thank Kaihua Sun, Teresa Monique Gunn, and Ted Clark for help with two-dimensional electrophoresis; David Gilbert for the eGFP-lamin A/C expression construct; Richard Roller and Bernard Roizman for antisera and recombinant viruses; Carol Duffy for help with confocal microscopy; James Lee Smith for help with FACs analysis and sorting; Klaus Osterrieder for comments on the manuscript; and members of the Baines laboratory for interesting discussions.

These studies were supported by grants R01AI 52341 and S10 RR020981 from the National Institutes of Health.

CHAPTER III

EFFECTS OF LAMIN A/C, LAMIN B1, AND VIRAL U_S3 KINASE ACTIVITY ON VIRAL INFECTIVITY, VIRION EGRESS, AND THE TARGETING OF HERPES SIMPLEX VIRUS U_L34-ENCODED PROTEIN TO THE INNER NUCLEAR MEMBRANE*

Fan Mou, Elizabeth Wills, Richard Park, and Joel D. Baines

Department of Microbiology and Immunology, College of Veterinary Medicine

Cornell University, Ithaca, NY 14853

* Reprinted from **Mou, F., E. G. Wills, R. Park, and J. D. Baines.** (2008). Effects of lamin A/C, lamin B1, and viral U_S3 kinase activity on viral infectivity, virion egress, and the targeting of herpes simplex virus U_L34-encoded protein to the inner nuclear membrane. J Virol 82:8094-104.

Abstract

Previous results indicated that the U_L34 protein (pU_L34) of herpes simplex virus 1 (HSV-1) is targeted to the nuclear membrane and is essential for nuclear egress of nucleocapsids. The normal localization of pU_L34 and virions requires the U_S3-encoded kinase that phosphorylates pU_L34 and lamin A/C. Moreover, pU_L34 was shown to interact with lamin A *in vitro*. In the present study, glutathione *S*-transferase/pU_L34 was shown to specifically pull down lamin A and lamin B1 from cellular lysates. To determine the role of these interactions on viral infectivity and pU_L34 targeting to the inner nuclear membrane (INM), the localization of pU_L34 was determined in *Lmna*$^{-/-}$ and *Lmnb1*$^{-/-}$ mouse embryonic fibroblasts (MEFs) by indirect immunofluorescence and immunogold electron microscopy in the presence or absence of U_S3 kinase activity. While pU_L34 INM targeting was not affected by the absence of lamin B1 in MEFs infected with wild-type HSV as viewed by indirect immunofluorescence, it localized in densely staining scallop-shaped distortions of the nuclear membrane in lamin B1 knockout cells infected with a U_S3 kinase-dead virus. Lamin B1 knockout cells were relatively less permissive for viral replication than wild-type MEFs, with viral titers decreased at least 10-fold. The absence of lamin A (i) caused clustering of pU_L34 in the nuclear rim of cells infected with wild-type virus, (ii) produced extensions of the INM bearing pU_L34 protein in cells infected with a U_S3 kinase-dead mutant, (iii) precluded accumulation of virions in the perinuclear space of cells infected with this mutant, and (iv) partially restored replication of this virus. The latter observation suggests that lamin A normally impedes viral infectivity and that U_S3 kinase activity partially alleviates this impediment. On the other hand, lamin B1 is necessary for optimal viral replication, probably through its well-documented effects on many cellular pathways. Finally, neither lamin A nor B1 was absolutely required for targeting pU_L34 to the

INM, suggesting that this targeting is mediated by redundant functions or can be mediated by other proteins.

Introduction

Herpesvirus nucleocapsids are assembled in the nucleus and become enveloped initially at the inner nuclear membrane (INM) in a reaction termed primary envelopment (4). The herpes simplex virus U_L31 and U_L34 proteins (pU_L31 and pU_L34, respectively) and their orthologs in other herpesviruses are targeted to the INM and are required for the primary envelopment reaction in many cell lines (70, 113, 169, 170, 181).

Upon infection of restrictive cells such as Vero and Hep2 with herpes simplex virus (HSV) deletion mutants lacking U_L31 or U_L34, nucleocapsids remain in the nucleoplasm and infectious titers are reduced at least 1,000-fold (22, 110, 175).

The U_L34 protein is a type II integral membrane protein of 30,000 M_r, with a predicted 250-amino-acid (aa) nucleoplasmic domain, a 23-aa transmembrane domain, and 5 aa in the perinuclear space (121, 188). The U_L31 protein is a largely hydrophobic phosphoprotein of 32,000 M_r that requires interaction with pU_L34 for targeting to the nucleoplasmic face of the INM (121, 169, 230). While pU_L31 and pU_L34 are incorporated into nascent virions, they are undetectable in extracellular virions, suggesting they are lost from the nascent virion when its envelope fuses with the outer nuclear membrane (62, 170). This observation is consistent with the most prominent model of virion egress in which the de-enveloped nucleocapsid subsequently gains a new envelope by budding into cytoplasmic membranes (194). In the absence of the activity of a serine kinase encoded by alphaherpesvirus genes, such as HSV-1 U_S3, or upon deletion of the HSV genes encoding glycoproteins B and H (gB and gH, respectively), virions accumulate aberrantly in the perinuclear space, suggesting that U_S3, gB, and

gH promote the fusion of the nascent virion envelope with the outer nuclear membrane (54, 94, 170, 176, 220). Interestingly, lamin A, pU_L31, and pU_L34 are phosphorylated by the U_S3 kinase, and the kinase activity is required for smooth localization of the U_L31/U_L34 complex throughout the nuclear rim of infected cells (46, 71, 91, 100). Otherwise, the U_L31/U_L34 complex accumulates aberrantly in discrete foci located at the nuclear rim. At least some of these foci are adjacent to areas of the perinuclear space in which virions accumulate.

How the pU_L31/pU_L34 complex is targeted to budding sites at the INM is an important but unresolved question. Host proteins are sufficient for targeting the complex to the INM because transiently expressed pU_L31 and pU_L34 are cotargeted to the nuclear rim in the absence of other viral proteins (79, 107). A current model proposes that most INM-destined integral membrane proteins in the endoplasmic reticulum use a subset of cytosolic nuclear localization signals to target them past the nuclear pore membrane to the INM via a karyopherin β1-driven pathway (26, 34). The proteins then become anchored to the INM by interaction with relatively immobile elements of the nuclear lamina (50). The nuclear lamina comprises a complex network of proteins that line the entire nucleoplasmic surface of the INM, structurally support the nucleus, and interact with chromatin (72). Intermediate filaments made of proteins called lamins comprise the major structural component of the nuclear lamina (59, 118). Lamins consist of two types, designated A and B. An alternatively spliced version of lamin A produces lamin type C that has a unique carboxyl terminus (59). Lamin B is expressed from two homologous genes, which encode lamin B1 and lamin B2 (76, 77). We previously showed that both pU_L31 and pU_L34 interact with lamin A produced in rabbit reticulocyte lysates, suggesting that this interaction might play a role in anchoring pU_L31/pU_L34 to the INM (162).

The main goal in initiating the current work was to test whether lamins are required for targeting of the pU_L31/pU_L34 complex to the inner nuclear membrane.

Materials and methods

Cells and viruses. Wild-type virus HSV-1(F) and a mutant HSV-1(F), containing a lysine-to-alanine mutation in U_S3 codon 220 (K220A), have been described and were obtained from B. Roizman and R. J. Roller, respectively. The viruses were grown and titers were determined on Vero cells as described previously.

Hep2 cell lines engineered to express green fluorescent protein (GFP) fused to the N terminus of lamin A/C have been described previously (128). An immortalized lamin A/C knockout mouse embryonic fibroblast (MEF) cell line lacking the gene encoding lamin A/C (*Lmna*$^{-/-}$) was a gift from Colin Stewart, NIH (201). To enhance cell adherence, *Lmna*$^{-/-}$ cells were propagated on cultureware pretreated with poly-L-lysine before seeding. Control MEFs (3T3) were obtained from Robert Weiss (Cornell University). This treatment precluded adherence of lamin B1 knockout MEFs (*Lmnb1*$^{-/-}$), and corresponding wild-type MEFs (*Lmnb1*$^{+/+}$) were a generous gift from Karen Reue and have been described elsewhere (217). Pretreatment with poly-L-lysine precluded adherence of these cells and was not used in their propagation. All MEFs were grown in growth medium (Dulbecco's modified Eagle's medium supplemented with 10% fetal bovine serum and antibiotics), except that the *Lmnb1*$^{-/-}$ MEFs and their control wild-type cells were supplemented with additional nonessential amino acids (Gibco) and Glutamax (Gibco).

Antibodies and immunofluorescence. Polyclonal chicken antibody against pU_L34 was a kind gift of Richard Roller and has been described elsewhere (173). Purified polyclonal chicken immunoglobulin Y (IgY) directed against lamin A/C was made

in our laboratory and has been published previously (162). Mouse monoclonal antibody directed against lamin A/C and goat polyclonal IgG directed against lamin B were purchased from Santa Cruz Biotechnology (catalog numbers sc-7292 and sc-6216, respectively).

For immunofluorescence, MEFs grown on glass coverslips were infected with 5.0 PFU of wild-type HSV-1(F) or U_S3(K220A) HSV-1 per cell. Thirteen hours later, cells were fixed with 3% paraformaldehyde in phosphate-buffered saline (PBS) for 20 min, quenched with 50 mM NH_4Cl for 15 min, and then permeabilized with 0.1% Triton X-100. Nonspecific immunoreactivity was blocked by reaction with 10% human serum in PBS for 1 hour at room temperature and another 1 hour with 10% BlockHen II (Aves Lab). The cells were then reacted with anti-pU_L34 chicken IgY diluted 1:400 and goat polyclonal anti-lamin B antibody diluted 1:100 in PBS plus 1% bovine serum albumin for 1 h at room temperature as needed. Bound primary antibodies were recognized by Texas Red- or fluorescein isothiocyanate-conjugated anti-immunoglobulins (Jackson ImmunoResearch).

One-step viral growth curves. *Lmna*$^{-/-}$ and 3T3 MEFs grown in 12-well plates pretreated with poly-L-lysine were infected with 5 PFU of HSV-1(F) or U_S3(K220A) HSV-1 per cell. After 1 h of incubation at 37°C, residual surface infectivity was inactivated with a low-pH wash (40 mM citric acid [pH 3.0], 10 mM KCl, 135 mM NaCl). A similar approach was used for the lamin B knockout cells and 3T3 control MEFS infected in parallel, except that cultureware was not pretreated. At the indicated time points, the cultures were frozen and thawed to lyse the cells, and infectious virus was titrated by plaque assay on Vero cells. Mean values of two independent experiments and corresponding standard deviations were calculated and plotted.

GST pull-down assay and mass spectrometry. Approximately 4 x 10^8 Hep2 cells were infected with 5 PFU/cell of wild-type HSV-1(F). At 16 h postinfection the cells were lysed in 30 ml modified radioimmunoprecipitation assay buffer {50 mM Tris-HCl [pH 7.4], 150 mM NaCl, 1% 3-[(3-cholamidopropyl)-dimethylammonio]-1-propanesulfonate, 0.5% Na-deoxycholate, 0.1% sodium dodecyl sulfate [SDS], 1 mM EDTA} containing 1x Complete protease inhibitor cocktail (Roche) and phosphatase inhibitor (10 mM NaF, 10 mM Na_3VO_4) with gentle rocking for 2 h at 4°C. The lysate was clarified by centrifugation at 10,000 x *g* for 20 min at 4°C, and the supernatant was reacted with glutathione-Sepharose beads (GE) at 4°C. A glutathione *S*-transferase (GST)-pU_L34 fusion protein was affinity purified from lysates of *Escherichia coli* using glutathione-Sepharose beads as described previously (162). The fusion protein was then covalently cross-linked to the Sepharose beads by reaction with 5 mM bis(sulfosuccinimidyl)suberate (Pierce) according to the manufacturer's protocol. GST identically cross-linked to Sepharose beads served as a control. After overnight incubation of the precleared HSV-infected cell lysate with the protein-Sepharose beads bearing GST or GST-pU_L34 at 4°C, the beads were washed two times with ice-cold modified radioimmunoprecipitation assay buffer and then three times with 0.5% Tween 20-PBS. The bound proteins were eluted by boiling for 10 min in SDS-polyacrylamide gel electrophoresis sample buffer (10 mM Tris-HCl [pH 8.0], 10 mM β-mercaptoethanol, 20% glycerol, 5% SDS, trace amounts of bromophenol blue). The eluted proteins were then separated electrophoretically on a 10% polyacrylamide gel (SDS-polyacrylamide gel electrophoresis) and visualized by Sypro ruby staining. Bands overrepresented in the pU_L34-GST pull-down relative to that with GST were excised and submitted for mass spectrometric analysis at the Biotechnology Resource Center, Cornell University, where the proteins in the gel were digested by trypsin and the masses of derived peptides determined by liquid chromatography-mass spectrome-

try (LC-MS). Peptides were identified by comparison to the NCBI Human database using MASCOT software (Matrix Science).

In separate experiments, the GST-pU_L34 fusion protein bound to glutathione-Sepharose beads was reacted with lysates of uninfected Hep2 cells, and proteins bound to the beads were eluted, electrophoretically separated, and identified by LC-MS as described above.

Immunoblotting. Nitrocellulose sheets bearing proteins of interest were blocked in 5% nonfat milk plus 0.2% Tween 20 for at least 2 hrs. The membrane was then probed with lamin A/C mouse monoclonal antibody. Primary antibody was detected by horseradish peroxidase-conjugated bovine anti-mouse secondary antibody (Santa Cruz Biotechnology). All bound immunoglobulins were visualized by enhanced chemiluminescence (Pierce) followed by exposure to X-ray film. Signals were quantified using NIH Image software.

Conventional and immunogold electron microscopy. Cells were fixed with 4% paraformaldehyde (Electron Microscopy Sciences) and 0.25% glutaraldehyde (Electron Microscopy Sciences) in 0.1 M sodium phosphate buffer, pH 7.4, for 30 min at room temperature and then 90 min at 4°C. Cells were washed three times for 5 min each with the same buffer and then dehydrated with a graduated series of ethanol concentrations (10%, 30%, 50%, 70%, and 100%) at 4°C and then –20°C. This was followed by stepwise infiltration with LR-White resin (catalogue no. 14381; Electron Microscopy Sciences) over the course of 48 h at –20°C. Samples were dispensed into gel capsules, and the resin was polymerized at 50°C for 18 h. Thin sections (60 to 90 nm thick) were collected on 300-mesh nickel grids (Ted Pella, Inc., Redding, CA) and floated on drops for the following procedures.

For electron microscopic immunostaining, grids were blocked with 10% normal goat serum and 10% human serum in PBS-0.05% Tween (PBST) and 1% fish gelatin for 15 min at room temperature and were incubated on drops of pU_L34-specific chicken antibody diluted 1:100 in PBST plus 1% fish gelatin for 3 h in a humidity chamber at room temperature. After incubation, grids were washed by brief passage over a series of 3 drops in a high-salt buffer (phosphate-buffered 750 mM NaCl, 0.05% Tween, and 1% fish gelatin) and then 5 drops of 1x PBST and fish gelatin. The secondary antibody, donkey anti-chicken immunoglobulin conjugated with 12-nm colloidal gold, was diluted 1:100 in PBST-1% fish gelatin and reacted for 1 h in a humidity chamber at room temperature. The grids were then washed as before on 6 successive drops of PBST-1% fish gelatin and then rinsed in a beaker of 200 ml of filtered water. Grids were air dried at room temperature prior to staining with 2% aqueous uranyl acetate for 20 min and then Reynolds lead citrate for 7 min. Stained grids were viewed in a Philips 201 transmission electron microscope. Conventionally rendered negatives of electron microscopic images were scanned by using a Microtek Scanmaker 5 and Scanwizard Pro PPC 1.02 software. Positive images were rendered from digitized negatives with Adobe Photoshop software.

Conventional electron microscopy was performed as above except that the cells were fixed in 2.5% glutaraldehyde in 0.1 M Na-cacodylate pH 7.4, followed by 2% OsO_4 and embedded in Epon-Araldyte resin (EM Sciences).

Results

GST-pU_L34 interacts with lamins A and B1 in infected cell lysates. To identify interaction partners that associated with pU_L34, GST or GST fused to the N terminus of full-length pU_L34 (GST/pU_L34) was affinity purified from *Escherichia coli* cells. Lysates of uninfected Hep2 cells or Hep2 cells infected with wild-type HSV-1(F)

were then reacted with GST or the GST/U_L34 fusion protein bound to glutathione-Sepharose beads. Proteins were eluted from the beads in SDS sample buffer, electrophoretically separated on an SDS-polyacrylamide gel, and stained with Sypro ruby. Bands specifically emphasized or unique to the GST/pU_L34 reactions as opposed to reactions with GST alone were excised and digested with trypsin, and the masses of peptides were determined by LC-MS. Within a protein band from infected cell lysates corresponding to approximately 70,000 apparent M_r, the masses of 12 tryptic peptides matched tryptic peptides predicted for human lamin A (Table 3.1). Moreover, a band containing protein of an apparent M_r of 75,000 from uninfected Hep2 cells contained five peptides consistent with human lamin B1. These data indicate that pU_L34 interacts with lamin A/C and lamin B1 in cellular lysates. Although we cannot exclude the possibility that this interaction is indirect, the result combined with our previous observations showing that lamin A and pU_L34 interact in rabbit reticulocyte lysates argue for a direct interaction (162).

To determine whether lamin A/C and lamin B1 were specifically pulled down by GST/pU_L34, the material pulled down by pU_L34/GST and GST alone was electrophoretically separated on SDS-polyacrylamide gels, transferred to nitrocellulose, and probed with either mouse monoclonal antibody directed against lamin A/C or goat polyclonal antibody directed against lamin B (see Materials and Methods). As shown in Fig. 3.1, although some lamin A/C and B1 was bound to Sepharose beads bearing GST alone, the presence of GST-pU_L34 increased the amount of bound lamin A and B1 approximately by five fold as revealed by densitometry. In contrast, lamin C was not overrepresented in the GST/pU_L34 pull down, despite the fact that lamins A and C were present in roughly equal amounts in the infected cell lysate. These data confirm the specificity of the interaction between pU_L34 and lamins A and B1 in cellular lysates and suggest that lamin C is not bound by GST/pU_L34.

Table 3.1 Mass spectrometric parameters of lamin tryptic peptides from GST/pU$_L$34 pull-down assays.

Protein	Exp-*m/z*[a]	Exp-*M*r[b]	Calc-*M*r[c]	Peptide[d]
gi|27436946 Lamin A/C isoform 1 precursor [Homo sapiens]	415.7389	829.4633	829.4909	LQLELSK
	514.7929	1027.5712	1027.5662	LADALQELR
	544.6882	1087.3619	1088.5462	SLETENAGLR
	574.8158	1147.617	1147.5721	ITESEEVVSR
	594.3728	1186.731	1186.6306	LRDLEDSLAR
	680.3711	1358.7277	1358.679	SGAQASSTPLSPTR
	754.3094	1506.6042	1506.7348	TALINSTGEEVAMR
	783.8828	1565.7511	1565.7434	SVGGSGGGSFGDNLVTR
	535.6269	1603.8589	1604.8046	VAVEEVDEEGKFVR
	546.0125	1635.0156	1634.8297	TALINSTGEEVAMRK
	567.3505	1699.0295	1698.9628	IRIDSLSAQLSQLQK
	585.0183	1752.0331	1751.855	NSNLVGAAHEELQQSR
gi|5031877 Lamin B1 [Homo sapiens]	485.34	968.66	968.48	IGDTSVSYK
	577.88	1153.74	1153.61	AGGPTTPLSPTR
	455.29	1817.14	1816.92	SLETENSALQLQVTER
	407.28	2031.36	2031.01	LAQALHEMREQHDAQVR

[a] Mass-to-charge ratio (*m/z*) of experimental peptide.

[b] M_r of experimental tryptic peptide.

[c] Calculated M_r of lamin peptide from database.

[d] Amino acid sequence of matching peptide.

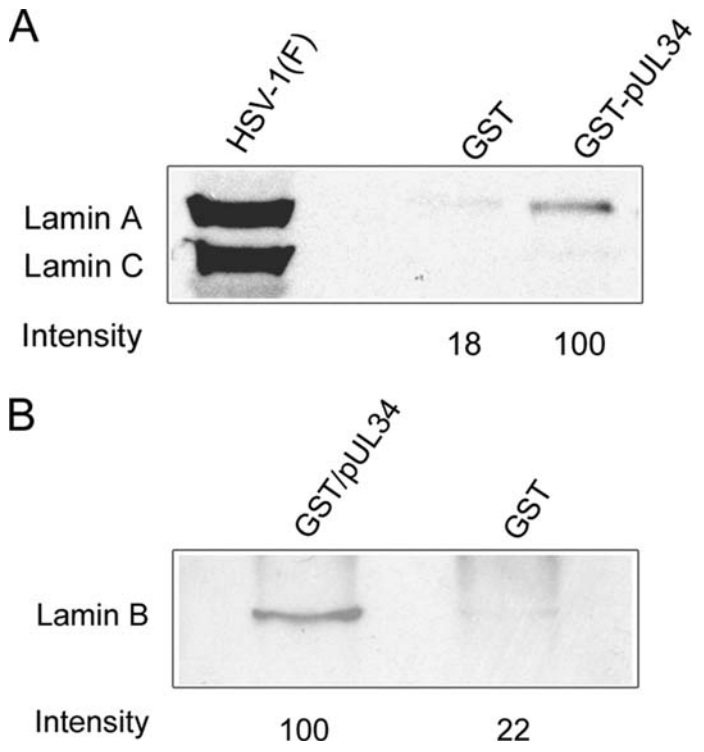

Figure 3.1 Immunoblots of lamin A/C and lamin B pulled down by GST and GST/pU$_L$34. Full-length pU$_L$34 fused to GST or GST alone on glutathione-Sepharose beads was reacted with HSV-1(F)-infected (A) or uninfected Hep2 cell (B) lysates, respectively. Proteins bound to GST fusion proteins were eluted and electrophoretically separated on SDS-polyacrylamide gels, transferred to nitrocellulose, and probed with either a mouse monoclonal antibody against lamin A/C (A) or goat polyclonal antibody against lamin B (B). Bound immunoglobulin was revealed by reaction with appropriate horseradish peroxidase-conjugated secondary antibodies followed by enhanced chemiluminescence. The signal intensities of protein bands were quantified and compared using Image J software, and the relative intensities of individual bands are indicated below corresponding lanes.

Lamin A/C is required for the proper distribution of pU_L34 in infected mouse embryonic fibroblasts. Given the above data suggesting that lamin A and pU_L34 interact in infected cells, we wanted to determine whether the pU_L34-lamin A interaction was involved in targeting pU_L34 to the nuclear membrane. To test this hypothesis, immortalized *Lmna*$^{-/-}$ MEFs or immortalized MEFs were infected with wild-type HSV-1(F), and the localization of pU_L34 was determined by indirect immunofluorescence and confocal microscopy. To assess nuclear shape, the cells were also immunostained with antibody directed against lamin B.

Preliminary experiments indicated that cytopathic effects consequential to HSV infection were accentuated in *Lmna*$^{-/-}$ MEFs as opposed to wild-type MEFs. Specifically, many *Lmna*$^{-/-}$ MEFs underwent dramatic rounding upon infection and subsequently detached from the culture dish by 14 h after infection. By 16 h postinfection, the *Lmna*$^{-/-}$ MEF nuclei were highly distorted in shape, with irregular pU_L34 staining in punctate foci that associated with the nuclear rim (data not shown). Because the exaggerated changes in nuclear shape at late times after infection might affect pU_L34-specific localization indirectly, the cells were fixed at 13 hours postinfection when effects on nuclear shape were less prominent. The cells were then permeabilized and immunostained with antibodies directed against pU_L34 and lamin B. The results are shown in Fig. 3.2.

Optical slices recorded from points midway between the top and adherent surface of the cells revealed that pU_L34-specific immunostaining localized at the nuclear rim of *Lmna*–/– cells, despite the absence of lamin A. On the other hand, the smooth distribution of pU_L34 seen in infected MEFs was not observed in cells lacking lamin A/C. Rather, considerable areas of the nuclear rim of *Lmna* knockout cells were stained with lamin B-specific antibody but lacked detectable pU_L34-specific immunostaining. Other regions of the nuclear rim contained areas with intense pU_L34 immunostaining,

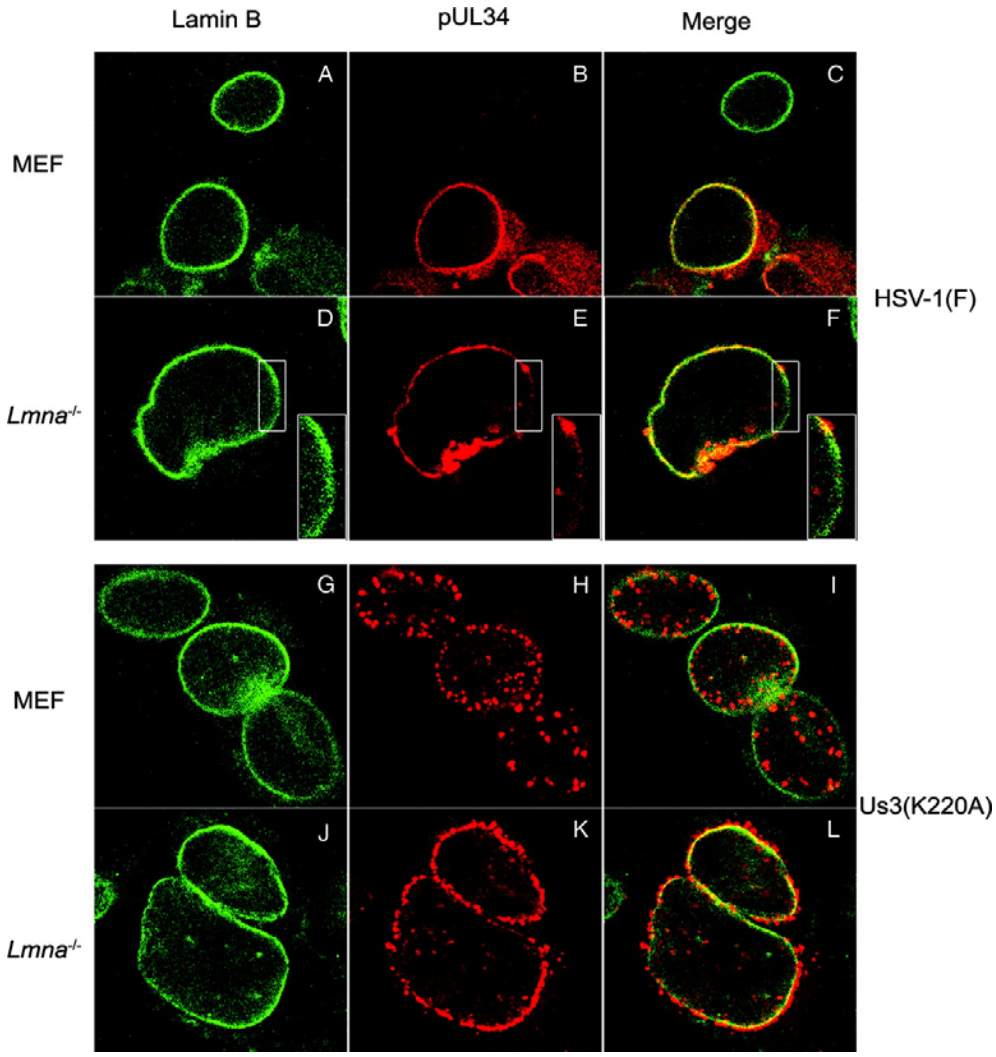

Figure 3.2 Indirect immunofluorescence localization of pU$_L$34 in HSV-1 infected MEFs containing or lacking lamin A/C. Control MEFs or *Lmna*$^{-/-}$ MEFs were infected with either wild-type HSV-1(F) (A to F) or U$_S$3 kinase-dead mutant virus (K220A) (G to L). At 13 h postinfection, cells were fixed in paraformaldehyde and immunostained for lamin B (green) and pU$_L$34 (red) and visualized by confocal microscopy. Optical sections for display were taken through a point between the top and bottom of cells. Insets contain magnified regions delimited by white rectangles in the same panel.

and these regions often overlapped lamin B immunostaining. We conclude that while lamin A/C is dispensable for localization of pU_L34 at the nuclear rim, its presence is required for the normal smooth localization of pU_L34 around the nuclear rim.

Given that lamin A/C was required for the normal distribution of pU_L34 throughout the nuclear rim, we next wanted to determine whether lamin A/C was necessary for localization of pU_L34 at the INM. To test this possibility, *Lmna*$^{-/-}$ or wild-type MEFs were infected with HSV-1(F), and thin sections of the infected cells were reacted with pU_L34-specific IgY followed by reaction with 12-nm colloidal gold-conjugated anti-IgY. As shown in Fig. 3.3, pU_L34-specific immunoreactivity was associated with both the inner and outer nuclear membranes of both cell types (Fig. 3.3A to C). We therefore conclude that lamin A/C is not required for targeting pU_L34 to the INM.

To determine the effects of lamin A/C on HSV-1 replication, *Lmna*$^{-/-}$ and wild-type MEFs were infected with 5.0 PFU/cell of wild-type HSV-1(F), and the virus infectivity was measured at various times after infection. The results, shown in Fig. 3.4, indicated very little difference in the amount of infectious virus produced from the two cell types at all time points. Thus, lamin A/C neither enhanced nor hindered production of wild-type HSV-1(F), at least at high multiplicities of infection.

Effects of U_S3 kinase activity on viral infectivity and localization of pU_L34 in the presence and absence of lamin A/C. The U_S3 kinase phosphorylates lamin A/C and pU_L34, promotes production of infectious virus, and optimizes nuclear egress of virions. To determine whether the effects of U_S3 kinase activity on nuclear egress and pU_L34 localization were dependent on lamin A/C, *Lmna*$^{-/-}$ or wild-type MEFs were infected either with a virus containing a mutation in U_S3 (K220A) that precludes

Figure 3.3. Ultrastructural localization of pU_L34 in MEFs or *Lmna*$^{-/-}$ MEFs infected with HSV-1(F) or U_S3 kinase-dead virus. (A) Wild-type MEFs were infected with HSV-1(F), and localization of pU_L34 was determined by reaction with pU_L34-specific IgY followed by reaction with anti-chicken immunoglobulin conjugated to 12-nm colloidal gold. Arrows indicate positions of gold beads indicative of pU_L34 localization. (B and C) An experiment similar to that in panel A, except that *Lmna*$^{-/-}$ MEFs were used. Colloidal gold beads are present on the INM and are indicated by arrows. (D) Immunogold localization of pU_L34 in MEFs infected with the U_S3 kinase-dead virus. Insets show increased magnifications of the boxed areas and presence of colloidal gold beads on the INM and perinuclear virions. (E and F) Conventionally fixed images of MEFs infected with U_S3 kinase-dead virus showing virions within pouches of nuclear membrane. (G) Immunogold localization of pU_L34 in *Lmna*$^{-/-}$ cells infected with U_S3 kinase-dead virus. Arrows show round extensions of the nuclear membrane emanating into the cytoplasm. The inset shows a negative image of a higher magnification of the boxed area and contains an extension of the INM heavily decorated with pU_L34-specific gold beads. The image is displayed as a negative to more clearly demonstrate the gold beads in white. Despite the presence of pU_L34, neither virions nor nucleocapsids accumulated within the extensions of nuclear membrane.

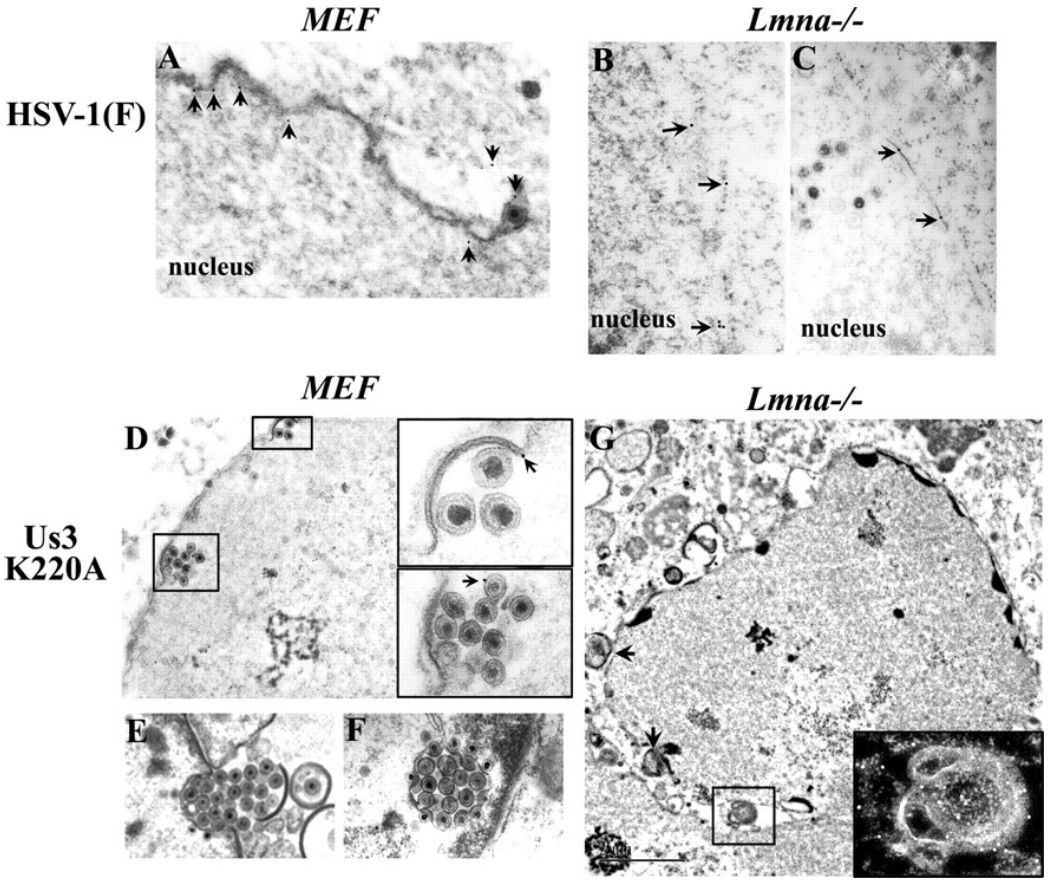
MEF
Lmna-/-
HSV-1(F)
A
B
C
nucleus
nucleus
nucleus
MEF
Lmna-/-
Us3
K220A
D
G
E
F

kinase activity or with wild-type HSV-1(F) virus. As shown in Fig. 3.2G to L, and consistent with results from other cell lines, both cell types exhibited a distribution of pU_L34 that differed from that of cells infected with the virus expressing active U_S3 kinase. Specifically, pU_L34 localized in punctate regions at the nuclear rim, as opposed to the more diffuse distribution seen in the presence of U_S3 kinase activity. On the other hand, the position of the pU_L34-containing foci in *Lmna*$^{-/-}$ cells was most often on the cytoplasmic side of the nuclear rim, whereas these foci were located mostly on the nucleoplasmic side of the nuclear rim in normal MEFs. The latter distribution resembled pU_L34 localization in other cell lines examined previously (174). Thus, although lamin A/C is not required for the punctate distribution of pU_L34 at the nuclear rim of cells infected with the U_S3 kinase-dead virus, it is required to retain these pU_L34-containing foci within the nucleoplasm.

To more precisely analyze the effects of U_S3 kinase activity on virion egress in the presence or absence of lamin A/C, thin sections of *Lmna* knockout MEFs and normal MEFs infected with wild-type and U_S3 kinase-dead viruses were examined by electron microscopy. As shown in Fig. 3.3D, virions accumulated aberrantly in pockets of nuclear membranes of cells infected with the U_S3 kinase-dead virus in normal MEFs. In most cases, these virion-containing regions were located internal to the nuclear rim. The appearance of infected lamin A knockout cells differed substantially in three respects. First, membranous structures that appeared to represent extensions of the INM were often observed (Fig. 3.3G and inset). Secondly, the space between the INM and ONM was often exaggerated relative to uninfected cells and cells infected with wild-type HSV-1(F). Third, virions were not observed to accumulate to a large extent in the perinuclear space, even upon infection with the U_S3 kinase-dead virus. We conclude that lamin A is required for (i) the accumulation of virions in discrete

regions of the perinuclear space normally seen in cells infected with the U_S3 kinase-dead virus and (ii) the morphology of the INM normally seen in infected cells.

To determine whether the concentrations of pU_L34 as revealed by immunofluorescence reflected localization of pU_L34 within the extensions of the INM observed in *Lmna* knockout cells, we performed immunogold electron microscopy on these cells infected with the U_S3 kinase-dead virus. Whereas immunoreactivity with pU_L34-specific antibody was not detected in any cell line infected with the U_L31 null virus (data not shown), extensions of INM were heavily decorated with gold beads reflecting the localization of pU_L34 (Fig. 3.3G, inset). Thus, pU_L34 localization in nuclear membrane extensions correlated with the punctate distribution of *Lmna* knockout cells infected with the U_S3 kinase-dead virus.

To determine the effects of lamin A/C and U_S3 kinase activity on viral infectivity, $Lmna^{-/-}$ MEFs or wild-type MEFs were infected with U_S3(K220A) or HSV-1(F) virus at 5.0 PFU/cell. At various times after infection the cells were lysed and the amount of infectious virus was determined by plaque assay on Vero cell monolayers. As shown in Fig. 3.4, the amount of virus produced by U_S3(K220A) was reduced by at least 10-fold at all times relative to the amount produced by HSV-1(F) regardless of whether the cells produced lamin A/C or not. Perhaps the most striking effect, as noted in previous studies (164, 174), was a delay in the onset of production of infectious virus in the absence of U_S3 kinase activity, resulting in a reduction in viral titer by more than 1,000-fold at 6 h postinfection. This delay occurred whether or not lamin A/C was produced. These data indicate that U_S3 kinase activity enhances both early and late production of infectious virus independently of its effects on lamin A/C.

Pertaining more to the purposes of this report was the observation that infection of $Lmna^{-/-}$ cells with the U_S3(K220A) virus yielded approximately 10-fold more infectious virus at 12 h postinfection relative to the amount produced in wild type MEFs.

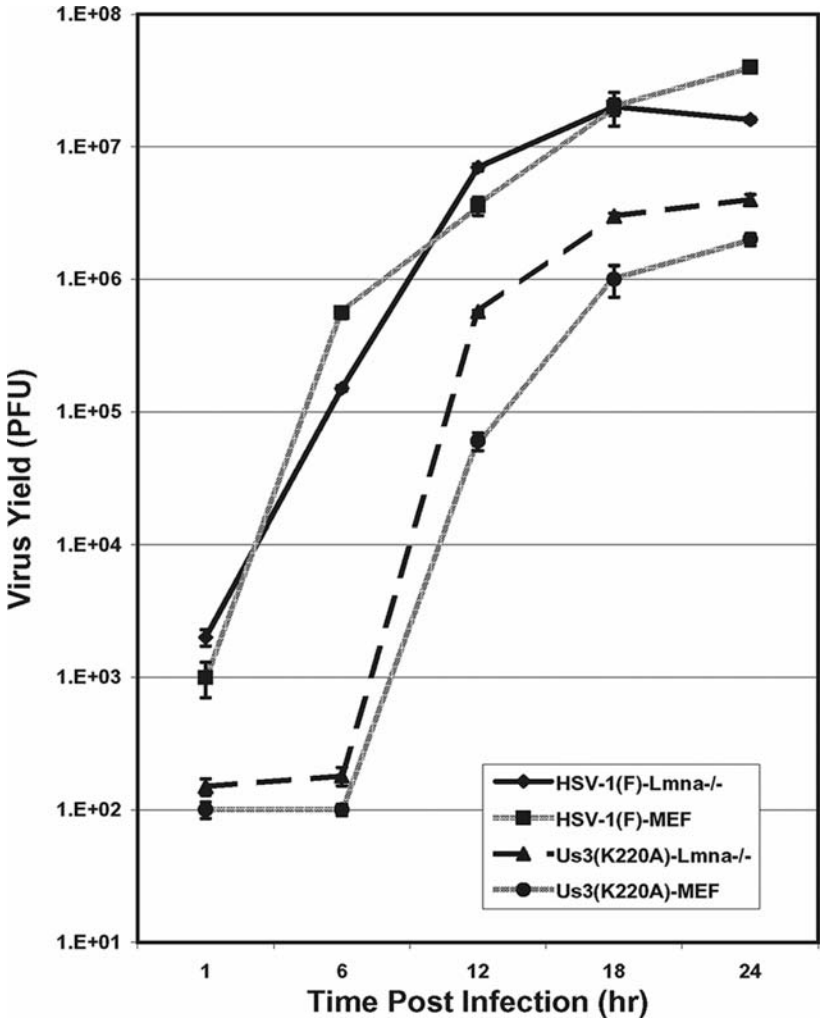

Figure 3.4 One-step growth curve of HSV-1 on normal MEFs or *Lmna*$^{-/-}$ MEFs. Cells were infected with either HSV-1(F) or U_S3(K220A) at 5 PFU per cell. Residual infectivity was inactivated by a low-pH wash at 1 hour postinfection. At the indicated time points, the whole culture was collected, virus was released by freeze-thawing, and infectivity was titrated on Vero cells. Experiments were performed in duplicate. Mean values are plotted, and standard deviations are represented by error bars.

The discrepancy in titer decreased later in infection, such that at 18 and 24 h after infection infectious virus produced by the Lmna knockout cells was increased only fivefold and threefold, respectively, over that obtained from normal MEFs. These data indicate that expression of lamin A/C decreases production of infectious virus and that U_S3 kinase activity partially relieves the lamin A/C-dependent impediment to viral replication.

Lamin B1 is dispensable for localization of pU_L34 to the nuclear rim but is required for normal viral growth. As shown in Table 3.1 and noted above, peptides in the pU_L34/GST pull-down assay were consistent with the predicted masses of tryptic peptides derived from four different regions of lamin B1. To determine whether the interaction between pU_L34 and lamin B was specific, the proteins pulled down with pU_L34/GST or GST were subjected to immunoblotting with lamin B-specific antibody. As shown in Fig. 3.1B, lamin B-specific immunoreactivity was readily detected in the pU_L34/GST pull-down assay, confirming the mass spectrometric analysis. Moreover, densitometry revealed that fivefold less immunoreactivity was detected in the material pulled down with GST. Thus, we conclude that the interaction with lamin B1 was specific, although we could not exclude the possibility that the interaction was indirect.

Given the potential interaction between pU_L34 and lamin B1, we determined whether lamin B1 plays a role in localization of pU_L31 and pU_L34 to the nuclear membrane by using a similar strategy as employed in the study of lamin A. Thus, MEFs lacking lamin B1 were obtained and infected with 5.0 PFU HSV-1(F) or U_S3(K220A) per cell, and the localization of pU_L34 was determined by indirect immunofluorescence 13 h later. As shown in Fig. 3.5, and unlike the effects caused by the absence of lamin A/C, the distribution of pU_L34-specific immunostaining in the

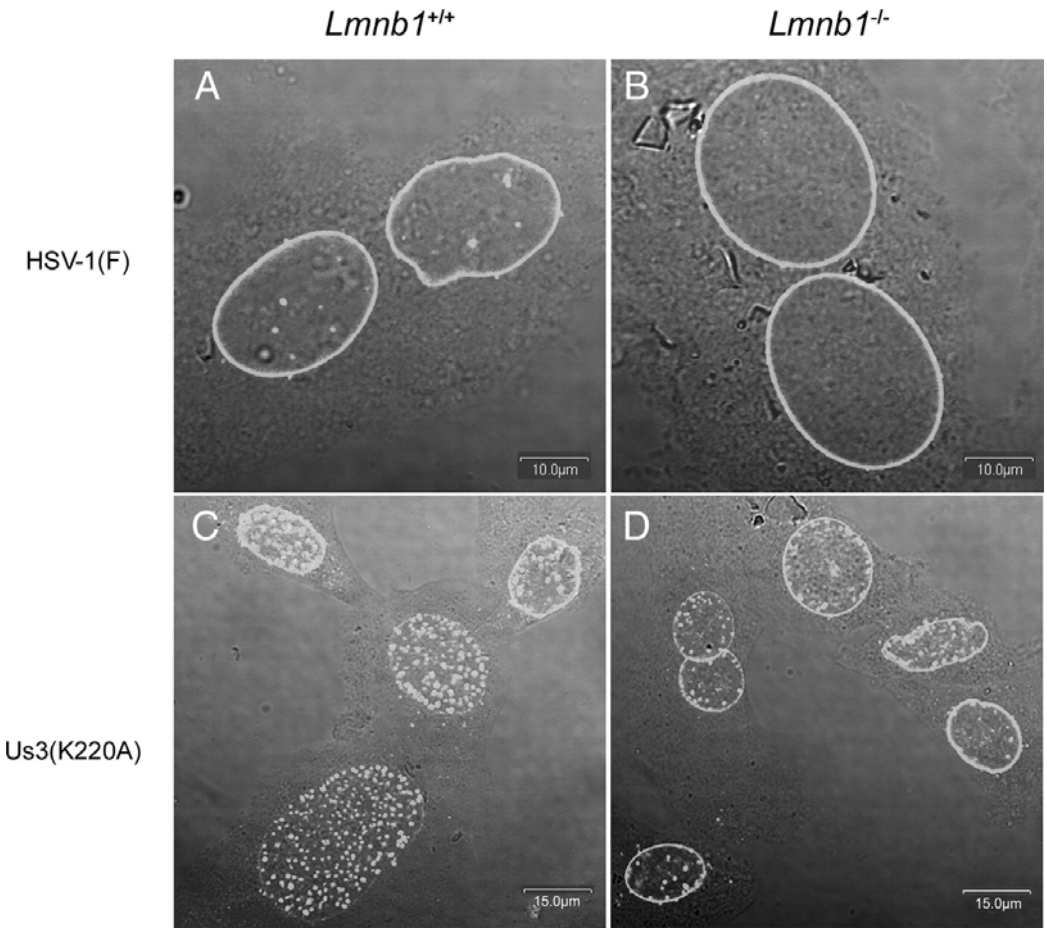

Figure 3.5 Confocal indirect immunofluorescence determination of the distribution of pU_L34 in HSV-1 infected MEFs containing or lacking lamin B1. Wild-type MEFs (A and C) or *Lmnb1*$^{-/-}$ MEFs (B and D) were infected with HSV-1(F) or Us3(K220A) virus, fixed at 13 h postinfection, and immunostained for pU_L34 as described in the legend to Fig. 2. The green channel and transmitted light from optical sections were taken near the middle of infected cells and digitally superimposed for illustrative purposes. The unaltered image was then converted to grayscale in Adobe Photoshop. Bar, 10 μM (upper panels) or 15 μM (lower panels).

lamin B knockout cells was not visibly altered from that seen in wild-type MEFs. On the other hand, HSV-induced cytopathic effects were accentuated in the lamin B1 knockout cells compared with infected normal MEFs. The alteration in cell morphology as a consequence of virus infection was severe enough to pose difficulties in maintaining the lamin B knockout cells on coverslips late after infection (data not shown).

To determine the effects of the U_S3 kinase on distribution of pU_L34 in the absence of lamin B1, the *Lmnb1* knockout cells and wild-type MEFs were infected with the U_S3(K220A) virus and the localization of pU_L34 was determined by indirect immunofluorescence. As shown in Fig. 3.5, pU_L34 localized in a similar punctate distribution at the nuclear rim of both cell lines. On the other hand, the foci in the lamin B1 knockout cells appeared less numerous than those observed in the wild-type MEFs infected with the U_S3 kinase-dead virus.

As shown in Fig. 3.6C, D, and E, representative electron microscopic images of many cells examined revealed that, unlike the case in the lamin A knockout cells, lamin B1 knockout cells infected with the U_S3 kinase-dead virus contained regions of nuclear membrane bearing virions. A feature unique to these cells infected with this virus was the presence of very densely staining scalloped-shaped extensions of what appeared to be the nuclear membrane (Fig. 3.6D and E). These observations taken together with the indirect immunofluorescence studies indicate that lamin B1 is dispensable for targeting of pU_L34 to the nuclear rim of infected MEFs, but it is required for normal nuclear membrane morphology of cells infected with the U_S3 kinase-dead virus.

Immunogold electron microscopy experiments were also performed to determine the localization of pU_L34 in the lamin B1 knockout cells. As shown in Fig. 3.6B, gold beads indicative of the localization of pU_L34 localized at the nuclear rim of cells

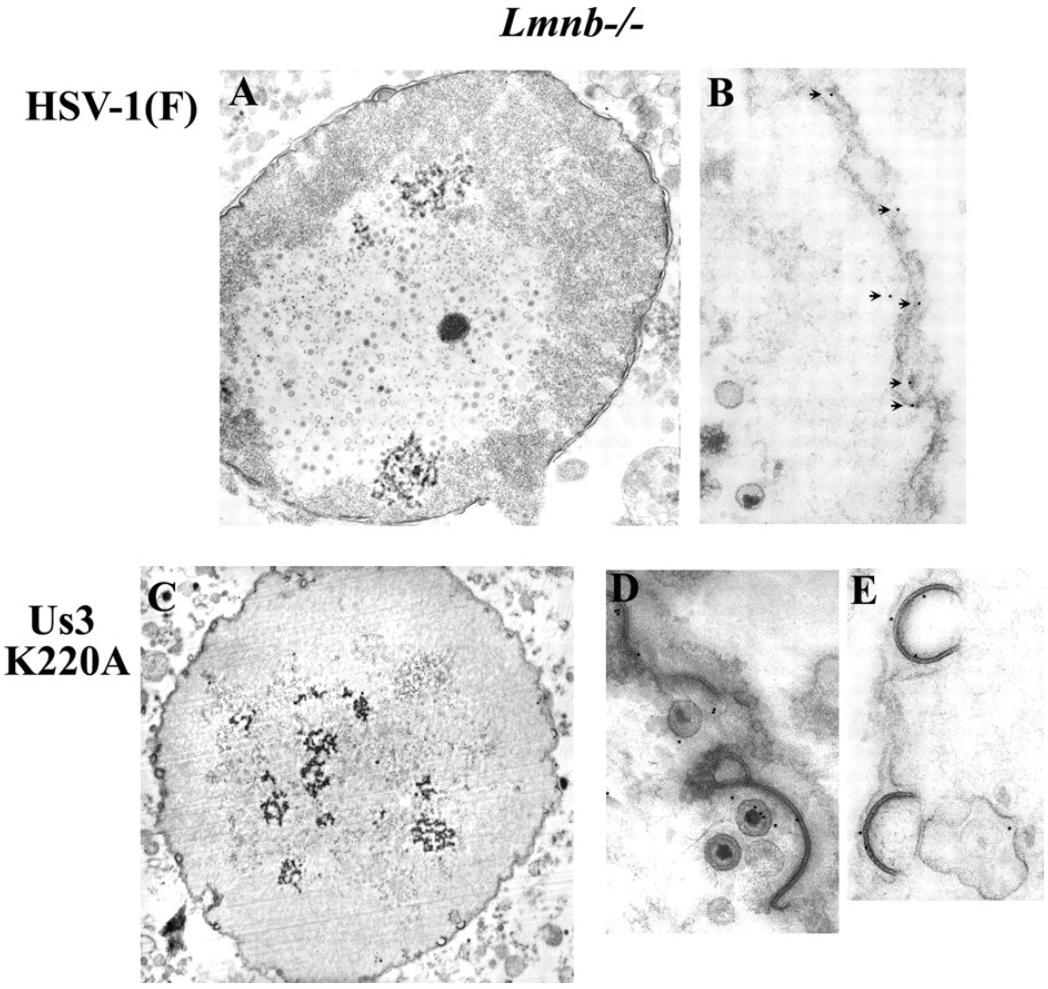

Figure 3.6 Localization of pU$_L$34 in *Lmnb1*$^{-/-}$ cells infected with HSV-1(F) or U$_S$3(K220A) viruses. (A) Low magnification of an HSV-1(F)-infected cell. (B) Section of nuclear membrane of cell infected with HSV-1(F). Positions of gold beads indicative of pU$_L$34 localization are indicated by arrows. (C) Low magnification of lamin B1 knockout MEF cell infected with U$_S$3 kinase-dead virus. (D and E) Higher magnification of cells infected with U$_S$3 kinase-dead virus, showing several gold beads associated with scalloped dense-staining nuclear membrane and perinuclear virions. As a size standard, capsids are 125 nm in diameter.

infected with the wild-type virus. Moreover, pU_L34-specific immunoreactivity was noted at the INM of lamin B1 knockout cells infected with the U_S3 kinase-dead mutant. This immunostaining localized mostly within the densely staining, scallop-shaped regions of the nuclear membrane or was associated with nearby virions (Fig. 3.6D and E). These data therefore indicate that lamin B1 is dispensable for targeting pU_L34 to the INM but necessary for the normal morphology of the nuclear membrane in the absence of U_S3 kinase activity.

We next examined the effects of the absence of lamin B1 on viral infectivity in the presence and absence of the U_S3 kinase. As shown in Fig. 3.7, the lamin B1 knockout cells were less permissive to HSV replication than normal MEFs, regardless of whether the U_S3 kinase was active. Specifically, titers at all time points in wild-type MEFs were at least 10-fold greater than those reached in the lamin B1 knockout cells infected with either wild-type virus or the U_S3 mutant virus. We therefore conclude that lamin B1 contributes substantially to the production of infectious virus, but this does not reflect a role in targeting pU_L34 to the INM.

Discussion

Taken together, the data presented herein indicate that targeting of pU_L34 to the INM and aggregation in the absence of U_S3 kinase activity are not dependent on expression of lamin A/C or B1, despite the observation that these proteins were shown to interact with pU_L34 in infected cell lysates. On the other hand, the absence of lamin A/C altered the normal smooth distribution of pU_L34 as revealed by indirect immunofluorescence, suggesting that it is directly or indirectly involved in pU_L34 distribution within the nuclear rim. In contrast, lamin B1 was entirely dispensable for pU_L34 targeting to the nuclear rim, as viewed by indirect immunofluorescence, and to the INM, as viewed by immunogold electron microscopy. Thus, lamin A or lamin A-

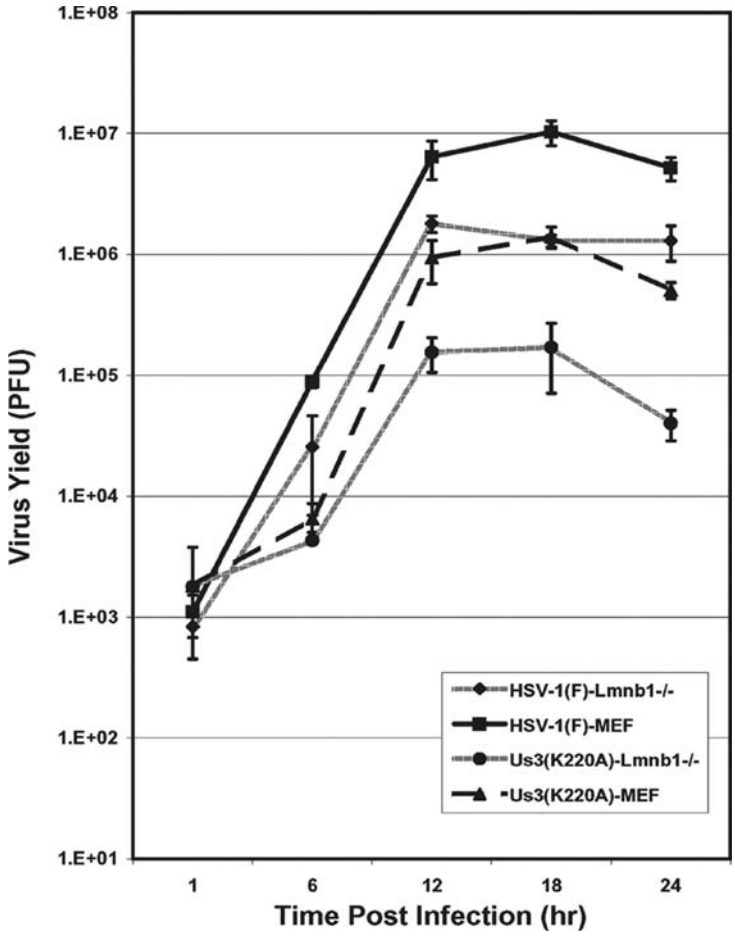

Figure 3.7 Growth curves of HSV-1(F) or U_S3 kinase-dead virus in MEFs or *Lmnb1*$^{-/-}$ MEFs. The experiment was performed similarly to that described in the legend to Fig. 3.4.

interacting components of the nuclear lamina are more relevant to pU_L34 targeting than lamin B1 or lamin B1-interacting components. The effects of lamin A on pU_L34 targeting may reflect effects of lamin A on lamina mechanics and stiffness, functionswhich are largely independent of lamin B1 (102). Alternatively, data obtained in this study and in previous work in which lamin A, pU_L31, and pU_L34 were shown to interact in pull-down assays from rabbit reticulocyte lysates suggest that the lamin A-pU_L34 interaction is direct and may play a role in pU_L34 targeting (162). The data are also consistent with the observation that emerin, a lamin A-interacting protein, can interact with pU_L34 and is displaced in HSV-infected cells in a pU_L34-dependent manner (103). Whether the emerin-pU_L34 interaction is mediated through interactions with lamin A/C will require further studies. A final possibility is that lamin B1 is involved in INM targeting of pU_L34, but lamin A confers redundant functions that compensate for the absence of lamin B1.

An untested but widely accepted hypothesis is that the nuclear lamina poses a barrier that herpesviruses must breach to allow nucleocapsids access to the INM for envelopment. Along these lines, previous observations indicated that the lamina is disrupted in HSV-infected cells in a pU_L31/pU_L34-dependent manner (15, 128, 162, 185, 186). Several studies have identified mechanisms by which pU_L31/pU_L34 of HSV may accomplish nuclear lamina disruption. Specifically, protein kinase C-δ and -α have been shown to be recruited to the nuclear membrane in a pU_L31/pU_L34-dependent manner to augment lamin B phosphorylation, whereas U_S3 has been shown to phosphorylate lamin A directly in vitro and to be required for its optimal phosphorylation in infected cells (128, 146). Moreover, pU_L31/pU_L34 may have their own lamina-depolymerizing activities inasmuch as overexpression of these proteins in the absence of other proteins is sufficient to disrupt the lamina, and locally high concentrations of pU_L31/pU_L34 exaggerate adjacent lamina perforations (15, 128, 162, 185). The obser-

vation in this study that lamin A knockout cells are more permissive to replication of a U_S3 kinase-dead virus at high multiplicities of infection further argues that at least lamin A poses a barrier to replication (and presumably nucleocapsid envelopment) and that U_S3 helps to overcome this barrier. Thus, disruption of the lamina might indeed reflect an important role for these proteins in promoting virion budding at the INM.

Despite their relative permissiveness to virus replication at high multiplicities of infection, the lamin A knockout cells exhibited altered NM morphology when infected with the U_S3 kinase-dead virus. Specifically, exaggerated extensions of the INM and increased space between the INM and ONM were noted. Because these effects were precluded by U_S3 kinase activity, it follows that substrates of U_S3 kinase other than lamin A are responsible for these phenotypes. Previous studies reported increased spacing between the INM and ONM upon overexpression of U_L34, pU_L31/pU_L34-dependent alterations of the nuclear lamina, and budding from the INM upon coexpression of pU_L31 and pU_L34 of pseudorabies virus in the absence of capsids (93, 236). Thus, the effects on nuclear membrane morphology induced by the combined absence of U_S3 kinase activity and lamin A might be consequential to increased concentration of pU_L34/pU_L31 in certain regions of the INM. This is consistent with the observation by immunogold electron microscopy that pU_L34 was specifically detected in the unusual nuclear membrane extensions observed in this study.

Also interesting to us was the absence of virions trapped within the perinuclear space of the *Lmna* knockout MEFs infected with the U_S3 kinase-dead virus, despite the fact that this feature was commonplace in similarly infected normal MEFs. Thus, lamin A is somehow required for the observed retention of virions in discrete regions within the perinuclear space. We speculate that this reflects the general permissivity of primary envelopment in the lamin A knockout cells. Thus, capsids may bud through the INM at multiple sites in the absence of lamin A, whereas the positions of envelop-

ment sites are more restricted by the lamin A-imposed barrier in normal MEFs. The absence of U_S3 kinase activity would still delay fusion of the virion envelope and ONM, but the wide dispersal of virions in the perinuclear space of *Lmna* knockout cells would preclude virion aggregation. Alternatively, we cannot rule out the possibility that the nuclear envelope is generally more fragile in the lamin A knockout cells, thus precluding stable association of virions within the perinuclear space of cells as they are pelleted prior to fixation for electron microscopy.

We also noted that pU_L34-containing regions mostly localized external to the nuclear membrane in lamin A knockout cells infected with the U_S3 kinase mutant but internal to the nuclear membrane in MEFs or lamin B1 knockout cells infected with this virus. We speculate that lamin A, by enhancing lamina stiffness, restrains locally high concentrations of the pU_L31/pU_L34 complex from inducing cytoplasmic protrusions of the nuclear membrane, although we cannot exclude more indirect mechanisms.

In striking contrast to the results with lamin A, *Lmnb1* knockout MEFs were less permissive to viral replication at high multiplicities of infection, and this was observed in both the presence and absence of U_S3 kinase activity. The role of lamin B1 in HSV infection is unclear, but it is required for a number of important nuclear functions including transcription, DNA replication, cell signaling, and optimal reassembly of the nucleus after mitosis (196). Thus, disturbance of any of these or related functions might render the cells less permissive by impairing the machinery that the virus ultimately needs to commandeer for optimal infection. This may be one reason why alteration of the nuclear lamina during viral infection is mostly limited to very discrete regions. Such a strategy might limit detrimental effects on the cell while still allowing nucleocapsids to bud through the INM.

Acknowledgements

We thank Richard Roller for the U_S3 kinase-dead virus and pU_L34 antibody, Karen Reue for the *Lmnb1* knockout and control MEFs, and Colin Stewart for the *Lmna* knockout MEFs.

These studies were supported by R01 grant AI52341 from the National Institutes of Health.

CHAPTER IV

PHOSPHORYLATION OF THE U_L31 PROTEIN OF HERPES SIMPLEX VIRUS 1 BY THE U_S3 ENCODED KINASE REGULATES LOCALIZATION OF THE NUCLEAR ENVELOPMENT COMPLEX AND EGRESS OF NUCLEOCAPSIDS

Fan Mou, Elizabeth Wills, and Joel D. Baines

Department of Microbiology and Immunology, College of Veterinary Medicine

Cornell University, Ithaca, NY 14853

Abstract

Herpes simplex virus 1 (HSV-1) nucleocapsids bud through the inner nuclear membrane (INM) into the perinuclear space to obtain a primary viral envelope. This process requires a protein complex at the INM composed of the U_L31 and U_L34 gene products. While it is clear that the viral kinase encoded by U_S3 regulates the localization of pU_L31/pU_L34 within the INM, the molecular mechanism by which this is accomplished remains enigmatic. Here, we have determined that (i) the N-terminus of pU_L31 is indispensable for the protein's normal function and contains up to 6 serines that are phosphorylated by the U_S3 kinase during infection. (ii) Phosphorylation at these 6 serines was not essential for productive infection, but was necessary for optimal viral growth kinetics. (iii) In the presence of active U_S3 kinase, changing the serines to alanine caused the pU_L31/pU_L34 complex to aggregate at the nuclear rim and caused some virions to accumulate aberrantly in herniations of the nuclear membrane, much as in cells infected with a U_S3 kinase-dead mutant. (iv) Replacement of the 6 serines of pU_L31 with glutamic acid largely restored the smooth distribution of pU_L34/pU_L31 at the NM, and precluded the accumulation of virions in herniations whether or not U_S3 kinase was active, but also precluded optimal primary envelopment of nucleocapsids. These observations indicate that phosphorylation of pU_L31 by pU_S3 represents an important regulatory event in the virion egress pathway that can account for much of pU_S3's role in nuclear egress. The data also suggest that the dynamics of pU_L31 phosphorylation modulate both primary envelopment and subsquent fusion of the nascent virion envelope with the outer nuclear membrane.

Introduction

The U_L31 and U_L34 proteins of herpes simplex virus 1 (HSV-1) form a complex that locates at the inner nuclear membrane (INM) of infected cells (163, 164). This

complex is essential for budding of nucleocapsids through the INM into the perinuclear space (163, 173). pU_L34, an integral membrane protein with a 247 amino acid nucleoplasmic domain, binds pU_L31 and holds the latter in close approximation to the INM (117, 163, 232, 235). Both proteins become incorporated into nascent virions indicating they directly or indirectly interact with nucleocapsids during the budding event (164). Interestingly, co-expression of the pseudorabies virus homologs of HSV pU_L31 and pU_L34 are sufficient to induce budding from the INM in the absence of other viral proteins (91).

The most prominent model of nuclear egress proposes that the step following primary envelopment involves fusion of the perinuclear virion envelope with the outer nuclear membrane (ONM), allowing subsequent steps in which the de-enveloped capsid engages budding sites in the Golgi or trans-Golgi network (123, 194). The U_S3 protein is a promiscuous kinase that phosphorylates pU_L31, pU_L34, and several other viral and cellular components (13, 14, 20, 89, 103, 128, 129, 152, 153, 156, 174). In the absence of pU_S3 kinase activity (i) virions accumulate within the perinuclear space, often causing distensions of this space that herniate into the nucleoplasm (93, 164, 174), (ii) the pU_L31/pU_L34 complex is mislocalized at the nuclear rim from a smooth pattern to discrete foci that accumulate adjacent to nuclear membrane herniations and (iii) the onset of infectious virus production is delayed (128, 174).

Aberrant accumulations of perinuclear virions similar to those observed in cells infected with U_S3 kinase-dead viruses have been observed in cells infected with viruses lacking the capacity to produce glycoproteins H and B (gH and gB, respectively) (56). Because these proteins are required for fusion with the plasma membrane or endocytic vesicles during HSV entry (3, 65, 161), it has been speculated that the accumulation of perinuclear virions in the absence of gH and gB reflects a failure in the apparatus that normally mediates fusion between the nascent virion envelope and

ONM. By extension of this hypothesis, pU_S3 might act to trigger this perinuclear fusion event.

The substrate(s) of pU_S3 kinase responsible for the altered localization of the pU_L31/pU_L34 complex and aberrant accumulation of perinuclear virions is unknown. In one study to identify such a substrate, it was determined that precluding phosphorylation of pU_L34 was not responsible for the nuclear egress defects induced by the absence of pU_S3 or its kinase activity (174). The current study was therefore undertaken to investigate the hypothesis that pU_S3-mediated phosphorylation of pU_L31 is critical to regulate nuclear egress. Evidence presented herein indicates that aspects of the U_S3 kinase-dead phenotype, including retention of virions in the perinuclear space, mislocalization of the pU_L31/pU_L34 complex, and delayed onset of virus replication, can be replicated by precluding pU_L31 phosphorylation in the presence or absence of pU_S3 kinase activity. The data also suggest that dynamic phosphorylation of pU_L31 is important for efficient primary envelopment of nucleocapsids.

Materials and methods

Cells and viruses. Wild type virus HSV-1(F), U_L31 null virus, and mutant virus containing a Lysine to Alanine mutation in U_S3 codon 220 (K220A), have been described and were obtained from B. Roizman and R. J. Roller, respectively (24, 49, 174). The HSV-1(F) and U_S3(K220A) viruses were propagated and titered on Vero cells, whereas the U_L31 null virus was grown and titered on a U_L31-expressing rabbit skin cells described previously (107).

Plasmids. For transient expression, the U_L31 gene was cloned into the pcDNA3 vector (Invitrogen) or into the pBudCE4.1 vector (Invitrogen) with a FLAG epitopic tag on the 3' end as indicated. Full length U_L31 ORF in pcDNA3 was previously de-

scribed (163). The U_L31-pcDNA3 then served as a template for other pcDNA3 or pBudCE4.1 constructs using PCR primers listed in Table 4.1. pGEX4T vectors (Amersham) were used for GST fusion expression plasmids. The construction of GST fused to full length U_L31 was also reported previously (163). Standard cloning methods were used to generate a series of GST fusion subclones. Briefly, U_L31 sequences were amplified from HSV-1 (F) genomic DNA using the primers listed in Table 4.1. The amplicons were first ligated into the pCR2.1 vector (Invitrogen) using TA cloning, and were flanked by EcoRI restriction sites as a result. The EcoRI fragments containing U_L31 sequences were subcloned into the EcoRI site of the pGEX4T vector (Amersham) in frame with the GST gene. To generate the point mutant plasmids, U_L31 were amplified from the corresponding mutant viral BAC DNAs bearing such mutations (described below); these amplicons were then cloned into the pGEX4T vector at the EcoRI and XhoI sites.

Recombinant viruses and BAC mutagenesis. A series of recombinant viruses were constructed using en passant mutagenesis of a bacterial artificial chromosome (BAC) containing the entire HSV-1(F) genome as previously described (205). Briefly, a PCR amplicon bearing fragments containing a Kan resistance cassette, Sce-I restriction endonucleae site and desired mutations flanked by homologous regions to the target gene was generated with primer pairs listed in Table 4.2 and pEPkan-S plasmid as template. The resulting amplicons were electroporated into recombination competent GS1783 *E. coli*, which harbors the target BAC and a Sce1 endonuclease gene integrated into its genome (a kind gift of Greg Smith). Following Kanamycin resistance screening and restriction length polymorphism (RFLP) confirmation, the Kan^R sequence was removed by RED recombination between internal homologous sequences that were generated through SceI cleavage, which was initiated by arabinose-induced

Table 4.1 Vectors and primers used to generate U_L31 subclones (restriction sites used for cloning were underlined and Flag sequence was colored in red).

Plasmids	UL31 codons	Vectors	Primers
U_L31(dN)-pCDNA3	AA 45-306	pcDNA3	5'-ATACTCGAGATGCCGCCTCACG-3' 5'-TATACTCGAGCTACGGCGGAGGAAAC-3'
U_L31-Flag	AA 1-306	pBudCE 4.1	5'-ATACTCGAGACCTATGTATGACACCGACCC-3' 5'-ATAAGATCTTACTTATCGTCGTCATCCTTGTAATCCGGCGGAGGAAACTC-3'
U_L31(dN)-Flag	AA 45-306	pBudCE 4.1	5'-ATACTCGAGACCTATGCCGCCTCACG-3' 5'-ATAAGATCTTACTTATCGTCGTCATCCTTGTAATCCGGCGGAGGAAACTC-3'
GST-U_L31 (1-50aa)	AA 1-50	pCR2.1 pGEX4T-2	5'-ATGTATGACACCGACCCCCATC-3' 5'-TTTGCGGGCGTGAGGC-3'
GST-U_L31 (52-165aa)	AA 52-165	pCR2.1 pGEX4T-1	5'-TCTCGAGATGGAGGAGCTGTGTTTAC-3' 5'-TCTAGGCCAACACGACCAA -3'
GST-U_L31 (159-265aa)	AA 159-265	pCR2.1 pGEX4T-1	5'-GCTCGAGATGGTGGCCTCCTTGGTC-3' 5'-CCTAGTCCGTGGGTTTCTCTGCGTT-3'
GST-U_L31 (255-306)	AA 259-306	pCR2.1 pGEX4T-1	5'-CCTCGAGATGGGCAACGCAGAGAAACC-3' 5'-CCTACGGCGGAGGAAACTC-3'
GST-U_L31(SA3)	AA 1-306	pGEX4T-1	5'-TAGAATTCATGTATGACACCGACCCCCATC-3' 5'-TATACTCGAGCTACGGCGGAGGAAAC-3'
GST-U_L31(SA6)	AA 1-306	pGEX4T-1	5'-TAGAATTCATGTATGACACCGACCCCCATC-3' 5'-TATACTCGAGCTACGGCGGAGGAAAC-3'

Table 4.2 Primers for BAC mutagenesis (introduced mutations were colored in red).

BAC	Primers
U_L31(dN)	5'-ATC TCG CTC CTG TCC CTG GAG CAC ACC CTG TGT ACC TAT GCC GCC TCA CGC CCG CAA ACA TAG GGA TAA CAG GGT-3' 5'-GCT CGT GTA AAC ACA GCT CCT GTT TGC GGG CGT GAG GCG GCA TAG GTA CAC AGG GTG TGC GCC AGT GTT ACA ACC-3'
U_L31(SA3)	5'-TCG ATC TCG CTC CTG TCC CTG GAG CAC ACC CTG TGT ACC TAT GTA TGA CAC CGA CCC CAT CGC CGC GGC GCC CGG CCC GGG CCC TAT CAC GGC AAG GAG CGC CGG CGG GCG CGC TCC TCT GCG GCC GGC GTA GGG ATA ACA GGG T-3' 5'-GGC CCC GAT AGC GCT GGC GCT CGT GTA AAC ACA GCT CCT GTT TGC GGG CGT GAG GCG GCA GGC TCT TCC GGG CGG CCC GAC GCA CCA CGC CCA GAG TCC CGC CGG CCG CAG AGG AGC GCG CCC GCC GGC GCT CCT TGC CAG TGT TAC AAC C-3'
U_L31(SA6)	5'-GCC CGG GCC CTA TCA CGG CAA GGA GCG CCG GCG GGC GCG CGC TGC TGC GGC CGG CGG GAC TCT GGG CGT GGT GCG TCG GGC CGC CCG GAA GTA GGG ATA ACA GGG T-3' 5'-CGT GTA AAC ACA GCT CCT GTT TGC GGG CGT GAG GCG GCA GTG CCT TCC GGG CGG CCC GAC GCA CCA CGC CCA GAG TCC CGC CGC CAG TGT TAC AAC C-3'
U_L31(SAR)	5'-GGG CCT CCC GGA AGA GCC TGC CGC CTC ACG CCC GCA AAC AGG AGC TGT GTT TAC ACG AGC TAG GGA TAA CAG GGT-3' 5'-GCT CGT GTA AAC ACA GCT CCT GTT TGC GGG CGT GAG GCG GCA TAG GTA CAC AGG GTG TGC GCC AGT GTT ACA ACC-3' Amplicon generated using above primers were PCR fused with a second amplicon generated from wild type HSV-1 (F) genomic DNA with primer pair 5'-tgcatagcgttgcgtgcc-3' and 5'-tttgcgggcgt gaggc-3' to obtain the 5' extension required for homologous recom-bination.

Table 4.2 (Continued)

BAC	Primers
U_L31(SAE)	5'-CCC GGG CCC TAT CAC GGC AAG GAG CGC CGG CGG GCG CGC GAA GAA GCG GCC GGC GGG ACT CTG GGC GTG GTG CGT CGG GCC GCC CTA GGG ATA ACA GGG T-3' 5'-GTG TAA ACA CAG CTC CTG TTT GCG GGC GTG AGG CGG CAG TTC CTT CCG GGC GGC CCG ACG CAC CAC GCC CAG AGT CCC GCC GGC CGC CAG TGT TAC AAC C-3'
U_L31(SE6)	5'-TCG ATC TCG CTC CTG TCC CTG GAG CAC ACC CTG TGT ACC TAT GTA TGA CAC CGA CCC CAT CGC CGC GGC GAA CGG CCC GGG CCC TAT CAC GGC AAG GAG CGC CGG CGG GAA CGC GAA GAA GCG GCC GGC GTA GGG ATA ACA GGG T-3' 5'-GGC CCC GAT AGC GCT GGC GCT CGT GTA AAC ACA GCT CCT GTT TGC GGG CGT GAG GCG GCA GTT CCT TCC GTT CGG CCC GAC GCA CCA CGC CCA GAG TCC CGC CGG CCG CTT CTT CGC GTT CCC GCC GGC GCT CCT TGC CAG TGT TAC AAC C-3'
U_L31(SE6)/ U_S3(K220A)	5'-TGA CAG CAG CCA TCC AGA TTA CCC CCA ACG GGT AAT CGT GGC GGC GGG GTG GTA CAC GAG CAT AGG GAT AAC AGG GTA ATC GAT TT-3' 5'-CAG TCG CGC CTC GTG GCT CGT GCT CGT GTA CCA CCC CGC CGC CAC GAT TAC CCG TTG GGG GTG CCA GTG TTA CAA CCA ATT AAC C-3'

SceI expression in GS1783 *E. coli*. Positive clones were verified through Kanamycin selection and further by RFLP and DNA sequencing (not shown). Rabbit skin cells were transfected with the BAC and a plasmid encoding FRT recombinase to remove the BAC sequences as described previously (107). Viral plaques were propagated into viral stocks using Vero cells.

All the BACs were designated according to their genotypes. Before obtaining the U_L31(SA6) BAC, the sequence of the U_L31 gene from 3 to 132 nucleotides was first deleted from wild type HSV-1 (F) BAC, producing an intermediate BAC designated U_L31(dN). The deleted region bearing designed mutations was then inserted, thus changing codons 11, 24 and 40 from serine into alanine. The resulting BAC was named U_L31(SA3), which then served as the parental BAC to generate U_L31(SA6) BAC by changing serine codons 26, 27 and 43 to alanine. The repair BAC U_L31(SAR) was created by repeating the deletion step starting with the U_L31(SA6) BAC, thus re-generating the intermediate U_L31(dN) genotype, followed by insertion of wild type sequences. In a separate experiment, this U_L31(dN) BAC served as the recipient of mutations changing codons 11, 24, 26, 27, 40 and 43 to those encoding glutamic acid. This BAC was designated BAC U_L31(SE6). The U_L31(SAE) BAC was derived from the BAC U_L31(SA6) by mutating alanine codons 26, 27 and 43 into glutamic acid codons. Incorporation of mutations substituting lysine codon 220 of U_S3 with alanine in the U_L31(SE6) BAC led to the double mutant BAC UL31(SE6)/Us3(K220A).

***In vitro* U_S3 kinase assays.** A kinase assay was performed using purified GST-pU_S3 essentially as described previously (128). Briefly, 0.1 μg GST-pU_S3 was incubated separately with approximately 1 μg of pU_L31-GST fusion proteins partially purified from *E. coli* and bound to glutathione Sepharose beads. The kinase reaction was performed for 30 minutes at 30^{o}C in 50 μl pU_S3 specific kinase buffer (50mM Tris

[pH9.0], 20mM MgCl2, 0.1% NP40, 1mM DTT) containing 10 μM ATP and 10 μCi [γ-^{32}P] ATP (Amersham). The Sepharose beads bearing the fusion proteins were then washed three times with TNE buffer (20 mM Tris-HCl [pH 8.0], 100 mM NaCl, 1 mM EDTA). The proteins were eluted in SDS-PAGE sample buffer (10 mM Tris-HCl [pH 8.0], 10 mM β-mercaptoethanol, 20% glycerol, 5% SDS, trace amounts of bromophenol blue)] and subjected to electrophoresis in a 12% polyacrylamide gel in the presence of 0.1% SDS. Gels were then stained with Coomassie brilliant blue, dried and autoradiographed using X-ray film (Pierce).

Transient complementation assay. Hep2 cells were seeded at 90% confluence in 12 well plates and were transfected with 1.6 μg plasmid DNA using lipofectamine (Invitrogen). After 20 hr incubation at 37^{o}C, the cells were infected with 5.0 PFU per cell of the U_L31 null virus. At 24 hpi, whole cell cultures were lysed for viral titering on U_L31 expressing rabbit skin cells. Experiments were performed in duplicate. Means and standard deviations were calculated and plotted.

One-step viral growth assay. 100% confluent Vero cells grown in 12-well plates were infected with 5.0 PFU per cell of the indicated viruses. After 1 hr incubation at 37^{o}C, residual surface infectivity was inactivated with a low-pH wash (40mM Citric Acid [pH 3.0], 10mM KCl, 135mM NaCl). At the indicated time points, the cultures were frozen and thawed to lyse the cells, and infectious virus was titrated by plaque assay on Vero cells. The mean values of two independent experiments and corresponding standard deviations were calculated and plotted.

Antibodies and Immunofluorescence assay. Polyclonal chicken antibody against pU_L34 was a kind gift from R. J. Roller. Rabbit anti-pU_L31 antisera were pre-

pared in our laboratory and was described previously (163). M2 mouse monoclonal antibody against the Flag epitopic tag was purchased from Sigma.

Hep2 cells growing on glass coverslips were mock infected or were infected with the indicated viruses at an MOI of 5 PFU/cell for 16 hrs. Cells were fixed with 3% PFA for 15 min. In experiments where the pre-adsorbed pU_L31-specific rabbit polyclonal antibody was to be used, the cells were treated for another 15 min at –20 C in methanol. The cells were then permeabilized with 0.1% Triton-X 100 and reacted with 10% human serum in phospho-buffered saline (PBS) to block nonspecific immunoreactivity, and subsequently probed with the pre-adsorbed pU_L31 antiserum diluted 1:50 in PBS supplemented with 1 % BSA. Thereafter, 10% BlockHen II (Aves Lab) was used for a second round of blocking before probing with a 1:400 dilution of chicken anti-pU_L34 polyclonal antibody. Bound primary antibodies were recognized by corresponding secondary antibodies conjugated with FITC or Texas Red, respectively (Jackson ImmunoResearch).

In some experiments, cells were transfected with equal amounts of U_L31-encoding plasmid DNA for 20 hrs prior to infection using lipofectamine (Invitrogen). Infected cells were processed for indirect immunofluorescence in the same way except that no methanol fixation was used, and the M2 anibody directed against the Flag epitope was diluted 1:100. Images were visualized and recorded using an Olympus confocal microscope. Digital images were processed with Adobe Photoshop.

Electron microscopy. Cells were first fixed with 2.5% glutaraldehyde in 0.1 M Na-cacodylate pH 7.4 (Electron Microscopy Sciences) for 30 min at room temperature and then 90 min at 4°C. After three 5 minute washes with the same buffer, the cells were fixed with 2% OsO4 in the same buffer and rinsed again. Cells were then dehydrated at 4^o C using a graduated series of ethanol concentrations (20%, 50%, 70%,

100%), and subsequent acetone/ethanol mixture (1:1), and finally, 100% acetone. This was followed by stepwise infiltration with Epon-Araldyte resin (EM Sciences) over the course of 64 hrs. Samples were dispensed into beem capsules, and the resin was polymerized at 80°C overnight. Thin sections (60 to 90 nm thick) were collected on 300-mesh copper grids and viewed in a Philips 201 transmission electron microscope. Conventionally rendered negatives of electron microscopic images were scanned by using Microtek Scanmaker 5 and Scanwizard Pro PPC 1.02 software. Positive images were rendered from digitized negatives with Adobe Photoshop software.

Results

The N-terminal domain of pU$_L$31 is functionally important to nuclear egress. The HSV-1 U$_L$31 protein is highly conserved among members of the herpesviridae. Interestingly, the first 50 amino acids of the N-terminal of U$_L$31 protein share little homology at the primary sequence level with other herpesvirus homologs. The clustered charged residues and hydrophilic nature distinguish this region from the remainder of HSV-1 pU$_L$31, which is mostly hydrophobic (not shown). To investigate the functional relevance of this charged region of pU$_L$31, a truncated U$_L$31 gene U$_L$31(dN) lacking the region from codon 2 to 44 was transfected into Hep2 cells and its ability to support replication of the U$_L$31 null HSV-1 mutant was determined by plaque assay. Plasmids bearing the full length U$_L$31 open reading frame and vector DNA (pCDNA3) served as positive and negative controls, respectively. Viral infectivity at 24 hr post infection was titrated on U$_L$31 complementing cells.

As shown in Fig. 4.1A, expression of full length pU$_L$31 increased the yield of infectious virus more than 100 fold above the background levels produced by transfection of vector DNA. In contrast to this result, the plasmid encoding N-terminally truncated pU$_L$31 produced only a 5-fold enhancement of viral yield over background. This

Figure 4.1 Functional analysis of the N-terminus of pU$_L$31. (A) Ability of pU$_L$31 mutants to support replication of a U$_L$31 null virus. Hep2 cells were transfected with a pcDNA3 vector plasmid or plasmids bearing full length U$_L$31(FL) or the N-terminally deleted U$_L$31(dN) used in panel A. The cells were then infected with the U$_L$31 null virus. Infectivity at 24 hpi was determined by freeze/thawing the infected cells, followed by titration on U$_L$31 complementing cell lines. Experiments were performed in duplicate. Each histogram represents the mean value, and the mean +/- standard deviations are indicated by error bars. **(B)** pU$_L$31 localization and ability to target pU$_L$34 to the nuclear rim. Hep2 cells were transfected with plasmids encoding Flag-tagged full length U$_L$31 [U$_L$31(FL); a to c] or U$_L$31 lacking the first 43 amino acid codons [U$_L$31(dN)] (d to f). The cells were then infected with a U$_L$31 null virus. Cells were stained with M2 antibody directed against the Flag tag (green) and pU$_L$34 (red), and images were captured by confocal microscopy.

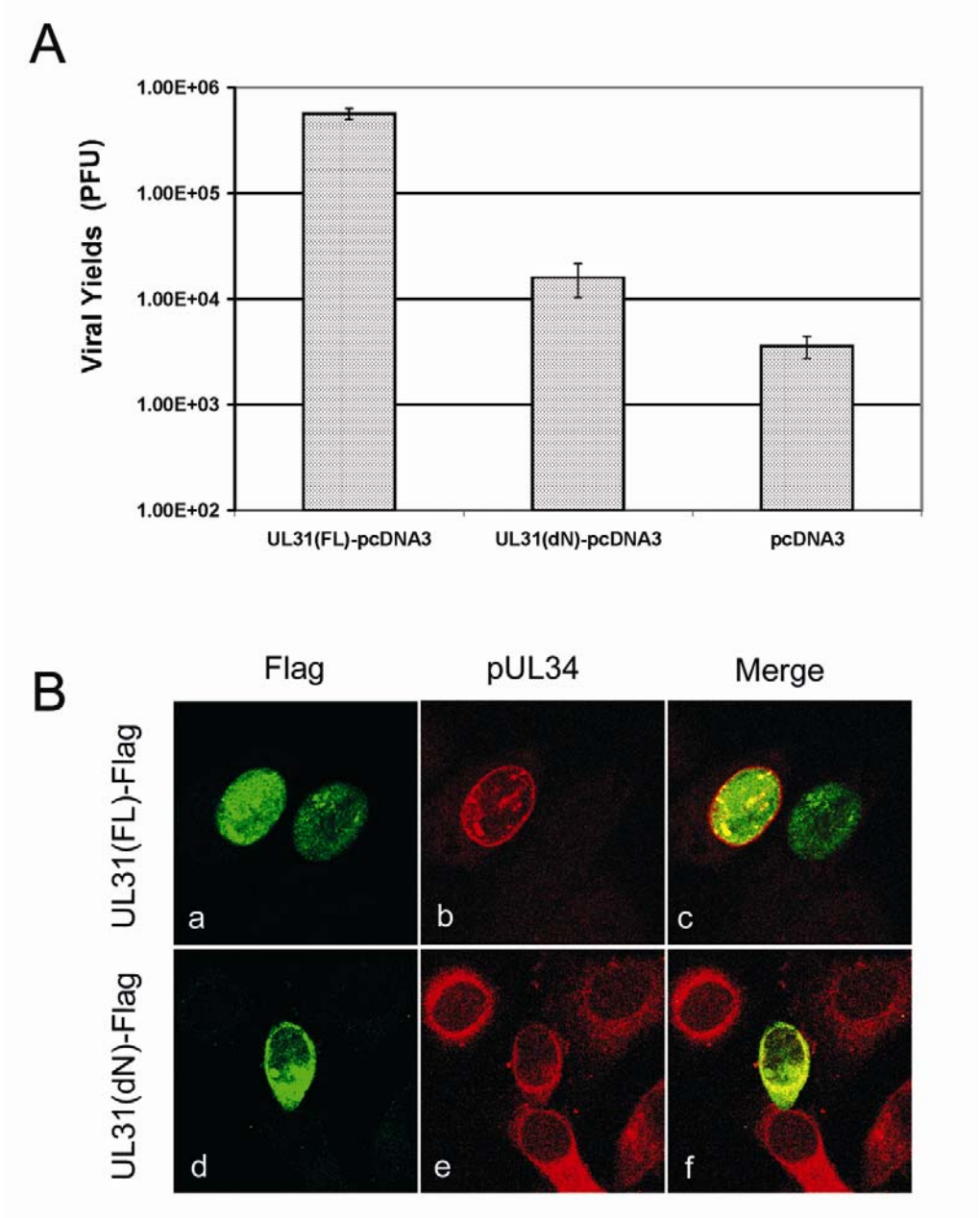
A
Viral Yields (PFU)
1.00E+06
1.00E+05
1.00E+04
1.00E+03
1.00E+02
UL31(FL)-pcDNA3
UL31(dN)-pcDNA3
pcDNA3
B
Flag
pUL34
Merge
UL31(FL)-Flag
UL31(dN)-Flag
a
b
c
d
e
f

result indicated that the N-terminal domain is important for full function of the HSV-1 U_L31 protein.

To determine the role of the pU_L31 N-terminus in targeting the pU_L31/pU_L34 complex to the nuclear rim, Hep2 cells were transfected with plasmids encoding either full length pU_L31, or the N-terminally truncated protein fused to a Flag epitopic tag. The cells were subsequently infected with the U_L31 deletion virus and were fixed and immunostained with the FLAG-specific antibody and polyclonal pU_L34-specific IgY. As shown in Fig. 4.1B, the full length pU_L31-Flag-specific immunostaining colocalized with pU_L34-specific immunostaining at the nuclear rim. In contrast to this result, the cells expressing pU_L31(dN), and subsequently infected with the U_L31 deletion virus contained Flag-specific immunostaining (denoting the location of truncated pU_L31) mostly in the cytoplasm. Under these conditions, pU_L34 specific immunostaining co-localized with pUL31 in the cytoplasm adjacent to the nucleus. The pattern of pU_L34-specific immunostaining was reminiscent of the pattern of pU_L34 distribution in cells infected with U_L31 null viruses (107, 163), and was similar whether or not pU_L31-Flag was detected in a particular cell. These observations imply that the N-terminus of U_L31 protein is required for strict localization of the pU_L31/pU_L34 complex to the nuclear rim.

The pU_L31 N-terminal domain harbors multiple phosphorylation sites of the viral U_S3 kinase. The N-terminal sequence of pU_L31 is arginine and serine rich, which is reminiscent of U_S3 serine/threonine kinase phosphorylation motifs (155). Because it was already known that pU_L31 was a substrate of pU_S3, we hypothesized that U_S3 kinase phosphorylated pU_L31 at least some of the putative U_S3 phosphorylation motifs located at its N-terminus. pU_S3 phosphorylation sites on pU_L31 were therefore mapped as follows. The U_L31 codons 1-50, 51-165, 155-165, and 255-306 (Fig. 4.2A)

were fused to the gene encoding GST, and the corresponding fusion proteins were purified from *E. coli* by GST affinity chromatography. The purified proteins were then incubated with recombinant baculovirus-expressed U_S3 kinase in buffer containing [γ-^{32}P]-ATP. Reaction components were then separated on an SDS polyacrylamide gel, and the gel was stained with Coomassie brilliant blue, dried and exposed to X-ray film. As shown in Fig. 4.2B, equal amounts of all four fragments were present in the reactions (upper panel), but only the N-terminal 50 amino acids of pU_L31 were labeled with ^{32}P (lower panel).

Analysis of the primary sequence of this region indicated that 6 serine residues were in a context potentially consistent with pU_S3 phosphorylation sites (Fig. 4.2A). Of the 6 residues, Serines 11, 24, and 40 completely matched the predicted pU_S3 consensus motif (RnXS/T [n>=2]) (155), while the other 3 Serines (S26, 27, and 43) could not be excluded since the kinase was found to be more promiscuous than originally predicted (128). With this in mind, we systematically substituted these serines with alanines and tested the corresponding mutants for their capacity to be phosphorylated by pU_S3 *in vitro*. The constructs were designated pU_L31(SA3) (bearing S11, S24, and S40 changed to alanine codons) and pU_L31(SA6) which bears all 6 serines (S11, 24, 25, 26, 40, 43A) changed to alanines. Mixing GST fusion protein bearing these mutations with active U_S3 kinase and [^{32}P-ATP] revealed that wild type pU_L31 was heavily phosphorylated by U_S3 kinase, whereas mutating all 6 serines completely abolished phosphorylation. In contrast, the SA3 mutations decreased, but did not eliminate U_S3-dependent phosphorylation (Fig. 4.2C). The results revealed that the pU_L31 N-terminus contains multiple sites that U_S3 kinase can phosphorylate *in vitro*, and suggests that the protein is phosphorylated by the U_S3 kinase during infection as indicated previously (89).

Figure 4.2 Mapping pU_L31 phosphorylation sites of pU_S3 kinase. (A) Schematic illustration of full length U_L31 protein and its sub-fragments used in panel B, and the primary sequence showing potential phosphorylation sites (underlined). A series of constructs with point mutations used in subsequent experiments are listed. **(B)** *In vitro* kinase assay with sub-fragments of pU_L31. GST fusion proteins purified from E.coli were incubated with purified U_S3 kinase assay with sub-fragments of pU_L31. GST fusion proteins purified from *E. coli* were incubated with purified U_S3 kinase and [γ-P^{32}]ATP. The reaction products were electrophoretically separated on a denaturing gel and were stained by Coomassie brilliant blue, dried and exposed to X-ray film. **(C)** Wild type and mutant pU_L31 reacted with purified U_S3 kinase *in vitro*. Reactions were performed as in panel B. Reactants were separated on a denaturing gel, visualized by CBB staining, and dried. The presence or absence of phosphorylation was determined by autoradiography of the same gel.

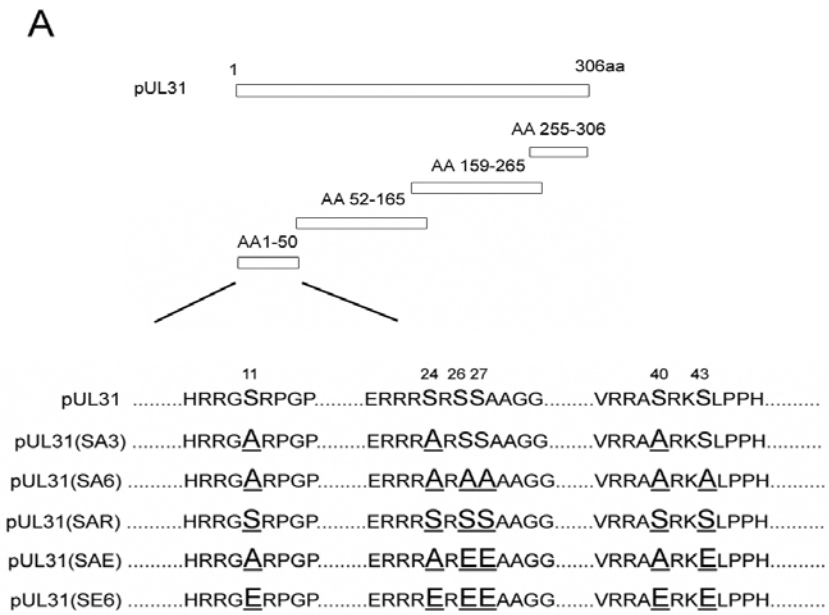
A
1
306aa
pUL31
AA 255-306
AA 159-265
AA 52-165
AA1-50
11
24 26 27
40 43
pUL31 .....HRRGSRPGP.....ERRRSRSSAAGG.....VRRASRKSLPPH.....
pUL31(SA3) .....HRRGARPGP.....ERRRARSSAAGG.....VRRAARKSLPPH.....
pUL31(SA6) .....HRRGARPGP.....ERRRARAAAAGG.....VRRAARKALPPH.....
pUL31(SAR) .....HRRGSRPGP.....ERRRSRSSAAGG.....VRRASRKSLPPH.....
pUL31(SAE) .....HRRGARPGP.....ERRRAREEAAGG.....VRRAARKELPPH.....
pUL31(SE6) .....HRRGERPGP.....ERRRERREEAAGG.....VRRAERKELPPH.....
B
GST-pUL31 (1-50aa)
GST-pUL31 (52-165aa)
GST-pUL31 (159-265aa)
GST-pUL31 (255-306aa)
CBB
Autoradiograph
1
2
3
4
C
GST-pUL31
GST-pUL31(SA6)
GST-pUL31(SA3)
CBB
Autoradiograph
1
2
3

Precluding phosphorylation of the pU_L31 N-terminus causes a delay in viral replication. We next proceeded to determine whether the N-terminus of pU_L31 was phosphorylated by U_S3 during viral infection. Recombinant viruses bearing the 6 Serine to Alanine mutations in U_L31 and its corresponding genetically repaired virus U_L31(SAR) were generated through BAC mutagenesis. Cells were infected with 5.0 PFU/cell of the wild type virus HSV-1(F), kinase dead virus U_S3(K220A), U_L31 mutant virus U_L31(SA6), or the repaired virus U_L31(SAR). At 16 hpi, the cells were harvested, and electrophoretically separated proteins were subjected to immunoblotting with pU_L31-specific antiserum.

The results, shown in Fig. 4.3, indicated that, (i) consistent with previous reports (89), phosphatase (PPase) treatment caused an increase in the electrophoretic mobility of the pU_L31-specific band of HSV-1(F) (lanes 1 and 2). The migration of this band was similar to that of non-treated pU_L31 from cells infected with U_S3(K220A) (lane 3), indicating that pU_S3 played an important role in phosphorylation of pU_L31 during infection directly or indirectly. (ii) The electrophoretic mobility of pU_L31 from U_S3(K220A) infected cells was also accelerated by PPase addition (lane 3 and 4), indicating that while pU_S3 is important for pU_L31 phosphorylation, other kinases also play a role. (iii) Substitution of all 6 serines by alanines increased the electrophoretic migration of U_L31 protein. PPase treatment did not cause a mobility change of this mutant (lane 5 and 6) indicating that this was the only phosphorylation site of pU_L31, at least as detected by one dimensional electrophoresis. In contrast, the mobility of pU_L31 expressed by the genetically repaired virus U_L31(SAR) (lane 7 and 8), was greatly increased by PPase treatment, confirming that the pU_L31 phosphorylation was successfully blocked by the SA6 mutations. (iv) All of the non-mutated pU_L31 proteins (lanes 1, 3, 7) produced wider bands than their PPase treated counterparts (lanes 2, 4, 8), implying the existence of heterogeneously phosphorylated pU_L31 species

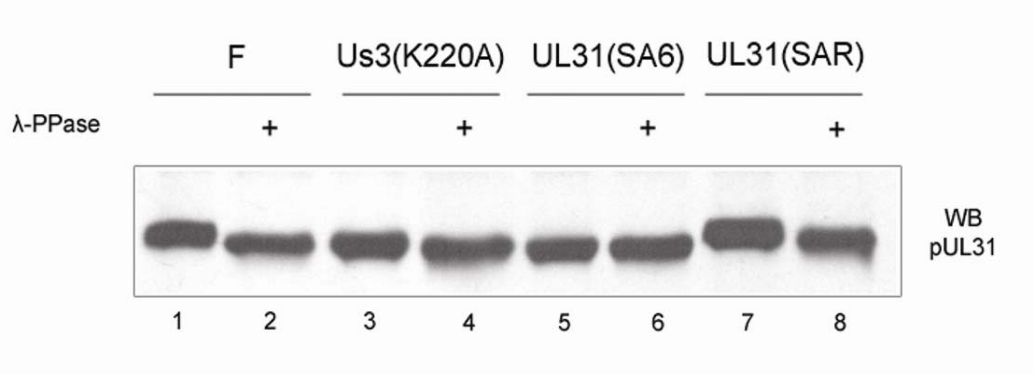

Figure 4.3 Immunoblot to determine the phosphorylation state of pU_L31 during infection with wild type and mutant viruses. Hep2 cells were infected with wild type HSV-1(F) (lanes 1, 2), U_S3(K220A) (lanes 3, 4), U_L31(SA6) (lanes 5, 6), or U_L31(SAR) (lane 7, 8) viruses for 16hrs. The lysates were treated or untreated with bacteriophage lambda phosphatase as indicated. Cell lysates were electrophoretically resolved on denaturing polyacrylamide gels, electrically transferred to nitrocellulose, and probed with antibody to pU_L31.

during infection. (v) Unexpectedly, the PPase treated U_L31 proteins of HSV-1(F) and U_L31(SAR) viruses (lane 2, 8) migrated slightly slower than the pU_L31 of U_S3(K220A) virus. This finding suggested either that not all phosphorylation is precluded by PPase treatment, or that active U_S3 kinase induces post-translational modifications other than phosphorylation on pU_L31 in infected cells.

We then conducted one-step viral growth assays to gauge the infectivity of the U_L31(SA6) virus. Cells were infected with 5 PFU/cell of U_L31(SA6), the restored virus U_L31(SAR), wild type HSV-1(F), or U_S3(K220A) at an MOI of 5 and viral yields at the indicated time points were titered on Vero cells. As shown in Fig. 4.4, the U_L31(SA6) and U_S3(K220A) viruses displayed a similar pattern of viral growth over time. Of note was a nearly 10-fold decrease in titer at 12 hpi compared to that of the wild type virus; on the other hand, both recombinant viruses produced titers similar to HSV-1(F) at 24 hpi. Impaired viral growth was eliminated by repairing the SA6 mutation inasmuch as the virus U_L31(SAR) replicated as efficiently as HSV-1(F). We conclude from these data that precluding phosphorylation of pU_L31 mimics the growth defect of the U_S3 kinase dead virus.

Precluding phosphorylation of the pU_L31 N-terminus mimics the effects of U_S3 kinase deficiency in pU_L31/pU_L34 complex localization and perinuclear virion accumulation. Although the absence of U_S3 kinase activity causes a defect in capsid nuclear egress, including mislocalization of pU_L34 at the nuclear rim and accumulation of primary enveloped virions in the perinuclear space, the responsible kinase substrate has not been identified. Because the growth kinetics of U_L31(SA6) virus and U_S3(K220A) were very similar, we compared the localization of pU_L34 and virions in cells infected with the U_L31(SA6) and U_S3 kinase dead viruses.

Hep2 cells were infected with either wild type HSV-1(F), U_S3(K220A),

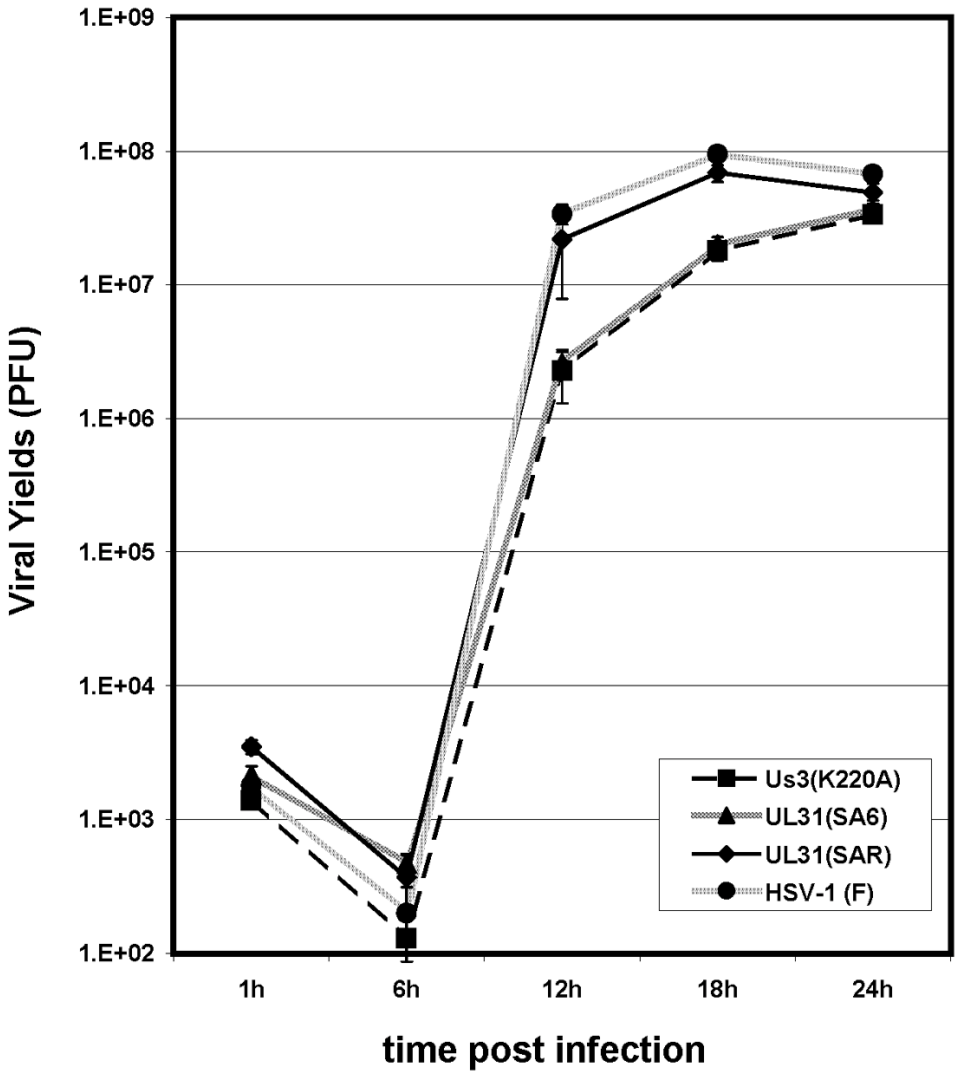

Figure 4.4 One-step growth curves of wild type and mutant viruses. Hep-2 cells were infected with either wild type HSV-1(F), U_S3(K220A), U_L31(SA6), or U_L31(SAR) viruses at an MOI of 5. After adsorption for one hour, residual infectivity was inactivated by a low-pH wash. At the indicated time points, pooled intracellular and extracellular viral infectivity was titrated on Vero cells. Experiments were done in duplicate. Mean values are plotted and deviations are represented by error bars.

U_L31(SA6), or the U_L31(SAR) virus for 16 hours, at which time the cells were immunostained with antibodies against pU_L31 and pU_L34 and visualized by confocal microscopy (Fig. 4.5). Consistent with previous reports, the pU_L31 and U_L34 proteins co-localized smoothly along the nuclear envelope in cells infected with HSV-1(F). Deactivation of the U_S3 kinase as in cells infected with the U_S3(K220A) virus induced discrete foci of pU_L31 and pU_L34 at the nuclear rim. In cells infected with the U_L31(SA6) virus, the focal distribution of pU_L31/pU_L34 appeared very similar to that of cells infected with U_S3(K220A). The aberrant distribution of pU_L31/pU_L34 was restored to the wild type distribution in cells infected with the genetically repaired virus U_L31(SAR).

To examine the effects of pU_L31 phosphorylation on the distribution of virions, cells were infected with wild type HSV-1(F), U_S3(K220A), U_L31(SA6), or the U_L31(SAR)viruses, embedded, and thin sections were stained and examined by electron microscopy. As shown in Fig. 4.6, U_L31(SA6) viral infection produced nuclear membrane invaginations containing multiple primary enveloped virions. The distribution of these virions resembled that of cells infected with U_S3(K220A) virus implying an egress defect, but was dissimilar to the appearance of cells infected with HSV-1(F) or the restored virus U_L31(SAR) (not shown).

We conclude that phosphorylation of pU_L31 is necessary for proper localization of the pU_L31/pU_L34 complex in the nuclear rim, and for optimal egress of virions from the perinuclear space.

pU_L31/pU_L34 distribution is dependent on the acidity of the pU_L31 N-terminus. In preliminary studies, localization of pU_L31/pU_L34 in cells infected with a virus [designated U_L31(SA3)] expressing pU_L31 with point mutations S11A, S24A and S40A was undistinguishable from that in cells infected with wild type virus (not

Figure 4.5 Confocal immunofluorescence staining of pU_L31 and pU_L34 in HSV-1 infected Hep2 cells. Cells were infected with either the wild type HSV-1(F) [designated (F)], U_S3(K220A), U_L31(SA6), or U_L31(SAR) viruses. After 16 hours the cells were fixed in paraformaldehyde and methanol, permeabilized, immunostained for pU_L31 (green) and pU_L34 (red), and visualized by confocal microscopy. Optical sections were taken through the middle of cells.

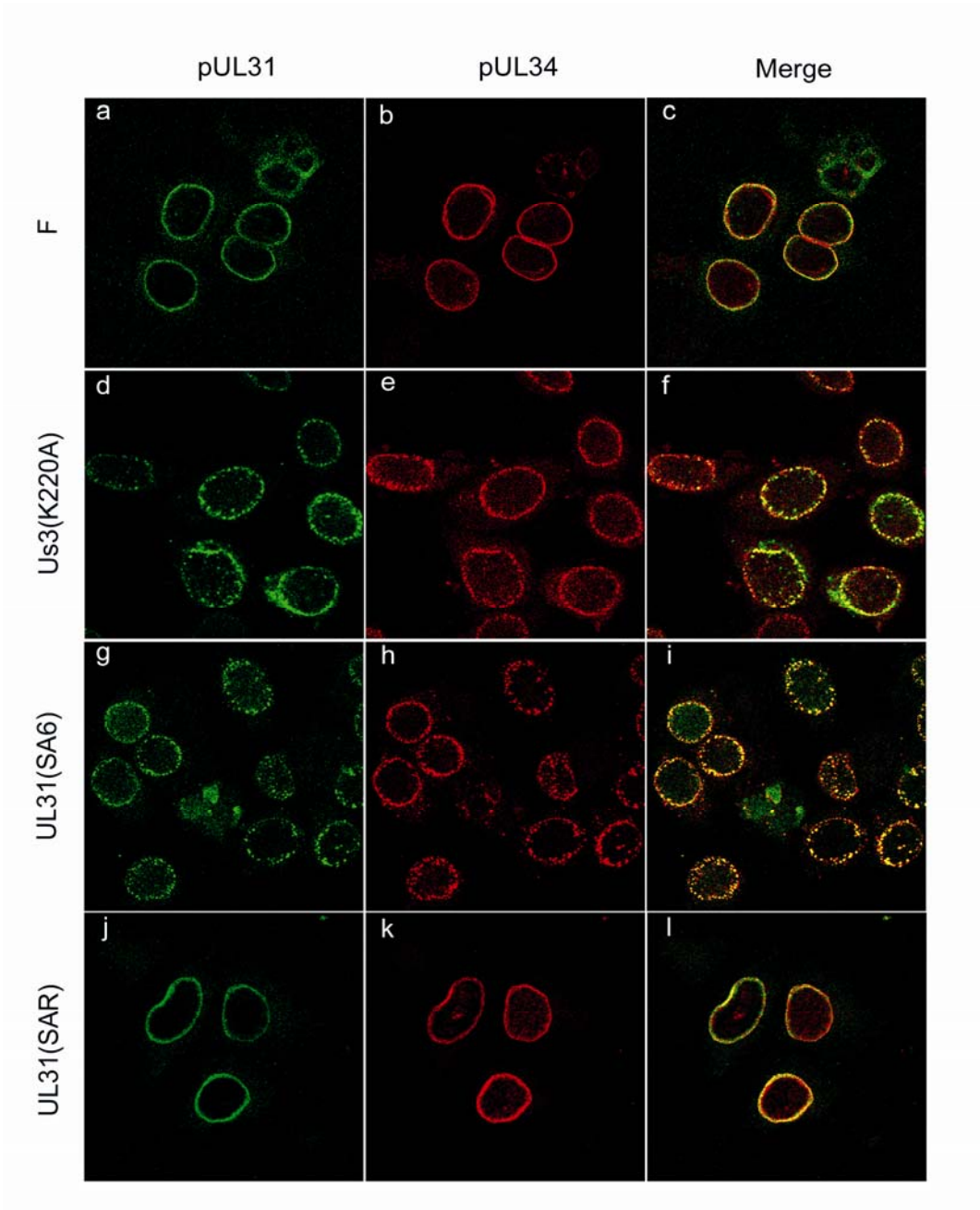
pUL31
pUL34
Merge
F
Us3(K220A)
UL31(SA6)
UL31(SAR)
a
b
c
d
e
f
g
h
i
j
k
l

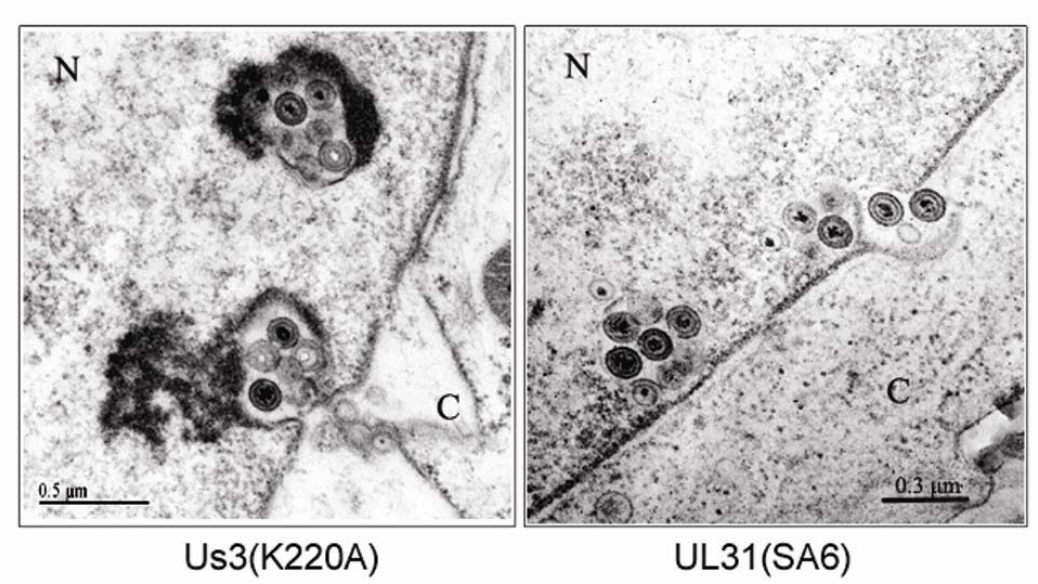

Figure 4.6 Electron microscopy of Hep2 cells infected with HSV mutants. Cells were infected for 16 hours with the indicated viruses, fixed, embedded, sectioned, stained, and examined in a transmission electron microscope. Images show primary enveloped virion accumulation in Hep2 cells infected by U_S3(K220A) viruses or U_L31(SA6) viruses. (N, nucleus; C, cytoplasm). The scale in μM is indicated.

shown). This observation suggested that phosphorylation at sites S25, S26 and/or S43 were sufficient to enable pU_L31 to function properly. With this in mind, two pseudo-phosphorylated pU_L31 expressing viruses were generated, one termed U_L31(SAE) encoded residues 11, 24 and 40 as alanines while residues 25, 26 and 43 were changed to glutamic acid, and U_L31(SE6), which had all six residues changed to glutamic acid (diagrammed in Fig. 4.2A).

Immunoflourescence analysis of the pU_L31 and pU_L34 distribution in cells infected with these viruses revealed phenotypic differences (Fig 4.7). Specifically, U_L31(SAE) still produced punctate pU_L31/pU_L34-specific staining like the U_L31(SA6) or U_S3(K220A) viruses, whereas these proteins were distributed smoothly throughout the nuclear rim in cells infected with U_L31(SE6). Taken together with the distribution patterns of pU_L31/pU_L34 in cells infected with of U_L31(SA3) and U_L31(SA6) viruses, the data indicated that acidity of the pU_L31 N-terminus was a critical factor mediating pU_L31/pU_L34 localization.

In order to confirm the rescuing effect of the acidity of pU_L31 in pU_L31/pU_L34 complex localization, and to see if effecters of U_S3 other than U_L31 play a role, a novel virus was generated in which the mutation abolishing U_S3 kinase activity was introduced into the U_L31(SE6) virus, resulting in a double mutant virus U_L31(SE6)/U_S3(K220A). Analysis of the distribution of the pU_L31/pU_L34 complex in cells infected with this mutant indicated that the complex localized in a smooth distribution at the nuclear rim in contrast to what would be expected in cells infected with U_S3(K220A). Thus the rescuing phenotype of completely pseudo-phosphorylated pU_L31 was dominant over the inactive U_S3 kinase phenotype. These observations suggested that pU_L31 is the major substrate of U_S3 kinase responsible for regulating the localization of pU_L31/pU_L34 at the nuclear rim.

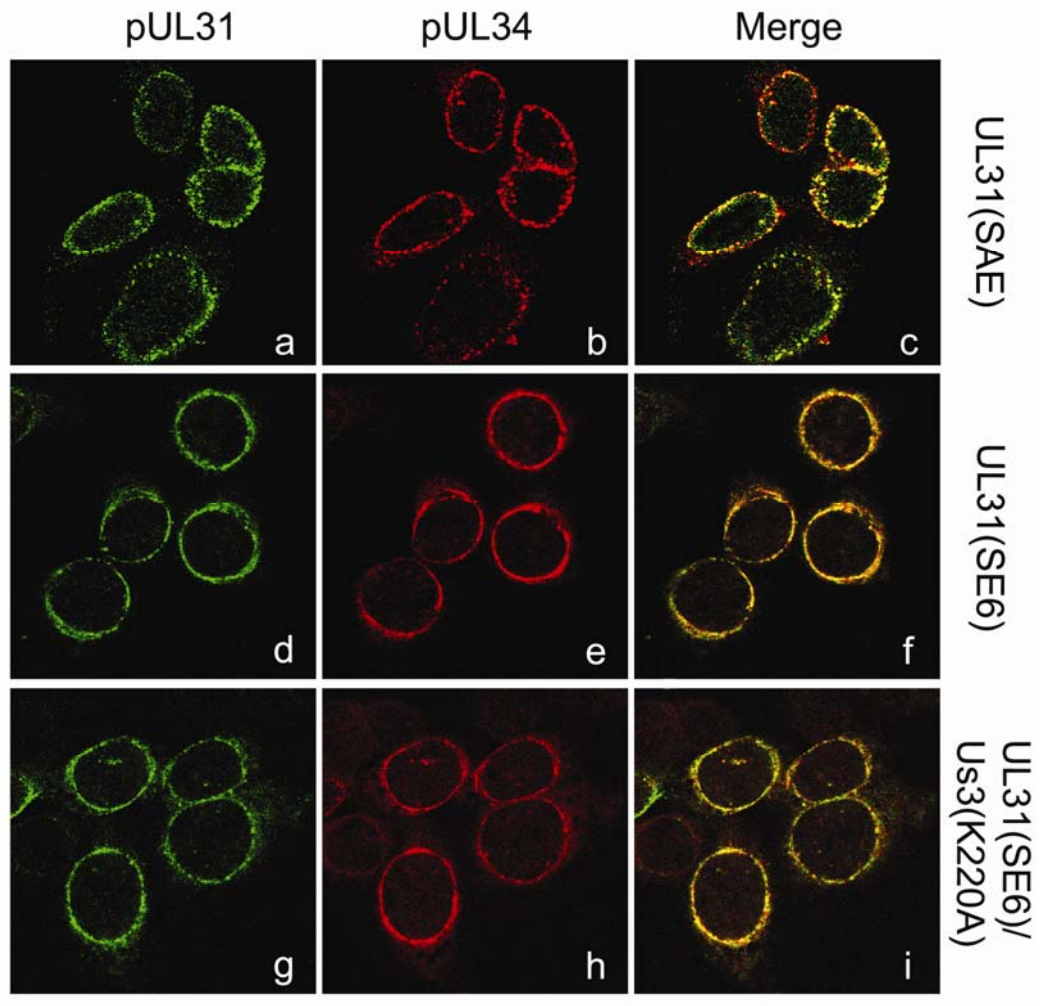

Figure 4.7 pU_L31 and pU_L34 localization in Hep2 Cells infected with pseudo-phosphorylated U_L31 viruses. Hep2 cells were infected with the indicated viruses and were fixed at 16 hours after infection in paraformaldehyd and methanol. The cells were then immunostainned for pU_L31 (green) and pU_L34 (red) and visualized by confocal microscopy. Optical sections were taken through the middle of cells.

Pseudo-phosphorylated pU$_L$31 inhibits primary envelopment of nucleocapsids. Based on the immunofluorescence data above, we presumed that unlike the U$_S$3 kinase-dead virus, (i) the U$_L$31(SE6) virus and U$_L$31(SE6)/U$_S$3(K220A) viruses would not induce herniations of nuclear membrane containing perinuclear virions, and (ii) would replicate as efficiently as wild type HSV-1. To test the first prediction, cells were infected with these viruses and examined by electron microscopy 16 hours later. Consistent with the first hypothesis, no excessive perinuclear virion accumulation was observed in cells infected with either virus over that seen in cells infected with wild type HSV-1(F). Inconsistent with the second hypothesis, however, very few viral particles were detected in the cytoplasm or on the cell surface of cells infected with the U$_L$31(SE6) or U$_L$31(SE6)/U$_S$3(K220A) viruses. This was the case despite ample numbers of capsids within nuclei of these cells. Counting a representative 9 cell sections indicated that whereas the ratio of cytoplasmic to intranuclear capsids was approximateley 1.55 in cells infected with HSV-1(F), this ratio was only 0.11 in cells infected with the mutant virus U$_L$31(SE6) virus and 0.02 for the U$_L$31(SE6)/U$_S$3(K220A) double mutant (Table 4.3). These data suggest that the mutant virions were enveloped at the inner nuclear membrane less efficiently than their wild type counterparts.

To further investigate the phenotype of the U$_L$31(SE6) and U$_L$31(SE6)/U$_S$3(K220A) viruses, cells were infected with these viruses at 5.0 PFU/cell and the amount of infectious virus was determined at various times after infection. As shown in Fig. 4.8, the U$_L$31(SE6) and U$_L$31(SE6)/U$_S$3(K220A) viruses produced less infectious virus throughout the infection compared to HSV-1(F). The most marked discrepancy was observed at 12 hpi, when the amount of infectious U$_L$31(SE6) virus was reduced approximately 10 fold compared to that of HSV-1(F), whereas the U$_L$31(SE6)/U$_S$(K220A) virus titer was reduced more than 20 fold. As shown previously, the U$_S$3(K220A) virus also displayed a 10 fold lower titer at 12 hpi compared to

Table 4.3 Subcellular distribution of viral particles in Hep2 cells infected for 16 hrs (examined by EM).

Virus	Total intracellular viral particle numbers			Cells counted	*Average Ratio (C/N)*
	Nuclear (N)	Cytoplasmic (C)	Perinuclear (PN)		
HSV-1 (F)	73	113	10	9	1.55
U_L31(SE6)	186	21	0	9	0.11
U_L31(SE6)/ U_S3(K220A)	129	3	2	9	0.02

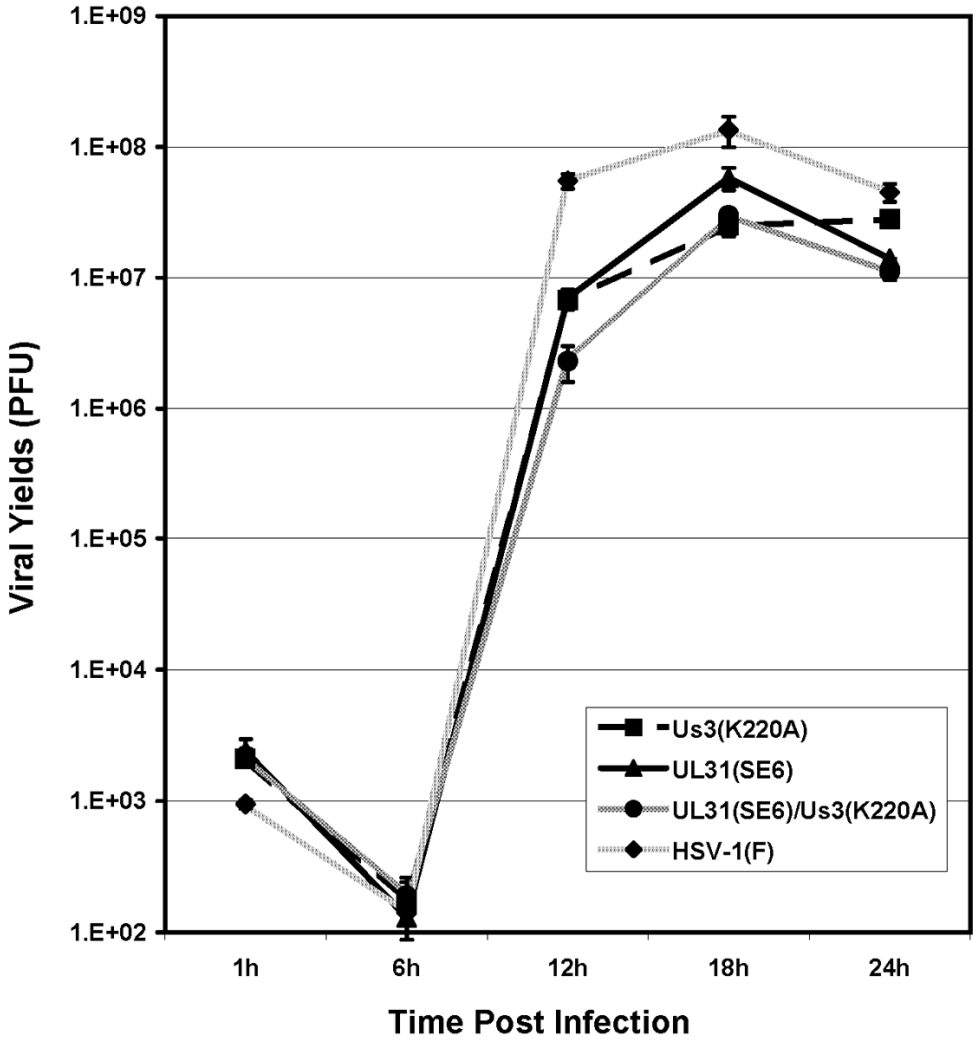

Figure 4.8 One-step growth curves of pseudo-phosphorylated U_L31 viruses. Hep-2 cells were infected with either wild type HSV-1(F), U_S3(K220A), U_L31(SE6), or U_L31(SE6)/U_S3(K220A) at an MOI of 5 PFU/cell. Residual viruses were inactivated by a low-pH wash at 1 hpi. At the indicated time points, virus in the whole culture was collected and titrated on Vero cells. Experiments were done in duplicate. Mean values are plotted and simple standard deviations are represented by error bars.

HSV-1(F) but eventually produced infectious virus titers approaching those of the wild type virus. In contrast to this result, the two U_L31 mutants reached their peak titers at 18 hpi, and never reached infectious titers approaching those of wild type HSV-1(F). These data indicate that the nuclear egress defects of the U_L31 mutants are more persistent than that of the U_S3(K220A) virus, suggesting a defect in primary envelopment that does not diminish as infection proceeds. We also noted that the double mutant U_L31(SE6)/U_S3(K220A) replicated slightly less efficiently than either of the viruses with single mutations, indicating that the pseudo-phosphorylated pU_L31 is insufficient to complement fully the contribution of U_S3 kinase activity to viral infectivity.

Discussion

Normally, nucleocapsid budding through the inner nuclear membrane and fusion of the nascent virion envelope with the outer nuclear membrane is highly efficient. This conclusion comes from the observation that during wild type virus infection, there is rarely extensive virion accumulation in the perinuclear space. In cells infected with U_S3 kinase-dead viruses however, the accumulation of perinuclear virions in herniations of the perinuclear space is commonplace. This aberrant virion accumulation likely reflects an imbalance between the rate of delivery into localized regions of the perinuclear space and the rate of exit from these regions. Taken from this perspective, the U_S3 kinase might serve to decrease the numbers of virions in particular perinuclear regions because its activity disperses the nuclear envelopment complex widely throughout the nuclear membrane. Thus, the rate of exit from the nucleoplasm is similar to wild type virus, but the number of envelopment sites is increased, and perinuclear virions do not accumulate in particular regions. On the other side of the inner nuclear membrane, U_S3 may promote fusion of the perinuclear virion envelope with the outer nuclear membrane.

Perhaps the most important finding of the current work is that most of the U_S3 nuclear egress phenotype, including mislocalization of the pU_L31/pU_L34 complex and virion accumulation in herniations of the perinuclear space, can be mimicked by precluding phosphorylation of pU_L31 at its N-terminus. Thus, U_S3 mediates much of its effects in nuclear egress through phosphorylation of pU_L31. Aggregation of pU_L31/pU_L34 may restrict sites of budding causing nucleocapsids to continue budding into herniations already containing multiple perinuclear virions, thereby overwhelming the fusion machinery. There is otherwise no evidence that the rate of budding into the perinuclear space is impaired by the absence of phosphorylation of pU_L31.

Our data also indicate that the pseudo-phosphorylated pU_L31(SE6) is defective in primary envelopment of nucleocapsids at the INM, and is insufficient to complement the full function of U_S3 kinase. Thus, some functions of U_S3 kinase activity important to viral replication are mediated by substrates other than pU_L31. We speculate that these other substrates may include an impaired or mis-triggered fusion apparatus that mediates fusion between the virion envelope and ONM (possibly mediated through gB and gH). It is unclear whether the pU_L31(SE6) mutation interferes with the fusion event because the paucity of perinuclear virions in cells infected with this mutation precludes assessment of this possibility.

Together, the data suggest that the function of pU_L31 is tightly and dynamically controlled by phosphorylation. Based on all the data presented herein, we hypothesize that there is a mixed population of both unphosphorylated and phosphorylated pU_L31 (Fig. 4.9). At primary envelopment sites in the inner nuclear membrane, the unphosphorylated form is involved in initiation of the budding reaction, possibly by direct or indirect interaction with the nucleocapsid or other egress components, whereas the phosphorylated form coexists and is required to prevent pU_L31/pU_L34 aggregation. Once in the perinuclear space, pre-existing or newly phosphorylated pU_L31 is needed

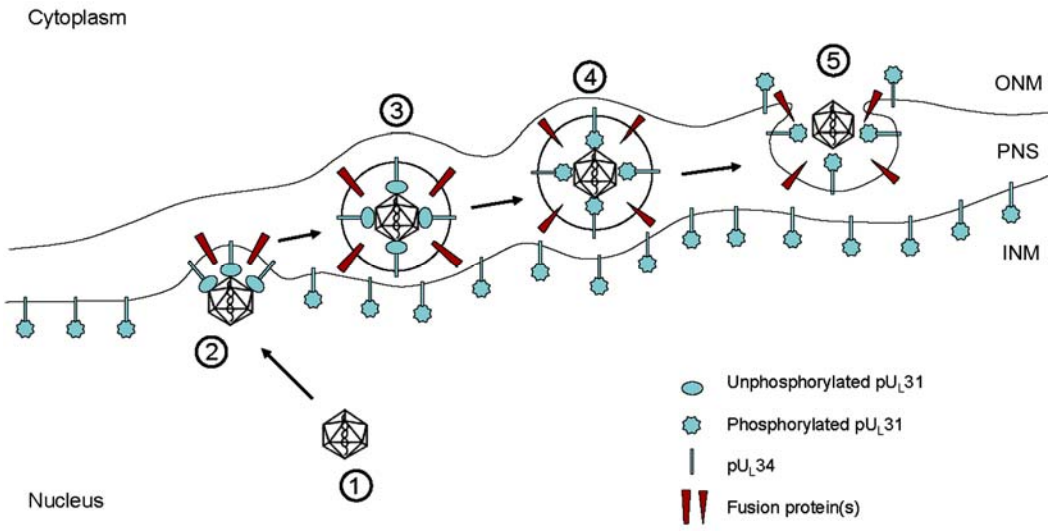

Figure 4.9 Proposed model of dynamic phosphorylation of pU_L31 during HSV nuclear egress. In HSV infected cells, phosphorylated pU_L31 are scattered through the inner nuclear membrane (INM) via interaction with pU_L34. DNA-filled capsids (1) contact the INM at the sites where unphosphorylated pU_L31 are concentrated to inititate the primary envelopment reaction (2). Capsids translocate into the perinuclear space (PNS) with an envelope containing fusion proteins (3). In the PNS, phosphorylated forms of pU_L31 induce conformational changes in the fusion proteins (4). These alterations trigger the fusion of the envelope with the outer nuclear membrane (ONM) and subsequent release of capsids into the cytoplasm (5).

to promote the fusion of the perinuclear virion with the ONM, probably by altering protein-protein interactions to activate the fusion proteins gH and gB.

Finally, we note that in our previous study of cellular lamin A/C, we reasoned that one possibility to explain the punctate distribution of pU_L31/pU_L34 in cells infected with U_S3 kinase-dead viruses was that this aberrant distribution reflected mobility constraints caused by a hypophosphorylated, and therefore less permeable, nuclear lamina. The current observation that the U_L31/U_L34 proteins are of punctate distribution in cells infected with the U_L31(SA6) mutant argue against this possibility because these cells contain active pU_S3, which would be expected to phosphorylate lamin A/C. Thus phosphorylation of lamin A/C is separable from functions required for the proper localization of pU_L31/pU_L34.

CHAPTER V

SUMMARY AND FUTURE STUDIES

Summary

The research goal of my study is to understand the machinery mediating the nuclear egress of HSV-1 capsids. The work initiated with the observation that in cells infected with a mutant HSV defective in U_S3 kinase, enveloped virions accumulate in invaginations of the inner nuclear membrane (INM), and viral production is delayed compared to wild type HSV-1(F) virus. The kinase therefore is postulated to regulate the capsid egress from the nucleus. This process involves primary envelopment at the INM and de-envelopment at the outer nuclear membrane (ONM) and requires the U_L31 and U_L34 proteins. Several substrates of pU_S3 have been identified and investigated for their role in this process, but had yet to be implicated.

In order to determine the U_S3 substrate(s) responsible, an *in vitro* assay system using baculovirus-expressed pU_S3 was established. As shown in Chapter II, nuclear lamin A/C was identified as a potential substrate and could be dissolved partially *in vitro* by U_S3 kinase activity. This was further confirmed by an *in vivo* assay showing that lamin A/C was hyper-phosphorylated during HSV infection and a full spectrum of phosphorylation required pU_S3 activity. The nuclear lamina was found to be dramatically perforated when U_S3 kinase was deactivated; and the essential nuclear egress complex pU_L31/pU_L34 aggregated near those lamina perforations. Given that phosphorylation is a common strategy to rearrange lamina structure, I hypothesized that the lack of pU_S3 activity caused a decrease in the phosphorylation of lamin A/C, which in turn made the lamina less flexible and hence restricted the pU_L31/pU_L34 distribution. However, an alternative possibility was that pU_L31/pU_L34 aggregation might mechanically perforate the lamina.

The nuclear lamina has long been considered a potential barrier for viral capsids to access primary envelopment sites at the inner nuclear membrane; together with the above hypothesis, I proceeded to investigate the roles of certain types of lamins during HSV-1 infection, using lamin knockout MEFs. In chapter III, pU_L34 positioning and general permissivity of wild type and U_S3 kinase dead viral infection was examined in *Lmna*$^{-/-}$ or *Lmnb1*$^{-/-}$ MEFs. I found the two lamin types contributed differently to viral infection. Lamin A/C was dispensable for the infections. In particular, the replication of U_S3 kinase dead virus was augmented and produced no perinuclear virion accumulation. The localization of pU_L34 was slightly altered upon the loss of lamin A/C in both viral infections, but it still aggregated in discrete foci in the absence of U_S3 kinase activity. In contrast, lamin B1 was required for efficient replication of both viruses. U_S3 mutant virus still induced perinuclear virion herniations, although pU_L34 aggregated in a less extensive fashion. These findings led to the conclusions that (i) lamin A/C and lamin B1 have different roles during HSV-1 infection; (ii) pU_L31/pU_L34 aggregates independently of lamin proteins, although lamins do play a direct or indirect role modifying the localization of the complex.

The substrate mediating pU_S3 activity was finally discovered, as described in chapter IV. pU_L31 was recognized as the major downstream effecter of pU_S3 regulatory pathway by using a phosphorylation-deficient U_L31 mutant that reproduced the defect seen in cells infected with the U_S3 mutant virus, even in the presence of the active U_S3 kinase. The mimicked defects included pU_L31/pU_L34 aggregation, perinuclear virion herniations, and slower viral replication kinetics. I went on to further confirm and characterize the functional significance of the pU_S3/pU_L31 catalytic relationship and found some interesting results. When pU_L31 was constantly phosphorylated in an artificial manner, pU_L31/pU_L34 was properly positioned on the nuclear rim but the primary envelopment of capsids was impaired. Introducing a mutation ablating

U_S3 kinase activity did not alter the distribution of the pU_L31/pU_L34 complex or induce nuclear membrane herniations, but the viral replication was more decreased than with either mutation alone. These data imply that phosphorylation of pU_L31 may be a dynamic event during infection and also that pU_S3 has to phosphorylate substrate(s) other than pU_L31 to exert its full contribution to HSV-1 replication. Hence, I propose that there is a mixed population of pU_L31. The unphosphorylated form is present to initiate the primary envelopment process by interacting with capsids or other egress components, while the phosphorylated form is required to prevent pU_L31/pU_L34 complex from aggregating. At the subsequent de-envelopment stage, phosphorylation of pU_L31 and other substrates are needed to promote the fusion of the nascent viral envelope with the ONM.

Future studies

(i) The proposed model of pU_L31 phosphorylation does not address whether there are two static or interchanging populations of pU_L31 and what is their relative ratio. Hence it will be interesting to determine when cells are co-infected by the phospho-deficient U_L31(SA6) and pseudo-phosphorylated U_L31(SE6) viruses, how these two static pU_L31 populations will interact. An approach allowing precise switch-off and -on of the U_S3 kinase activity will be very useful to characterize the process in more spatial and temporal details. To achieve this goal, solving pU_S3 structure and generating a specific inhibitor to the kinase would be useful.

(ii) The core question remaining unanswered is the specific mechanism by which the pU_L31/pU_L34 complex initiates primary envelopment of capsids. Co-expressing the pU_L31/pU_L34 homologs of pseudorabies virus is sufficient to induce vesicles derived from the INM in the absence of other viral proteins (91). Therefore, it is necessary to test if pU_L34 alone is capable of such a function inasmuch as pU_L34 can be

properly targeted to the INM in rabbit skin cells in the absence of pU_L31, and pU_L31 is less essential for viral replication in this particular cell line (107).

Since the research strategies are hampered by difficulties involved in working with nuclei, it will be very useful if we could reconstruct primary envelopment machinery on the plasma membrane. pU_L34 is a type II membrane protein and may be delivered to the cell surface via genetic engineering or by interaction with synthesized liposomes. pU_L31 is easier to manipulate because its NLS is in the poorly conserved N-terminal domain that appears to be dispensable for interaction with pU_L34 (unpublished data). If the system works, and budding vesicles are induced from plasma membrane, it means the process does not need nuclear components, and the vesicles can be harvested for composition analysis to identify additional cellular factors.

Alternatively, leaving pU_L31/pU_L34 on the nuclear rim, we may take advantage of the aggregates induced by the U_S3 mutation, with the assumption that the essential egress components are enriched in these pU_L31/pU_L34 containing microdomains. In this case, cross-linking and *in vivo* labeling strategies may allow us to isolate functional candidates.

(iii) It is equally important to determine the structure of pU_L31 and pU_L34. Primary sequence analysis only inefficiently predicts any obvious structural or functional domains in the two proteins. In particular, it is indicated in Chapter IV that the phosphorylation at pU_L31 N-terminus may induce significant conformational changes in the protein that is required for efficient primary envelopment and de-envelopment. Therefore, structural analysis will greatly help elucidate the nature of the protein functions.

BIBLIOGRAPHY

1. **Abbotts, A. P., V. G. Preston, M. Hughes, A. H. Patel, and N. D. Stow.** 2000. Interaction of the herpes simplex virus type 1 packaging protein UL15 with full-length and deleted forms of the UL28 protein. J Gen Virol **81:**2999-3009.

2. **Adelman, K., B. Salmon, and J. D. Baines.** 2001. Herpes simplex virus DNA packaging sequences adopt novel structures that are specifically recognized by a component of the cleavage and packaging machinery. Proc Natl Acad Sci U S A **98:**3086-91.

3. **Atanasiu, D., J. C. Whitbeck, T. M. Cairns, B. Reilly, G. H. Cohen, and R. J. Eisenberg.** 2007. Bimolecular complementation reveals that glycoproteins gB and gH/gL of herpes simplex virus interact with each other during cell fusion. Proc Natl Acad Sci U S A **104:**18718-23.

4. **Baines, J. D., and C. Duffy.** 2006. Nucleocapsid assembly and envelopment of herpes simplex virus, p. 175-204. *In* R. M. Sandri-Goldin (ed.), Alpha herpesviruses: pathogenesis, molecular biology and infection control. Caister Scientific Press, Norfolk, United Kingdom.

5. **Baines, J. D., and S. K. Weller.** 2005. Cleavage and packaging of herpes simplex virus 1 DNA, p. 135-150. *In* C. E. Catalano (ed.), Viral Genome Packaging Machines: Genetics, Structure, and Mechanism. Landes Bioscience, Austin, TX.

6. **Baines, J. D., E. Wills, R. J. Jacob, J. Pennington, and B. Roizman.** 2007. Glycoprotein M of herpes simplex virus 1 is incorporated into virions during budding at the inner nuclear membrane. J Virol **81:**800-12.

7. **Balliet, J. W., and P. A. Schaffer.** 2006. Point mutations in herpes simplex virus type 1 oriL, but not in oriS, reduce pathogenesis during acute infection of mice and impair reactivation from latency. J Virol **80:**440-50.

8. **Baringer, J. R.** 1976. The biology of herpes simplex virus infection in humans. Surv Ophthalmol **21:**171-4.

9. **Baringer, J. R., and P. Swoveland.** 1973. Recovery of herpes-simplex virus from human trigeminal ganglions. N Engl J Med **288:**648-50.

10. **Batterson, W., D. Furlong, and B. Roizman.** 1983. Molecular genetics of herpes simplex virus. VIII. further characterization of a temperature-sensitive mutant defective in release of viral DNA and in other stages of the viral reproductive cycle. J Virol **45:**397-407.

11. **Batterson, W., and B. Roizman.** 1983. Characterization of the herpes simplex virion-associated factor responsible for the induction of alpha genes. J Virol **46:**371-7.

12. **Beard, P. M., N. S. Taus, and J. D. Baines.** 2002. DNA cleavage and packaging proteins encoded by genes U(L)28, U(L)15, and U(L)33 of herpes simplex virus type 1 form a complex in infected cells. J Virol **76:**4785-91.

13. **Benetti, L., J. Munger, and B. Roizman.** 2003. The herpes simplex virus 1 US3 protein kinase blocks caspase-dependent double cleavage and activation of the proapoptotic protein BAD. J Virol **77:**6567-73.

14. **Benetti, L., and B. Roizman.** 2004. Herpes simplex virus protein kinase US3 activates and functionally overlaps protein kinase A to block apoptosis. Proc Natl Acad Sci U S A **101:**9411-6.

15. **Bjerke, S. L., and R. J. Roller.** 2006. Roles for herpes simplex virus type 1 UL34 and US3 proteins in disrupting the nuclear lamina during herpes simplex virus type 1 egress. Virology **347:**261-76.

16. **Booy, F. P., W. W. Newcomb, B. L. Trus, J. C. Brown, T. S. Baker, and A. C. Steven.** 1991. Liquid-crystalline, phage-like packing of encapsidated DNA in herpes simplex virus. Cell **64:**1007-15.

17. **Bowzard, J. B., R. J. Visalli, C. B. Wilson, J. S. Loomis, E. M. Callahan, R. J. Courtney, and J. W. Wills.** 2000. Membrane targeting properties of a herpesvirus tegument protein-retrovirus Gag chimera. J Virol **74:**8692-9.

18. **Cai, W. Z., S. Person, S. C. Warner, J. H. Zhou, and N. A. DeLuca.** 1987. Linker-insertion nonsense and restriction-site deletion mutations of the gB glycoprotein gene of herpes simplex virus type 1. J Virol **61:**714-21.

19. **Campadelli-Fiume, G., F. Farabegoli, S. Di Gaeta, and B. Roizman.** 1991. Origin of unenveloped capsids in the cytoplasm of cells infected with herpes simplex virus 1. J Virol **65:**1589-95.

20. **Cartier, A., T. Komai, and M. G. Masucci.** 2003. The Us3 protein kinase of herpes simplex virus 1 blocks apoptosis and induces phosporylation of the Bcl-2 family member Bad. Exp Cell Res **291:**242-50.

21. **Cereghini, S., and M. Yaniv.** 1984. Assembly of transfected DNA into chromatin: structural changes in the origin-promoter-enhancer region upon replication. EMBO J **3:**1243-53.

22. **Challberg, M. D.** 1986. A method for identifying the viral genes required for herpesvirus DNA replication. Proc Natl Acad Sci U S A **83:**9094-8.

23. **Chang, Y. E., and B. Roizman.** 1993. The product of the UL31 gene of herpes simplex virus 1 is a nuclear phosphoprotein which partitions with the nuclear matrix. J Virol **67:**6348-56.

24. **Chang, Y. E., C. Van Sant, P. W. Krug, A. E. Sears, and B. Roizman.** 1997. The null mutant of the U(L)31 gene of herpes simplex virus 1: construction and phenotype in infected cells. J Virol **71:**8307-15.

25. **Church, G. A., and D. W. Wilson.** 1997. Study of herpes simplex virus maturation during a synchronous wave of assembly. J Virol **71:**3603-12.

26. **Clement, C., V. Tiwari, P. M. Scanlan, T. Valyi-Nagy, B. Y. Yue, and D. Shukla.** 2006. A novel role for phagocytosis-like uptake in herpes simplex virus entry. J Cell Biol **174:**1009-21.

27. **Clements, J. B., R. J. Watson, and N. M. Wilkie.** 1977. Temporal regulation of herpes simplex virus type 1 transcription: location of transcripts on the viral genome. Cell **12:**275-85.

28. **Collas, P., L. Thompson, A. P. Fields, D. L. Poccia, and J. C. Courvalin.** 1997. Protein kinase C-mediated interphase lamin B phosphorylation and solubilization. J Biol Chem **272:**21274-80.

29. **Conley, A. J., D. M. Knipe, P. C. Jones, and B. Roizman.** 1981. Molecular genetics of herpes simplex virus. VII. Characterization of a temperature-sensitive mutant produced by in vitro mutagenesis and defective in DNA synthesis and accumulation of gamma polypeptides. J Virol **37:**191-206.

30. **Costanzo, F., G. Campadelli-Fiume, L. Foa-Tomasi, and E. Cassai.** 1977. Evidence that herpes simplex virus DNA is transcribed by cellular RNA polymerase B. J Virol **21:**996-1001.

31. **Crump, C. M., B. Bruun, S. Bell, L. E. Pomeranz, T. Minson, and H. M. Browne.** 2004. Alphaherpesvirus glycoprotein M causes the relocalization of plasma membrane proteins. J Gen Virol **85:**3517-27.

32. **Davison, M. D., F. J. Rixon, and A. J. Davison.** 1992. Identification of genes encoding two capsid proteins (VP24 and VP26) of herpes simplex virus type 1. J Gen Virol **73 (Pt 10):**2709-13.

33. **de Bruyn Kops, A., and D. M. Knipe.** 1988. Formation of DNA replication structures in herpes virus-infected cells requires a viral DNA binding protein. Cell **55:**857-68.

34. **Deb, S., and M. Doelberg.** 1988. A 67-base-pair segment from the Ori-S region of herpes simplex virus type 1 encodes origin function. J Virol **62:**2516-9.

35. **Deiss, L. P., J. Chou, and N. Frenkel.** 1986. Functional domains within the a sequence involved in the cleavage-packaging of herpes simplex virus DNA. J Virol **59:**605-18.

36. **Desai, P., N. A. DeLuca, J. C. Glorioso, and S. Person.** 1993. Mutations in herpes simplex virus type 1 genes encoding VP5 and VP23 abrogate capsid formation and cleavage of replicated DNA. J Virol **67:**1357-64.

37. **Desai, P., and S. Person.** 1999. Second site mutations in the N-terminus of the major capsid protein (VP5) overcome a block at the maturation cleavage site of the capsid scaffold proteins of herpes simplex virus type 1. Virology **261:**357-66.

38. **Desai, P., G. L. Sexton, J. M. McCaffery, and S. Person.** 2001. A null mutation in the gene encoding the herpes simplex virus type 1 UL37 polypeptide abrogates virus maturation. J Virol **75:**10259-71.

39. **Desai, P., S. C. Watkins, and S. Person.** 1994. The size and symmetry of B capsids of herpes simplex virus type 1 are determined by the gene products of the UL26 open reading frame. J Virol **68:**5365-74.

40. **Desai, P. J.** 2000. A null mutation in the UL36 gene of herpes simplex virus type 1 results in accumulation of unenveloped DNA-filled capsids in the cytoplasm of infected cells. J Virol **74:**11608-18.

41. **Deshmane, S. L., and N. W. Fraser.** 1989. During latency, herpes simplex virus type 1 DNA is associated with nucleosomes in a chromatin structure. J Virol **63:**943-7.

42. **Diefenbach, R. J., M. Miranda-Saksena, M. W. Douglas, and A. L. Cunningham.** 2008. Transport and egress of herpes simplex virus in neurons. Rev Med Virol **18:**35-51.

43. **Dingwell, K. S., C. R. Brunetti, R. L. Hendricks, Q. Tang, M. Tang, A. J. Rainbow, and D. C. Johnson.** 1994. Herpes simplex virus glycoproteins E and I facilitate cell-to-cell spread in vivo and across junctions of cultured cells. J Virol **68:**834-45.

44. **Dingwell, K. S., and D. C. Johnson.** 1998. The herpes simplex virus gE-gI complex facilitates cell-to-cell spread and binds to components of cell junctions. J Virol **72:**8933-42.

45. **Dixon, R. A., and P. A. Schaffer.** 1980. Fine-structure mapping and functional analysis of temperature-sensitive mutants in the gene encoding the herpes simplex virus type 1 immediate early protein VP175. J Virol **36:**189-203.

46. **Dohner, K., A. Wolfstein, U. Prank, C. Echeverri, D. Dujardin, R. Vallee, and B. Sodeik.** 2002. Function of dynein and dynactin in herpes simplex virus capsid transport. Mol Biol Cell **13:**2795-809.

47. **Douglas, M. W., R. J. Diefenbach, F. L. Homa, M. Miranda-Saksena, F. J. Rixon, V. Vittone, K. Byth, and A. L. Cunningham.** 2004. Herpes simplex

virus type 1 capsid protein VP26 interacts with dynein light chains RP3 and Tctex1 and plays a role in retrograde cellular transport. J Biol Chem **279:**28522-30.

48. **Eggert, M., N. Radomski, D. Tripier, P. Traub, and E. Jost.** 1991. Identification of phosphorylation sites on murine nuclear lamin C by RP-HPLC and microsequencing. FEBS Lett **292:**205-9.

49. **Ejercito, P. M., E. D. Kieff, and B. Roizman.** 1968. Characterization of herpes simplex virus strains differing in their effects on social behaviour of infected cells. J Gen Virol **2:**357-64.

50. **Ellenberg, J., E. D. Siggia, J. E. Moreira, C. L. Smith, J. F. Presley, H. J. Worman, and J. Lippincott-Schwartz.** 1997. Nuclear membrane dynamics and reassembly in living cells: targeting of an inner nuclear membrane protein in interphase and mitosis. J Cell Biol **138:**1193-206.

51. **Enquist, L. W., P. J. Husak, B. W. Banfield, and G. A. Smith.** 1998. Infection and spread of alphaherpesviruses in the nervous system. Adv Virus Res **51:**237-347.

52. **Esclatine, A., B. Taddeo, and B. Roizman.** 2004. The UL41 protein of herpes simplex virus mediates selective stabilization or degradation of cellular mRNAs. Proc Natl Acad Sci U S A **101:**18165-70.

53. **Everett, R. D., and J. Murray.** 2005. ND10 components relocate to sites associated with herpes simplex virus type 1 nucleoprotein complexes during virus infection. J Virol **79:**5078-89.

54. **Farnsworth, A., K. Goldsmith, and D. C. Johnson.** 2003. Herpes simplex virus glycoproteins gD and gE/gI serve essential but redundant functions during acquisition of the virion envelope in the cytoplasm. J Virol **77:**8481-94.

55. **Farnsworth, A., and D. C. Johnson.** 2006. Herpes simplex virus gE/gI must accumulate in the trans-Golgi network at early times and then redistribute to cell junctions to promote cell-cell spread. J Virol **80:**3167-79.

56. **Farnsworth, A., T. W. Wisner, M. Webb, R. Roller, G. Cohen, R. Eisenberg, and D. C. Johnson.** 2007. Herpes simplex virus glycoproteins gB

and gH function in fusion between the virion envelope and the outer nuclear membrane. Proc Natl Acad Sci U S A **104:**10187-92.

57. **Favoreel, H. W., G. Van Minnebruggen, D. Adriaensen, and H. J. Nauwynck.** 2005. Cytoskeletal rearrangements and cell extensions induced by the US3 kinase of an alphaherpesvirus are associated with enhanced spread. Proc Natl Acad Sci U S A **102:**8990-5.

58. **Feierbach, B., S. Piccinotti, M. Bisher, W. Denk, and L. W. Enquist.** 2006. Alpha-herpesvirus infection induces the formation of nuclear actin filaments. PLoS Pathog **2:**e85.

59. **Fisher, D. Z., N. Chaudhary, and G. Blobel.** 1986. cDNA sequencing of nuclear lamins A and C reveals primary and secondary structural homology to intermediate filament proteins. Proc Natl Acad Sci U S A **83:**6450-4.

60. **Forest, T., S. Barnard, and J. D. Baines.** 2005. Active intranuclear movement of herpesvirus capsids. Nat Cell Biol **7:**429-31.

61. **Foster, T. P., J. M. Melancon, J. D. Baines, and K. G. Kousoulas.** 2004. The herpes simplex virus type 1 UL20 protein modulates membrane fusion events during cytoplasmic virion morphogenesis and virus-induced cell fusion. J Virol **78:**5347-57.

62. **Fuchs, W., H. Granzow, B. G. Klupp, M. Kopp, and T. C. Mettenleiter.** 2002. The UL48 tegument protein of pseudorabies virus is critical for intracytoplasmic assembly of infectious virions. J Virol **76:**6729-42.

63. **Gao, M., L. Matusick-Kumar, W. Hurlburt, S. F. DiTusa, W. W. Newcomb, J. C. Brown, P. J. McCann, 3rd, I. Deckman, and R. J. Colonno.** 1994. The protease of herpes simplex virus type 1 is essential for functional capsid formation and viral growth. J Virol **68:**3702-12.

64. **Garber, D. A., S. M. Beverley, and D. M. Coen.** 1993. Demonstration of circularization of herpes simplex virus DNA following infection using pulsed field gel electrophoresis. Virology **197:**459-62.

65. **Garner, J. A.** 2003. Herpes simplex virion entry into and intracellular transport within mammalian cells. Adv Drug Deliv Rev **55:**1497-513.

66. **Gelman, I. H., and S. Silverstein.** 1987. Dissection of immediate-early gene promoters from herpes simplex virus: sequences that respond to the virus transcriptional activators. J Virol **61:**3167-72.

67. **Gershon, A. A., D. L. Sherman, Z. Zhu, C. A. Gabel, R. T. Ambron, and M. D. Gershon.** 1994. Intracellular transport of newly synthesized varicella-zoster virus: final envelopment in the trans-Golgi network. J Virol **68:**6372-90.

68. **Godowski, P. J., and D. M. Knipe.** 1986. Transcriptional control of herpesvirus gene expression: gene functions required for positive and negative regulation. Proc Natl Acad Sci U S A **83:**256-60.

69. **Gonnella, R., A. Farina, R. Santarelli, S. Raffa, R. Feederle, R. Bei, M. Granato, A. Modesti, L. Frati, H. J. Delecluse, M. R. Torrisi, A. Angeloni, and A. Faggioni.** 2005. Characterization and intracellular localization of the Epstein-Barr virus protein BFLF2: interactions with BFRF1 and with the nuclear lamina. J Virol **79:**3713-27.

70. **Granzow, H., B. G. Klupp, W. Fuchs, J. Veits, N. Osterrieder, and T. C. Mettenleiter.** 2001. Egress of alphaherpesviruses: comparative ultrastructural study. J Virol **75:**3675-84.

71. **Granzow, H., B. G. Klupp, and T. C. Mettenleiter.** 2005. Entry of pseudorabies virus: an immunogold-labeling study. J Virol **79:**3200-5.

72. **Gruenbaum, Y., A. Margalit, R. D. Goldman, D. K. Shumaker, and K. L. Wilson.** 2005. The nuclear lamina comes of age. Nat Rev Mol Cell Biol **6:**21-31.

73. **Grunewald, K., P. Desai, D. C. Winkler, J. B. Heymann, D. M. Belnap, W. Baumeister, and A. C. Steven.** 2003. Three-dimensional structure of herpes simplex virus from cryo-electron tomography. Science **302:**1396-8.

74. **Heine, J. W., R. W. Honess, E. Cassai, and B. Roizman.** 1974. Proteins specified by herpes simplex virus. XII. The virion polypeptides of type 1 strains. J Virol **14:**640-51.

75. **Herold, B. C., R. J. Visalli, N. Susmarski, C. R. Brandt, and P. G. Spear.** 1994. Glycoprotein C-independent binding of herpes simplex virus to cells re-

quires cell surface heparan sulphate and glycoprotein B. J Gen Virol **75 (Pt 6):**1211-22.

76. **Hoger, T. H., G. Krohne, and W. W. Franke.** 1988. Amino acid sequence and molecular characterization of murine lamin B as deduced from cDNA clones. Eur J Cell Biol **47:**283-90.

77. **Hoger, T. H., K. Zatloukal, I. Waizenegger, and G. Krohne.** 1990. Characterization of a second highly conserved B-type lamin present in cells previously thought to contain only a single B-type lamin. Chromosoma **100:**67-9.

78. **Hong, Z., M. Beaudet-Miller, J. Durkin, R. Zhang, and A. D. Kwong.** 1996. Identification of a minimal hydrophobic domain in the herpes simplex virus type 1 scaffolding protein which is required for interaction with the major capsid protein. J Virol **70:**533-40.

79. **Igarashi, K., R. Fawl, R. J. Roller, and B. Roizman.** 1993. Construction and properties of a recombinant herpes simplex virus 1 lacking both S-component origins of DNA synthesis. J Virol **67:**2123-32.

80. **Izumi, M., O. A. Vaughan, C. J. Hutchison, and D. M. Gilbert.** 2000. Head and/or CaaX domain deletions of lamin proteins disrupt preformed lamin A and C but not lamin B structure in mammalian cells. Mol Biol Cell **11:**4323-37.

81. **Jackson, S. A., and N. A. DeLuca.** 2003. Relationship of herpes simplex virus genome configuration to productive and persistent infections. Proc Natl Acad Sci U S A **100:**7871-6.

82. **Jacob, R. J., L. S. Morse, and B. Roizman.** 1979. Anatomy of herpes simplex virus DNA. XII. Accumulation of head-to-tail concatemers in nuclei of infected cells and their role in the generation of the four isomeric arrangements of viral DNA. J Virol **29:**448-57.

83. **Jacobson, J. G., K. Yang, J. D. Baines, and F. L. Homa.** 2006. Linker insertion mutations in the herpes simplex virus type 1 UL28 gene: effects on UL28 interaction with UL15 and UL33 and identification of a second-site mutation in the UL15 gene that suppresses a lethal UL28 mutation. J Virol **80:**12312-23.

84. **Jayachandra, S., A. Baghian, and K. G. Kousoulas.** 1997. Herpes simplex virus type 1 glycoprotein K is not essential for infectious virus production in actively replicating cells but is required for efficient envelopment and translocation of infectious virions from the cytoplasm to the extracellular space. J Virol **71:**5012-24.

85. **Johnson, D. C., and M. T. Huber.** 2002. Directed egress of animal viruses promotes cell-to-cell spread. J Virol **76:**1-8.

86. **Johnson, D. C., and P. G. Spear.** 1982. Monensin inhibits the processing of herpes simplex virus glycoproteins, their transport to the cell surface, and the egress of virions from infected cells. J Virol **43:**1102-12.

87. **Johnson, D. C., M. Webb, T. W. Wisner, and C. Brunetti.** 2001. Herpes simplex virus gE/gI sorts nascent virions to epithelial cell junctions, promoting virus spread. J Virol **75:**821-33.

88. **Jovasevic, V., L. Liang, and B. Roizman.** 2008. Proteolytic cleavage of VP1-2 is required for release of herpes simplex virus 1 DNA into the nucleus. J Virol **82:**3311-9.

89. **Kato, A., M. Yamamoto, T. Ohno, H. Kodaira, Y. Nishiyama, and Y. Kawaguchi.** 2005. Identification of proteins phosphorylated directly by the Us3 protein kinase encoded by herpes simplex virus 1. J Virol **79:**9325-31.

90. **Klupp, B. G., W. Fuchs, H. Granzow, R. Nixdorf, and T. C. Mettenleiter.** 2002. Pseudorabies virus UL36 tegument protein physically interacts with the UL37 protein. J Virol **76:**3065-71.

91. **Klupp, B. G., H. Granzow, W. Fuchs, G. M. Keil, S. Finke, and T. C. Mettenleiter.** 2007. Vesicle formation from the nuclear membrane is induced by coexpression of two conserved herpesvirus proteins. Proc Natl Acad Sci U S A **104:**7241-6.

92. **Klupp, B. G., H. Granzow, G. M. Keil, and T. C. Mettenleiter.** 2006. The capsid-associated UL25 protein of the alphaherpesvirus pseudorabies virus is nonessential for cleavage and encapsidation of genomic DNA but is required for nuclear egress of capsids. J Virol **80:**6235-46.

93. **Klupp, B. G., H. Granzow, and T. C. Mettenleiter.** 2001. Effect of the pseudorabies virus US3 protein on nuclear membrane localization of the UL34 protein and virus egress from the nucleus. J Gen Virol **82:**2363-71.

94. **Klupp, B. G., R. Nixdorf, and T. C. Mettenleiter.** 2000. Pseudorabies virus glycoprotein M inhibits membrane fusion. J Virol **74:**6760-8.

95. **Koslowski, K. M., P. R. Shaver, J. T. Casey, 2nd, T. Wilson, G. Yamanaka, A. K. Sheaffer, D. J. Tenney, and N. E. Pederson.** 1999. Physical and functional interactions between the herpes simplex virus UL15 and UL28 DNA cleavage and packaging proteins. J Virol **73:**1704-7.

96. **Koslowski, K. M., P. R. Shaver, X. Y. Wang, D. J. Tenney, and N. E. Pederson.** 1997. The pseudorabies virus UL28 protein enters the nucleus after coexpression with the herpes simplex virus UL15 protein. J Virol **71:**9118-23.

97. **Kristensson, K., E. Lycke, M. Roytta, B. Svennerholm, and A. Vahlne.** 1986. Neuritic transport of herpes simplex virus in rat sensory neurons in vitro. Effects of substances interacting with microtubular function and axonal flow [nocodazole, taxol and erythro-9-3-(2-hydroxynonyl)adenine]. J Gen Virol **67 (Pt 9):**2023-8.

98. **Kristie, T. M., and B. Roizman.** 1986. Alpha 4, the major regulatory protein of herpes simplex virus type 1, is stably and specifically associated with promoter-regulatory domains of alpha genes and of selected other viral genes. Proc Natl Acad Sci U S A **83:**3218-22.

99. **Krohne, G.** 2004. Lamins. Methods Cell Biol **78:**573-96.

100. **La Boissiere, S., A. Izeta, S. Malcomber, and P. O'Hare.** 2004. Compartmentalization of VP16 in cells infected with recombinant herpes simplex virus expressing VP16-green fluorescent protein fusion proteins. J Virol **78:**8002-14.

101. **Lamberti, C., and S. K. Weller.** 1998. The herpes simplex virus type 1 cleavage/packaging protein, UL32, is involved in efficient localization of capsids to replication compartments. J Virol **72:**2463-73.

102. **Lammerding, J., L. G. Fong, J. Y. Ji, K. Reue, C. L. Stewart, S. G. Young, and R. T. Lee.** 2006. Lamins A and C but not lamin B1 regulate nuclear mechanics. J Biol Chem **281:**25768-80.

103. **Leach, N., S. L. Bjerke, D. K. Christensen, J. M. Bouchard, F. Mou, R. Park, J. Baines, T. Haraguchi, and R. J. Roller.** 2007. Emerin is hyperphosphorylated and redistributed in herpes simplex virus type 1-infected cells in a manner dependent on both UL34 and US3. J Virol **81:**10792-803.

104. **Lehman, I. R., and P. E. Boehmer.** 1999. Replication of herpes simplex virus DNA. J Biol Chem **274:**28059-62.

105. **Leuzinger, H., U. Ziegler, E. M. Schraner, C. Fraefel, D. L. Glauser, I. Heid, M. Ackermann, M. Mueller, and P. Wild.** 2005. Herpes simplex virus 1 envelopment follows two diverse pathways. J Virol **79:**13047-59.

106. **Liang, L., and J. D. Baines.** 2005. Identification of an essential domain in the herpes simplex virus 1 UL34 protein that is necessary and sufficient to interact with UL31 protein. J Virol **79:**3797-806.

107. **Liang, L., M. Tanaka, Y. Kawaguchi, and J. D. Baines.** 2004. Cell lines that support replication of a novel herpes simplex virus 1 UL31 deletion mutant can properly target UL34 protein to the nuclear rim in the absence of UL31. Virology **329:**68-76.

108. **Lockshon, D., and D. A. Galloway.** 1986. Cloning and characterization of oriL2, a large palindromic DNA replication origin of herpes simplex virus type 2. J Virol **58:**513-21.

109. **Loomis, J. S., R. J. Courtney, and J. W. Wills.** 2003. Binding partners for the UL11 tegument protein of herpes simplex virus type 1. J Virol **77:**11417-24.

110. **Lukonis, C. J., and S. K. Weller.** 1997. Formation of herpes simplex virus type 1 replication compartments by transfection: requirements and localization to nuclear domain 10. J Virol **71:**2390-9.

111. **Luxton, G. W., S. Haverlock, K. E. Coller, S. E. Antinone, A. Pincetic, and G. A. Smith.** 2005. Targeting of herpesvirus capsid transport in axons is cou-

pled to association with specific sets of tegument proteins. Proc Natl Acad Sci U S A **102:**5832-7.

112. **Luxton, G. W., J. I. Lee, S. Haverlock-Moyns, J. M. Schober, and G. A. Smith.** 2006. The pseudorabies virus VP1/2 tegument protein is required for intracellular capsid transport. J Virol **80:**201-9.

113. **Lycke, E., B. Hamark, M. Johansson, A. Krotochwil, J. Lycke, and B. Svennerholm.** 1988. Herpes simplex virus infection of the human sensory neuron. An electron microscopy study. Arch Virol **101:**87-104.

114. **Mackem, S., and B. Roizman.** 1980. Regulation of herpesvirus macromolecular synthesis: transcription-initiation sites and domains of alpha genes. Proc Natl Acad Sci U S A **77:**7122-6.

115. **Marschall, M., A. Marzi, P. aus dem Siepen, R. Jochmann, M. Kalmer, S. Auerochs, P. Lischka, M. Leis, and T. Stamminger.** 2005. Cellular p32 recruits cytomegalovirus kinase pUL97 to redistribute the nuclear lamina. J Biol Chem **280:**33357-67.

116. **Maul, G. G., A. M. Ishov, and R. D. Everett.** 1996. Nuclear domain 10 as preexisting potential replication start sites of herpes simplex virus type-1. Virology **217:**67-75.

117. **McGeoch, D. J., M. A. Dalrymple, A. J. Davison, A. Dolan, M. C. Frame, D. McNab, L. J. Perry, J. E. Scott, and P. Taylor.** 1988. The complete DNA sequence of the long unique region in the genome of herpes simplex virus type 1. J Gen Virol **69 (Pt 7):**1531-74.

118. **McKeon, F. D., M. W. Kirschner, and D. Caput.** 1986. Homologies in both primary and secondary structure between nuclear envelope and intermediate filament proteins. Nature **319:**463-8.

119. **McLauchlan, J., and F. J. Rixon.** 1992. Characterization of enveloped tegument structures (L particles) produced by alphaherpesviruses: integrity of the tegument does not depend on the presence of capsid or envelope. J Gen Virol **73 (Pt 2):**269-76.

120. **McNab, A. R., P. Desai, S. Person, L. L. Roof, D. R. Thomsen, W. W. Newcomb, J. C. Brown, and F. L. Homa.** 1998. The product of the herpes simplex virus type 1 UL25 gene is required for encapsidation but not for cleavage of replicated viral DNA. J Virol **72:**1060-70.

121. **McNamee, E. E., T. J. Taylor, and D. M. Knipe.** 2000. A dominant-negative herpesvirus protein inhibits intranuclear targeting of viral proteins: effects on DNA replication and late gene expression. J Virol **74:**10122-31.

122. **Mellerick, D. M., and N. W. Fraser.** 1987. Physical state of the latent herpes simplex virus genome in a mouse model system: evidence suggesting an episomal state. Virology **158:**265-75.

123. **Mettenleiter, T. C.** 2002. Herpesvirus assembly and egress. J Virol **76:**1537-47.

124. **Mettenleiter, T. C.** 2003. Pathogenesis of neurotropic herpesviruses: role of viral glycoproteins in neuroinvasion and transneuronal spread. Virus Res **92:**197-206.

125. **Mettenleiter, T. C., B. G. Klupp, and H. Granzow.** 2006. Herpesvirus assembly: a tale of two membranes. Curr Opin Microbiol **9:**423-9.

126. **Michael, K., B. G. Klupp, T. C. Mettenleiter, and A. Karger.** 2006. Composition of pseudorabies virus particles lacking tegument protein US3, UL47, or UL49 or envelope glycoprotein E. J Virol **80:**1332-9.

127. **Morrison, E. E., Y. F. Wang, and D. M. Meredith.** 1998. Phosphorylation of structural components promotes dissociation of the herpes simplex virus type 1 tegument. J Virol **72:**7108-14.

128. **Mou, F., T. Forest, and J. D. Baines.** 2007. US3 of herpes simplex virus type 1 encodes a promiscuous protein kinase that phosphorylates and alters localization of lamin A/C in infected cells. J Virol **81:**6459-70.

129. **Munger, J., and B. Roizman.** 2001. The US3 protein kinase of herpes simplex virus 1 mediates the posttranslational modification of BAD and prevents BAD-induced programmed cell death in the absence of other viral proteins. Proc Natl Acad Sci U S A **98:**10410-5.

130. **Muranyi, W., J. Haas, M. Wagner, G. Krohne, and U. H. Koszinowski.** 2002. Cytomegalovirus recruitment of cellular kinases to dissolve the nuclear lamina. Science **297:**854-7.

131. **Muylaert, I., and P. Elias.** 2007. Knockdown of DNA ligase IV/XRCC4 by RNA interference inhibits herpes simplex virus type I DNA replication. J Biol Chem **282:**10865-72.

132. **Nalwanga, D., S. Rempel, B. Roizman, and J. D. Baines.** 1996. The UL 16 gene product of herpes simplex virus 1 is a virion protein that colocalizes with intranuclear capsid proteins. Virology **226:**236-42.

133. **Newcomb, W. W., F. L. Homa, and J. C. Brown.** 2005. Involvement of the portal at an early step in herpes simplex virus capsid assembly. J Virol **79:**10540-6.

134. **Newcomb, W. W., F. L. Homa, D. R. Thomsen, F. P. Booy, B. L. Trus, A. C. Steven, J. V. Spencer, and J. C. Brown.** 1996. Assembly of the herpes simplex virus capsid: characterization of intermediates observed during cell-free capsid formation. J Mol Biol **263:**432-46.

135. **Newcomb, W. W., F. L. Homa, D. R. Thomsen, B. L. Trus, N. Cheng, A. Steven, F. Booy, and J. C. Brown.** 1999. Assembly of the herpes simplex virus procapsid from purified components and identification of small complexes containing the major capsid and scaffolding proteins. J Virol **73:**4239-50.

136. **Newcomb, W. W., F. L. Homa, D. R. Thomsen, Z. Ye, and J. C. Brown.** 1994. Cell-free assembly of the herpes simplex virus capsid. J Virol **68:**6059-63.

137. **Newcomb, W. W., R. M. Juhas, D. R. Thomsen, F. L. Homa, A. D. Burch, S. K. Weller, and J. C. Brown.** 2001. The UL6 gene product forms the portal for entry of DNA into the herpes simplex virus capsid. J Virol **75:**10923-32.

138. **Newcomb, W. W., D. R. Thomsen, F. L. Homa, and J. C. Brown.** 2003. Assembly of the herpes simplex virus capsid: identification of soluble scaffold-portal complexes and their role in formation of portal-containing capsids. J Virol **77:**9862-71.

139. **Newcomb, W. W., B. L. Trus, F. P. Booy, A. C. Steven, J. S. Wall, and J. C. Brown.** 1993. Structure of the herpes simplex virus capsid. Molecular composition of the pentons and the triplexes. J Mol Biol **232:**499-511.

140. **Nicholson, P., C. Addison, A. M. Cross, J. Kennard, V. G. Preston, and F. J. Rixon.** 1994. Localization of the herpes simplex virus type 1 major capsid protein VP5 to the cell nucleus requires the abundant scaffolding protein VP22a. J Gen Virol **75 (Pt 5):**1091-9.

141. **Nicola, A. V., J. Hou, E. O. Major, and S. E. Straus.** 2005. Herpes simplex virus type 1 enters human epidermal keratinocytes, but not neurons, via a pH-dependent endocytic pathway. J Virol **79:**7609-16.

142. **Nicola, A. V., and S. E. Straus.** 2004. Cellular and viral requirements for rapid endocytic entry of herpes simplex virus. J Virol **78:**7508-17.

143. **Ogasawara, M., T. Suzutani, I. Yoshida, and M. Azuma.** 2001. Role of the UL25 gene product in packaging DNA into the herpes simplex virus capsid: location of UL25 product in the capsid and demonstration that it binds DNA. J Virol **75:**1427-36.

144. **Ojala, P. M., B. Sodeik, M. W. Ebersold, U. Kutay, and A. Helenius.** 2000. Herpes simplex virus type 1 entry into host cells: reconstitution of capsid binding and uncoating at the nuclear pore complex in vitro. Mol Cell Biol **20:**4922-31.

145. **Ottaviano, Y., and L. Gerace.** 1985. Phosphorylation of the nuclear lamins during interphase and mitosis. J Biol Chem **260:**624-32.

146. **Park, R., and J. D. Baines.** 2006. Herpes simplex virus type 1 infection induces activation and recruitment of protein kinase C to the nuclear membrane and increased phosphorylation of lamin B. J Virol **80:**494-504.

147. **Patel, A. H., F. J. Rixon, C. Cunningham, and A. J. Davison.** 1996. Isolation and characterization of herpes simplex virus type 1 mutants defective in the UL6 gene. Virology **217:**111-23.

148. **Person, S., S. Laquerre, P. Desai, and J. Hempel.** 1993. Herpes simplex virus type 1 capsid protein, VP21, originates within the UL26 open reading frame. J Gen Virol **74 (Pt 10):**2269-73.

149. **Poffenberger, K. L., and B. Roizman.** 1985. A noninverting genome of a viable herpes simplex virus 1: presence of head-to-tail linkages in packaged genomes and requirements for circularization after infection. J Virol **53:**587-95.

150. **Polcicova, K., K. Goldsmith, B. L. Rainish, T. W. Wisner, and D. C. Johnson.** 2005. The extracellular domain of herpes simplex virus gE is indispensable for efficient cell-to-cell spread: evidence for gE/gI receptors. J Virol **79:**11990-2001.

151. **Polvino-Bodnar, M., P. K. Orberg, and P. A. Schaffer.** 1987. Herpes simplex virus type 1 oriL is not required for virus replication or for the establishment and reactivation of latent infection in mice. J Virol **61:**3528-35.

152. **Poon, A. P., H. Gu, and B. Roizman.** 2006. ICP0 and the US3 protein kinase of herpes simplex virus 1 independently block histone deacetylation to enable gene expression. Proc Natl Acad Sci U S A **103:**9993-8.

153. **Poon, A. P., and B. Roizman.** 2005. Herpes simplex virus 1 ICP22 regulates the accumulation of a shorter mRNA and of a truncated US3 protein kinase that exhibits altered functions. J Virol **79:**8470-9.

154. **Purifoy, D. J., R. B. Lewis, and K. L. Powell.** 1977. Identification of the herpes simplex virus DNA polymerase gene. Nature **269:**621-3.

155. **Purves, F. C., A. D. Deana, F. Marchiori, D. P. Leader, and L. A. Pinna.** 1986. The substrate specificity of the protein kinase induced in cells infected with herpesviruses: studies with synthetic substrates [corrected] indicate structural requirements distinct from other protein kinases. Biochim Biophys Acta **889:**208-15.

156. **Purves, F. C., D. Spector, and B. Roizman.** 1991. The herpes simplex virus 1 protein kinase encoded by the US3 gene mediates posttranslational modification of the phosphoprotein encoded by the UL34 gene. J Virol **65:**5757-64.

157. **Purves, F. C., D. Spector, and B. Roizman.** 1992. UL34, the target of the herpes simplex virus U(S)3 protein kinase, is a membrane protein which in its unphosphorylated state associates with novel phosphoproteins. J Virol **66:**4295-303.

158. **Quinlan, M. P., L. B. Chen, and D. M. Knipe.** 1984. The intranuclear location of a herpes simplex virus DNA-binding protein is determined by the status of viral DNA replication. Cell **36:**857-68.

159. **Read, G. S., B. M. Karr, and K. Knight.** 1993. Isolation of a herpes simplex virus type 1 mutant with a deletion in the virion host shutoff gene and identification of multiple forms of the vhs (UL41) polypeptide. J Virol **67:**7149-60.

160. **Remillard-Labrosse, G., G. Guay, and R. Lippe.** 2006. Reconstitution of herpes simplex virus type 1 nuclear capsid egress in vitro. J Virol **80:**9741-53.

161. **Reske, A., G. Pollara, C. Krummenacher, B. M. Chain, and D. R. Katz.** 2007. Understanding HSV-1 entry glycoproteins. Rev Med Virol **17:**205-15.

162. **Reynolds, A. E., L. Liang, and J. D. Baines.** 2004. Conformational changes in the nuclear lamina induced by herpes simplex virus type 1 require genes U(L)31 and U(L)34. J Virol **78:**5564-75.

163. **Reynolds, A. E., B. J. Ryckman, J. D. Baines, Y. Zhou, L. Liang, and R. J. Roller.** 2001. U(L)31 and U(L)34 proteins of herpes simplex virus type 1 form a complex that accumulates at the nuclear rim and is required for envelopment of nucleocapsids. J Virol **75:**8803-17.

164. **Reynolds, A. E., E. G. Wills, R. J. Roller, B. J. Ryckman, and J. D. Baines.** 2002. Ultrastructural localization of the herpes simplex virus type 1 UL31, UL34, and US3 proteins suggests specific roles in primary envelopment and egress of nucleocapsids. J Virol **76:**8939-52.

165. **Rixon, F. J., C. Addison, A. McGregor, S. J. Macnab, P. Nicholson, V. G. Preston, and J. D. Tatman.** 1996. Multiple interactions control the intracellular localization of the herpes simplex virus type 1 capsid proteins. J Gen Virol **77 (Pt 9):**2251-60.

166. **Rixon, F. J., C. Addison, and J. McLauchlan.** 1992. Assembly of enveloped tegument structures (L particles) can occur independently of virion maturation in herpes simplex virus type 1-infected cells. J Gen Virol **73 (Pt 2):**277-84.

167. **Rock, D. L., and N. W. Fraser.** 1983. Detection of HSV-1 genome in central nervous system of latently infected mice. Nature **302:**523-5.

168. **Roizman, B.** 1991. Herpesviridae: a brief introduction, p. 841-847. *In* B. N. Fields, D. M. Knipe (ed.), Fundamental Virology. Raven Press, New York.

169. **Roizman, B., and A. Sears.** 1996. Herpes simplex viruses and their replication., p. 2231-2296. *In* B. N. Fields, D. M. Knipe, P. M. Howley (ed.), Fileds Virology, 3rd ed. Lippincott-Raven, Philadelphia, PA.

170. **Roizman, B., and D. M. Knipe.** 2001. Herpes simplex viruses and their replication., p. 2399-2460. *In* D. M. Knipe, P. M. Howley (ed.), Fileds Virology. Lippincott, William & Willkins, Philadelphia, PA.

171. **Roizman, B., and J. Baines.** 1991. The diversity and unity of Herpesviridae. Comp Immunol Microbiol Infect Dis **14:**63-79.

172. **Roizman, B., L. E. Carmichael, F. Deinhardt, G. de-The, A. J. Nahmias, W. Plowright, F. Rapp, P. Sheldrick, M. Takahashi, and K. Wolf.** 1981. Herpesviridae. Definition, provisional nomenclature, and taxonomy. The Herpesvirus Study Group, the International Committee on Taxonomy of Viruses. Intervirology **16:**201-17.

173. **Roller, R. J., Y. Zhou, R. Schnetzer, J. Ferguson, and D. DeSalvo.** 2000. Herpes simplex virus type 1 U(L)34 gene product is required for viral envelopment. J Virol **74:**117-29.

174. **Ryckman, B. J., and R. J. Roller.** 2004. Herpes simplex virus type 1 primary envelopment: UL34 protein modification and the US3-UL34 catalytic relationship. J Virol **78:**399-412.

175. **Saldanha, C. E., J. Lubinski, C. Martin, T. Nagashunmugam, L. Wang, H. van Der Keyl, R. Tal-Singer, and H. M. Friedman.** 2000. Herpes simplex virus type 1 glycoprotein E domains involved in virus spread and disease. J Virol **74:**6712-9.

176. **Salmon, B., C. Cunningham, A. J. Davison, W. J. Harris, and J. D. Baines.** 1998. The herpes simplex virus type 1 U(L)17 gene encodes virion tegument proteins that are required for cleavage and packaging of viral DNA. J Virol **72:**3779-88.

177. **Sambrook, J., E. F. Fritsch, and T. Maniatis.** 1989. Molecular cloning: a laboratory mannual, 2nd ed. Cold Spring Harbor Laboratory Press, Cold Spring Harbor, NY.

178. **Satoh, T., J. Arii, T. Suenaga, J. Wang, A. Kogure, J. Uehori, N. Arase, I. Shiratori, S. Tanaka, Y. Kawaguchi, P. G. Spear, L. L. Lanier, and H. Arase.** 2008. PILRalpha is a herpes simplex virus-1 entry coreceptor that associates with glycoprotein B. Cell **132:**935-44.

179. **Schrag, J. D., B. V. Prasad, F. J. Rixon, and W. Chiu.** 1989. Three-dimensional structure of the HSV1 nucleocapsid. Cell **56:**651-60.

180. **Scott, E. S., and P. O'Hare.** 2001. Fate of the inner nuclear membrane protein lamin B receptor and nuclear lamins in herpes simplex virus type 1 infection. J Virol **75:**8818-30.

181. **Shahin, V., W. Hafezi, H. Oberleithner, Y. Ludwig, B. Windoffer, H. Schillers, and J. E. Kuhn.** 2006. The genome of HSV-1 translocates through the nuclear pore as a condensed rod-like structure. J Cell Sci **119:**23-30.

182. **Sheaffer, A. K., W. W. Newcomb, J. C. Brown, M. Gao, S. K. Weller, and D. J. Tenney.** 2000. Evidence for controlled incorporation of herpes simplex virus type 1 UL26 protease into capsids. J Virol **74:**6838-48.

183. **Sheaffer, A. K., W. W. Newcomb, M. Gao, D. Yu, S. K. Weller, J. C. Brown, and D. J. Tenney.** 2001. Herpes simplex virus DNA cleavage and packaging proteins associate with the procapsid prior to its maturation. J Virol **75:**687-98.

184. **Shiba, C., T. Daikoku, F. Goshima, H. Takakuwa, Y. Yamauchi, O. Koiwai, and Y. Nishiyama.** 2000. The UL34 gene product of herpes simplex virus type 2 is a tail-anchored type II membrane protein that is significant for virus envelopment. J Gen Virol **81:**2397-405.

185. **Simpson-Holley, M., J. Baines, R. Roller, and D. M. Knipe.** 2004. Herpes simplex virus 1 U(L)31 and U(L)34 gene products promote the late maturation of viral replication compartments to the nuclear periphery. J Virol **78:**5591-600.

186. **Simpson-Holley, M., R. C. Colgrove, G. Nalepa, J. W. Harper, and D. M. Knipe.** 2005. Identification and functional evaluation of cellular and viral factors involved in the alteration of nuclear architecture during herpes simplex virus 1 infection. J Virol **79:**12840-51.

187. **Sinclair, M. C., J. McLauchlan, H. Marsden, and S. M. Brown.** 1994. Characterization of a herpes simplex virus type 1 deletion variant (1703) which under-produces Vmw63 during immediate early conditions of infection. J Gen Virol **75 (Pt 5):**1083-9.

188. **Skepper, J. N., A. Whiteley, H. Browne, and A. Minson.** 2001. Herpes simplex virus nucleocapsids mature to progeny virions by an envelopment --> deenvelopment --> reenvelopment pathway. J Virol **75:**5697-702.

189. **Smibert, C. A., B. Popova, P. Xiao, J. P. Capone, and J. R. Smiley.** 1994. Herpes simplex virus VP16 forms a complex with the virion host shutoff protein vhs. J Virol **68:**2339-46.

190. **Smiley, J. R.** 2004. Herpes simplex virus virion host shutoff protein: immune evasion mediated by a viral RNase? J Virol **78:**1063-8.

191. **Smiley, J. R., J. Duncan, and M. Howes.** 1990. Sequence requirements for DNA rearrangements induced by the terminal repeat of herpes simplex virus type 1 KOS DNA. J Virol **64:**5036-50.

192. **Sodeik, B., M. W. Ebersold, and A. Helenius.** 1997. Microtubule-mediated transport of incoming herpes simplex virus 1 capsids to the nucleus. J Cell Biol **136:**1007-21.

193. **Sourvinos, G., and R. D. Everett.** 2002. Visualization of parental HSV-1 genomes and replication compartments in association with ND10 in live infected cells. EMBO J **21:**4989-97.

194. **Stackpole, C. W.** 1969. Herpes-type virus of the frog renal adenocarcinoma. I. Virus development in tumor transplants maintained at low temperature. J Virol **4:**75-93.

195. **Stannard, L. M., S. Himmelhoch, and S. Wynchank.** 1996. Intra-nuclear localization of two envelope proteins, gB and gD, of herpes simplex virus. Arch Virol **141:**505-24.

196. **Stewart, C. L., K. J. Roux, and B. Burke.** 2007. Blurring the boundary: the nuclear envelope extends its reach. Science **318:**1408-12.

197. **Stow, N. D.** 2001. Packaging of genomic and amplicon DNA by the herpes simplex virus type 1 UL25-null mutant KUL25NS. J Virol **75:**10755-65.

198. **Stow, N. D., and E. C. Stow.** 1986. Isolation and characterization of a herpes simplex virus type 1 mutant containing a deletion within the gene encoding the immediate early polypeptide Vmw110. J Gen Virol **67 (Pt 12):**2571-85.

199. **Strang, B. L., and N. D. Stow.** 2005. Circularization of the herpes simplex virus type 1 genome upon lytic infection. J Virol **79:**12487-94.

200. **Subramanian, R. P., and R. J. Geraghty.** 2007. Herpes simplex virus type 1 mediates fusion through a hemifusion intermediate by sequential activity of glycoproteins D, H, L, and B. Proc Natl Acad Sci U S A **104:**2903-8.

201. **Sullivan, T., D. Escalante-Alcalde, H. Bhatt, M. Anver, N. Bhat, K. Nagashima, C. L. Stewart, and B. Burke.** 1999. Loss of A-type lamin expression compromises nuclear envelope integrity leading to muscular dystrophy. J Cell Biol **147:**913-20.

202. **Taus, N. S., B. Salmon, and J. D. Baines.** 1998. The herpes simplex virus 1 UL 17 gene is required for localization of capsids and major and minor capsid proteins to intranuclear sites where viral DNA is cleaved and packaged. Virology **252:**115-25.

203. **Taylor, T. J., E. E. McNamee, C. Day, and D. M. Knipe.** 2003. Herpes simplex virus replication compartments can form by coalescence of smaller compartments. Virology **309:**232-47.

204. **Thurlow, J. K., F. J. Rixon, M. Murphy, P. Targett-Adams, M. Hughes, and V. G. Preston.** 2005. The herpes simplex virus type 1 DNA packaging protein UL17 is a virion protein that is present in both the capsid and the tegument compartments. J Virol **79:**150-8.

205. **Tischer, B. K., J. von Einem, B. Kaufer, and N. Osterrieder.** 2006. Two-step red-mediated recombination for versatile high-efficiency markerless DNA manipulation in Escherichia coli. Biotechniques **40:**191-7.

206. **Topp, K. S., K. Bisla, N. D. Saks, and J. H. Lavail.** 1996. Centripetal transport of herpes simplex virus in human retinal pigment epithelial cells in vitro. Neuroscience **71:**1133-44.

207. **Torrisi, M. R., C. Di Lazzaro, A. Pavan, L. Pereira, and G. Campadelli-Fiume.** 1992. Herpes simplex virus envelopment and maturation studied by fracture label. J Virol **66:**554-61.

208. **Trus, B. L., F. P. Booy, W. W. Newcomb, J. C. Brown, F. L. Homa, D. R. Thomsen, and A. C. Steven.** 1996. The herpes simplex virus procapsid: structure, conformational changes upon maturation, and roles of the triplex proteins VP19c and VP23 in assembly. J Mol Biol **263:**447-62.

209. **Trus, B. L., N. Cheng, W. W. Newcomb, F. L. Homa, J. C. Brown, and A. C. Steven.** 2004. Structure and polymorphism of the UL6 portal protein of herpes simplex virus type 1. J Virol **78:**12668-71.

210. **Trus, B. L., W. W. Newcomb, N. Cheng, G. Cardone, L. Marekov, F. L. Homa, J. C. Brown, and A. C. Steven.** 2007. Allosteric signaling and a nuclear exit strategy: binding of UL25/UL17 heterodimers to DNA-Filled HSV-1 capsids. Mol Cell **26:**479-89.

211. **Turcotte, S., J. Letellier, and R. Lippe.** 2005. Herpes simplex virus type 1 capsids transit by the trans-Golgi network, where viral glycoproteins accumulate independently of capsid egress. J Virol **79:**8847-60.

212. **Ugolini, G., H. G. Kuypers, and P. L. Strick.** 1989. Transneuronal transfer of herpes virus from peripheral nerves to cortex and brainstem. Science **243:**89-91.

213. **Uprichard, S. L., and D. M. Knipe.** 1997. Assembly of herpes simplex virus replication proteins at two distinct intranuclear sites. Virology **229:**113-25.

214. **van Genderen, I. L., R. Brandimarti, M. R. Torrisi, G. Campadelli, and G. van Meer.** 1994. The phospholipid composition of extracellular herpes simplex virions differs from that of host cell nuclei. Virology **200:**831-6.

215. **van Leeuwen, H., G. Elliott, and P. O'Hare.** 2002. Evidence of a role for nonmuscle myosin II in herpes simplex virus type 1 egress. J Virol **76:**3471-81.

216. **Varmuza, S. L., and J. R. Smiley.** 1985. Signals for site-specific cleavage of HSV DNA: maturation involves two separate cleavage events at sites distal to the recognition sequences. Cell **41:**793-802.

217. **Vergnes, L., M. Peterfy, M. O. Bergo, S. G. Young, and K. Reue.** 2004. Lamin B1 is required for mouse development and nuclear integrity. Proc Natl Acad Sci U S A **101:**10428-33.

218. **Vittone, V., E. Diefenbach, D. Triffett, M. W. Douglas, A. L. Cunningham, and R. J. Diefenbach.** 2005. Determination of interactions between tegument proteins of herpes simplex virus type 1. J Virol **79:**9566-71.

219. **Wagner, E.** 1985. Individual HSV transcripts: Characterization of specific genes., p. 45-104. *In* B. Roizman (ed.), The Herpesviruses, vol. 3. Plenum Press, New York.

220. **Wagner, M. J., and W. C. Summers.** 1978. Structure of the joint region and the termini of the DNA of herpes simplex virus type 1. J Virol **27:**374-87.

221. **Warner, S. C., P. Desai, and S. Person.** 2000. Second-site mutations encoding residues 34 and 78 of the major capsid protein (VP5) of herpes simplex virus type 1 are important for overcoming a blocked maturation cleavage site of the capsid scaffold proteins. Virology **278:**217-26.

222. **Weinheimer, S. P., P. J. McCann, 3rd, D. R. O'Boyle, 2nd, J. T. Stevens, B. A. Boyd, D. A. Drier, G. A. Yamanaka, C. L. DiIanni, I. C. Deckman, and M. G. Cordingley.** 1993. Autoproteolysis of herpes simplex virus type 1

protease releases an active catalytic domain found in intermediate capsid particles. J Virol **67:**5813-22.

223. **Weir, J. P.** 2001. Regulation of herpes simplex virus gene expression. Gene **271:**117-30.

224. **Weller, S. K., A. Spadaro, J. E. Schaffer, A. W. Murray, A. M. Maxam, and P. A. Schaffer.** 1985. Cloning, sequencing, and functional analysis of oriL, a herpes simplex virus type 1 origin of DNA synthesis. Mol Cell Biol **5:**930-42.

225. **White, C. A., N. D. Stow, A. H. Patel, M. Hughes, and V. G. Preston.** 2003. Herpes simplex virus type 1 portal protein UL6 interacts with the putative terminase subunits UL15 and UL28. J Virol **77:**6351-8.

226. **Whitley, R. J., J. W. Gnann.** 1993. The epidemiology and clinical manifestation, p. 69-105. *In* B. Roizman (ed.), The Human Herpesviruses. Raven Press, New York.

227. **Whitley, R. J., and B. Roizman.** 2001. Herpes simplex virus infections. Lancet **357:**1513-8.

228. **Wild, P., M. Engels, C. Senn, K. Tobler, U. Ziegler, E. M. Schraner, E. Loepfe, M. Ackermann, M. Mueller, and P. Walther.** 2005. Impairment of nuclear pores in bovine herpesvirus 1-infected MDBK cells. J Virol **79:**1071-83.

229. **Wittels, M., and P. G. Spear.** 1991. Penetration of cells by herpes simplex virus does not require a low pH-dependent endocytic pathway. Virus Res **18:**271-90.

230. **Wolfstein, A., C. H. Nagel, K. Radtke, K. Dohner, V. J. Allan, and B. Sodeik.** 2006. The inner tegument promotes herpes simplex virus capsid motility along microtubules in vitro. Traffic **7:**227-37.

231. **Wu, C. A., N. J. Nelson, D. J. McGeoch, and M. D. Challberg.** 1988. Identification of herpes simplex virus type 1 genes required for origin-dependent DNA synthesis. J Virol **62:**435-43.

232. **Yamauchi, Y., C. Shiba, F. Goshima, A. Nawa, T. Murata, and Y. Nishiyama.** 2001. Herpes simplex virus type 2 UL34 protein requires UL31 protein for its relocation to the internal nuclear membrane in transfected cells. J Gen Virol **82:**1423-8.

233. **Yang, K., and J. D. Baines.** 2006. The putative terminase subunit of herpes simplex virus 1 encoded by UL28 is necessary and sufficient to mediate interaction between pUL15 and pUL33. J Virol **80:**5733-9.

234. **Yang, K., F. Homa, and J. D. Baines.** 2007. Putative terminase subunits of herpes simplex virus 1 form a complex in the cytoplasm and interact with portal protein in the nucleus. J Virol **81:**6419-33.

235. **Ye, G. J., and B. Roizman.** 2000. The essential protein encoded by the UL31 gene of herpes simplex virus 1 depends for its stability on the presence of UL34 protein. Proc Natl Acad Sci U S A **97:**11002-7.

236. **Ye, G. J., K. T. Vaughan, R. B. Vallee, and B. Roizman.** 2000. The herpes simplex virus 1 U(L)34 protein interacts with a cytoplasmic dynein intermediate chain and targets nuclear membrane. J Virol **74:**1355-63.

237. **Yu, D., and S. K. Weller.** 1998. Herpes simplex virus type 1 cleavage and packaging proteins UL15 and UL28 are associated with B but not C capsids during packaging. J Virol **72:**7428-39.

238. **Zhou, Z. H., D. H. Chen, J. Jakana, F. J. Rixon, and W. Chiu.** 1999. Visualization of tegument-capsid interactions and DNA in intact herpes simplex virus type 1 virions. J Virol **73:**3210-8.

239. **Zhou, Z. H., M. Dougherty, J. Jakana, J. He, F. J. Rixon, and W. Chiu.** 2000. Seeing the herpesvirus capsid at 8.5 A. Science **288:**877-80.

240. **Zhou, Z. H., J. He, J. Jakana, J. D. Tatman, F. J. Rixon, and W. Chiu.** 1995. Assembly of VP26 in herpes simplex virus-1 inferred from structures of wild-type and recombinant capsids. Nat Struct Biol **2:**1026-30.

241. **Zhou, Z. H., B. V. Prasad, J. Jakana, F. J. Rixon, and W. Chiu.** 1994. Protein subunit structures in the herpes simplex virus A-capsid determined from 400 kV spot-scan electron cryomicroscopy. J Mol Biol **242:**456-69.

242. **Zhu, Q., and R. J. Courtney.** 1994. Chemical cross-linking of virion envelope and tegument proteins of herpes simplex virus type 1. Virology **204:**590-9.